PB 161603

NBS

Technical Note No. 102

Boulder Laboratories

PERFORMANCE PREDICTIONS FOR SINGLE TROPOSPHERIC COMMUNICATION LINKS AND FOR SEVERAL LINKS IN TANDEM

BY

A. P. BARSIS, K. A. NORTON,

P. L. RICE, AND P. H. ELDER

U. S. DEPARTMENT OF COMMERCE
NATIONAL BUREAU OF STANDARDS

THE NATIONAL BUREAU OF STANDARDS

Functions and Activities

The functions of the National Bureau of Standards are set forth in the Act of Congress, March 3, 1901, as amended by Congress in Public Law 619, 1950. These include the development and maintenance of the national standards of measurement and the provision of means and methods for making measurements consistent with these standards; the determination of physical constants and properties of materials; the development of methods and instruments for testing materials, devices, and structures; advisory services to government agencies on scientific and technical problems; invention and development of devices to serve special needs of the Government; and the development of standard practices, codes, and specifications. The work includes basic and applied research, development, engineering, instrumentation, testing, evaluation, calibration services, and various consultation and information services. Research projects are also performed for other government agencies when the work relates to and supplements the basic program of the Bureau or when the Bureau's unique competence is required. The scope of activities is suggested by the listing of divisions and sections on the inside of the back cover.

Publications

The results of the Bureau's research are published either in the Bureau's own series of publications or in the journals of professional and scientific societies. The Bureau itself publishes three periodicals available from the Government Printing Office: The Journal of Research, published in four separate sections, presents complete scientific and technical papers; the Technical News Bulletin presents summary and preliminary reports on work in progress; and Basic Radio Propagation Predictions provides data for determining the best frequencies to use for radio communications throughout the world. There are also five series of nonperiodical publications: Monographs, Applied Mathematics Series, Handbooks, Miscellaneous Publications, and Technical Notes.

A complete listing of the Bureau's publications can be found in National Bureau of Standards Circular 460, Publications of the National Bureau of Standards, 1901 to June 1947 ($1.25), and the Supplement to National Bureau of Standards Circular 460, July 1947 to June 1957 ($1.50), and Miscellaneous Publication 240, July 1957 to June 1960 (Includes Titles of Papers Published in Outside Journals 1950 to 1959) ($2.25); available from the Superintendent of Documents, Government Printing Office, Washington 25, D. C.

NATIONAL BUREAU OF STANDARDS

Technical Note

102

August 1961

PERFORMANCE PREDICTIONS FOR SINGLE TROPOSPHERIC COMMUNICATION LINKS AND FOR SEVERAL LINKS IN TANDEM

by

A. P. Barsis, K. A. Norton, P. L. Rice, and P. H. Elder

DISTRIBUTED BY

UNITED STATES DEPARTMENT OF COMMERCE

OFFICE OF TECHNICAL SERVICES

WASHINGTON 25, D. C.

Price $ 3.00

TABLE OF CONTENTS

ABSTRACT

Performance of long-distance tropospheric communication circuits, either singly or in tandem, is predicted in terms of the probability of obtaining a specified grade of service or better for various percentages of time. The grade of service is determined by the minimum acceptable ratio of hourly median predetection-RMS-signal-to-RMS-noise for the type of intelligence to be transmitted.

The standard deviation of prediction errors depends upon the percentage of hours the specified grade of service is required and on parameters characterizing the propagation path. The possibility of reducing this standard deviation by making path-loss measurements is discussed. It is shown that no improvement is possible unless the test path is very nearly the same as the proposed operational path; in particular, unless the test path and operational paths have terminals less than one mile apart it is shown to be doubtful in most cases whether the observations will be useful in improving the reliability of the predicted performance of the proposed system. Assuming that the test path and proposed operational paths are identical, estimates are given of the number of days of observations required to halve the prediction uncertainty or, alternatively, to reduce it to 3 db; in some cases several years of observations are required.

A tutorial discussion is given in Appendix III of the concepts of the effective noise figure and the effective input noise temperature of a receiving system.

PERFORMANCE PREDICTIONS FOR SINGLE TROPOSPHERIC COMMUNICATION LINKS AND FOR SEVERAL LINKS IN TANDEM

by

A. P. Barsis, K. A. Norton, P. L. Rice, and P. H. Elder

1. INTRODUCTION

The utilization of tropospheric radio wave propagation for long distance communication circuits has become more and more important in recent years. The underlying physical principles for this mode of propagation are still a subject of discussion and some controversy and will not be treated here. Of more importance to the engineer is that a signal transmitted at very high and ultra-high frequencies through the troposphere over a long distance is subject to substantial amplitude variations which may be described statistically. Information contained in the signal will be affected by these variations, and may be misinterpreted by the receiving system if the amplitude happens to be too low compared to the inherent noise level of the receiving system or its surroundings.

Taking into account the characteristics of the propagation path, the receiving system, the type of information to be transmitted, and the nature of the signal variations, one may estimate the amount of transmitter power and the antenna size necessary to provide a given degree of reliability of the system for a specified percentage of the time. This degree of reliability is most easily thought of in terms of a maximum permissible error rate in teletype transmission and may be identified with a "grade of service". Conversely, for a given system the percentage of time that it is possible to provide a given reliability

of communication or grade of service may be estimated. Both results will be functions not only of the percentage of time for which this given grade of service is desired, but also, because of errors in the prediction, will be dependent on another statistical variable, namely the probability that the actual system performance and path parameters may be expected to conform to the theoretical assumptions made.

It will be shown how the probability of obtaining a predetermined grade of service or better during a given percentage of time is determined as a function of the system parameters. This probability will be called "service probability," and the percentage of time concerned will be termed "time availability," and expressed in percent of all hours. The grade of service will be defined as an hourly median predetection RMS-signal-to-RMS-noise ratio necessary to provide the desired maximum permissible teletype error rate, a corresponding quality of voice transmission, or any other desired measure of circuit reliability. For any particular communication link the procedure consists in calculating first the distribution of hourly median basic transmission loss values over the time period (generally all hours of the year) for which the prediction is desired. Relations between basic transmission loss and transmitter power requirements are easily established by the use of equipment parameters and specifications for the desired grade of service. Then, using reasonable assumptions about the prediction uncertainty, the service probability of a given system as a function of the time availability may be calculated and presented in graphical form.

Finally, a study is made of the possible reduction of prediction uncertainty by means of transmission loss measurements.

2. DETERMINATION OF SYSTEM POWER REQUIREMENTS

In the design of a complete communication system, there are a number of factors determining the optimum frequency, transmitter power and diversity configuration, as well as the service probability for a specified grade of service. In general, the transmitter power is related to equipment parameters, basic transmission loss, and path antenna gain by a simple formula given by Norton [1956]:

$$P_t = L_b - G_p + F + L_t + R + B - 204 \qquad (1)$$

where

P_t = transmitter power in decibels above one watt

L_b = basic transmission loss over the path in decibels

G_p = average path antenna gain in decibels

F = effective noise figure of the receiving system in decibels, including the effects of the receiver itself, the receiving antenna transmission line losses and the effects of external noise in the receiving antenna. See Appendix III.

L_t = transmitting antenna transmission line and associated losses, in decibels

R = hourly median RMS-signal-to-RMS-noise ratio in decibels in the predetection pass band. A given minimum value R_m characterizes a specified required grade of service. The RMS signal may consist of a modulated carrier with its sidebands, or only the modulated sidebands in the case of suppressed carrier systems.

B = $10 \log_{10} b$, where b is the predetection noise bandwidth in cycles per second as defined in Appendix III. The band

b should be made sufficiently wide so that it allows for the effect of drift between transmitter and receiver oscillators.

204 = a constant equal to $(-10 \log_{10} kt_o)$, where k is Boltzmann's constant, and the reference temperature t_o is taken to be 288.39^o Kelvin.

For a long-distance tropospheric propagation path the terms F, L_t, R_m, and B are determined by the choice of the equipment and the specified required grade of service. They are frequency dependent, but otherwise may be considered fixed when the frequency of the system has been selected. The basic transmission loss L_b and the path antenna gain G_p, however, are time dependent, and the resulting transmitter power P_t from (1) will be the same function of time as $(L_b - G_p)$. If (1) is solved for one of the other parameters, the solution will also be a function of time.

It has been found convenient and practical to distinguish between short-term and long-term variations of basic transmission loss. Variability within a single hour is arbitrarily classified as "short-term", and is allowed for by a minimum hourly median required signal-to-noise ratio, R_m. The quantity R_m is simply that number of decibels by which the predetection hourly median RMS signal level exceeds the RMS noise level in order to provide the specified grade of service during that hour. The study of long-term variability is then concerned with the variability of these hourly medians.

Within-the-hour fading characteristics are nearly always adequately described by the Rayleigh distribution, particularly in the case of those weak fields which determine the required power for

long-distance communication links. The required predetection hourly median RMS-signal-to-RMS-noise ratio R_m may be directly related to the binary or teletype error rate for various schemes of demodulation and various diversity configurations [Florman and Tary, 1961], assuming Rayleigh-distributed within-the-hour fading. For voice modulation, R_m may also be related to a voice channel signal-to-noise ratio required for a specified intelligibility under Rayleigh fading conditions. The grade of service given by R_m may be specified by the requirements of the user of the communication circuit. The designer of the circuit only has to meet the requirement that the grade of service defined by R_m, or better, will be available during a specified percentage of the hours, or alternatively, he has to determine the percentage of hours during which a specified grade of service, or better, is available, when certain types of equipment and various amounts of power are used. Thus the grade of service and its time availability are independent quantities which both enter into the final determination of service probability. Statistical variations in the short-term fading rates and fade durations are accounted for in determining R_m; they do not otherwise affect time availability.

Methods for calculating the hourly median basic transmission loss L_{bm} and its variability, and the average or hourly median path antenna gain G_p as functions of carrier frequency, path parameters, and antenna size are contained in an NBS Technical Note [Rice, Longley, and Norton, 1959], and an Air Force Technical Order, [1961], which also include references to earlier work by NBS and other authors. Time variations of the path antenna gain G_p are included in the time variations of basic transmission loss, so that G_p in (1) may be assumed to be an average value independent of time variations.

The prediction uncertainty concept which will be discussed later ties in directly with the transmission loss calculation procedures discussed in the Air Force Technical Order, [1961]; therefore, it is recommended that this work be used for performance predictions.

The expected variability of hourly median transmission loss values is expressed by an empirical function, V(p), which is combined with a reference value, L_{bm}, to give the value of basic transmission loss, $L_b(p)$, not exceeded during p percent of all hours within the time period considered. The percentage of hours, p, is called the time availability. In terms of basic transmission loss,

$$L_b(p) = L_{bm} - V(p) \text{ db} \tag{2a}$$

and in terms of field strength,

$$E_b(p) = E_{bm} + V(p) \text{ db} \tag{2b}$$

where $E_b(p)$ and E_{bm} are the field strength values corresponding to the basic transmission loss values $L_b(p)$ and L_{bm}, respectively. For the purpose of analyzing long-term variability, the year has been divided into eight time blocks, four of which apply to the winter months, and four to the summer months [Norton, Rice, and Vogler, 1955].* In accordance with the notation used in the Air Force Technical Order, [1961], L_{bm} is the Time Block 2 (November - April, 1300 - 1800 hours) median of hourly median basic transmission loss values. This value corresponds to the average winter afternoon hour and is identical to the reference value calculated by the methods of

* See Table I-1, page 88.

Rice, Longley, and Norton, [1959], or the Air Force Technical Order, [1961].

The time variability function, V(p), has also been discussed in detail in the Air Force Technical Order, [1961]. For long extra-diffraction tropospheric propagation paths V(p) depends on the angular distance θ. Figs. 1, 2, and 3 are graphs of $V(p, \theta)$ for all hours of the year, for the winter time block group (all hours for November through April), and for the summer time block group (all hours for May through October). Figs. 1, 2, or 3 may be used where the angular distance θ can be accurately determined from terrain profiles. $V(p, \theta)$ is most reliable for θ greater than 10 milliradians and for frequencies near 100 Mc/s. For the most recent prediction methods, the function $V(p, \theta)$ is replaced by a function $V(p, d)$, where d is the path distance in statute miles. Methods for determining $V(p, d)$ and pertinent graphs are given in the Air Force Technical Order, [1961].

Calculation of the path antenna gain G_p as a function of the free space antenna gains at the path terminal and other path and circuit parameters is given in a paper by Hartman and Wilkerson [1959], and also in the Air Force Technical Order, [1961].

Equation (2a) shows the relation between the basic transmission loss, $L_b(p)$, expected to be exceeded during (100-p)% of all the hours in a given time block, and the winter afternoon reference value of basic transmission loss L_{bm}. It is now practical to combine all constant or specified terms of (1) into a constant K_o and substitute into (2a), in order to obtain either an expression for the transmitter power required to deliver a fixed predetection hourly median RMS-signal-to-RMS-noise ratio R_m as a function of the

EXPECTED SIGNAL LEVEL, $V(p,\theta)$, EXCEEDED BY p PERCENT OF ALL HOURLY MEDIANS OBSERVED AT ANGULAR DISTANCE θ DURING ALL HOURS OF THE YEAR

$V(p,\theta)$ shows the deviation of all-day, all-year values, $L_b(p,\theta)$, relative to median basic transmission loss, L_{bm}, for the period November–April, 1 P.M.–6 P.M. (Time Block No. 2)

$L_b(p,\theta) = L_{bm} - V(p,\theta)$ decibels

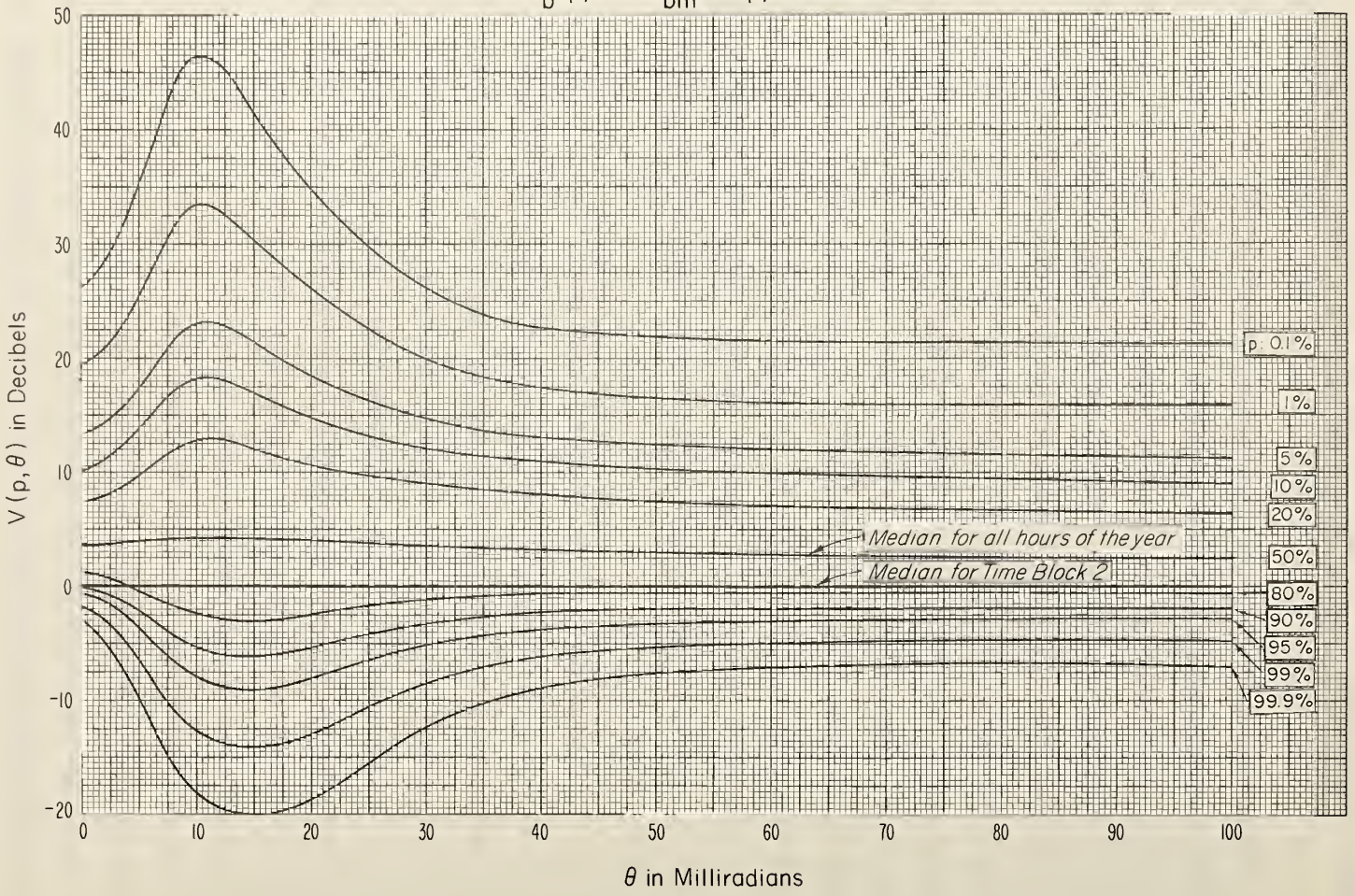

Figure 1

EXPECTED SIGNAL LEVEL, $V(p,\theta)$, EXCEEDED BY p PERCENT
OF ALL HOURS, WINTER
November – April, All Hours
$L_b(p,\theta) = L_{bm} - V(p,\theta)$ decibels

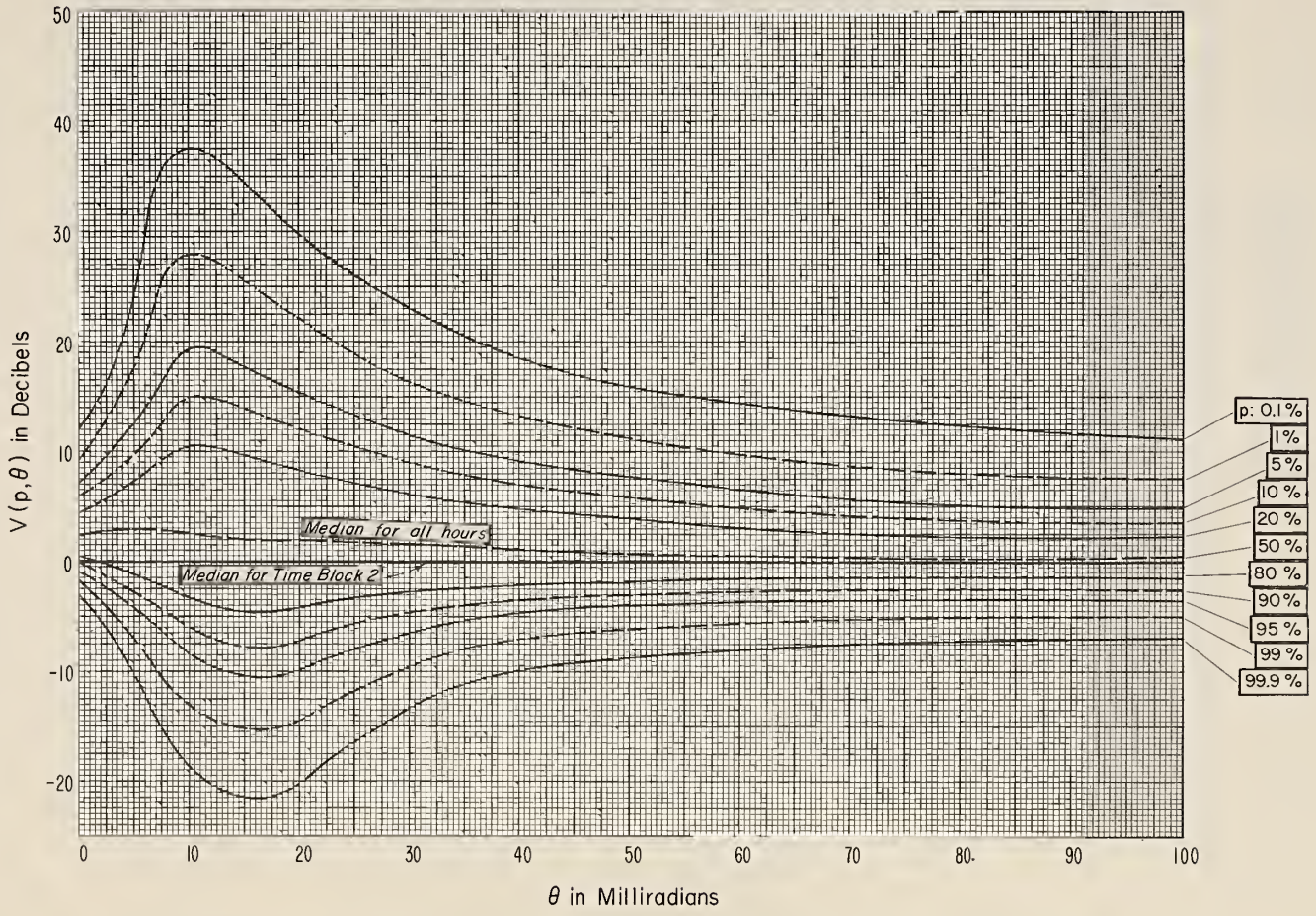

Figure 2

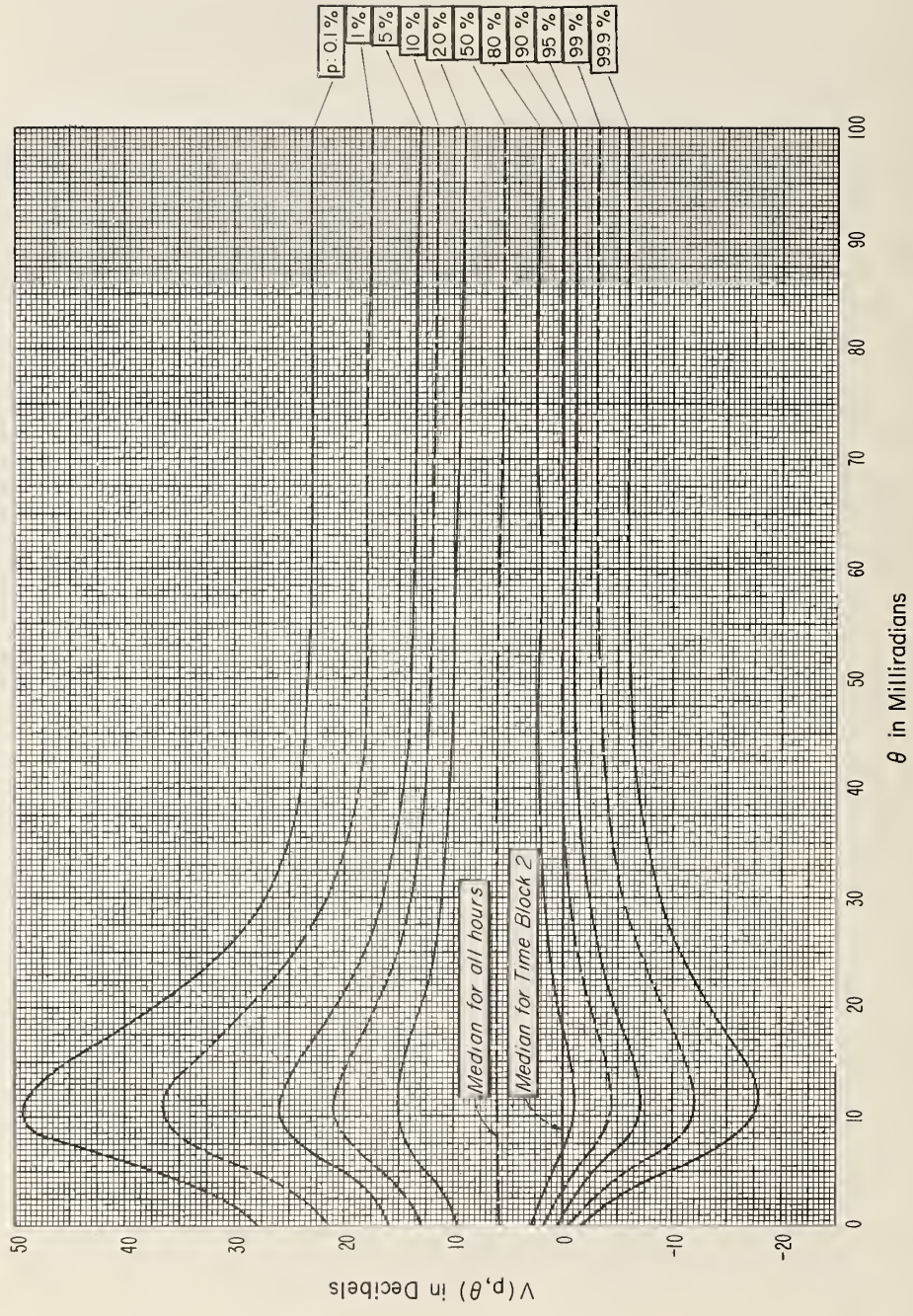
EXPECTED SIGNAL LEVEL, V(p,θ), EXCEEDED BY p PERCENT
OF ALL HOURS, SUMMER
May - October, All Hours
$L_b(p,\theta) = L_{bm} - V(p,\theta)$ decibels
p: 0.1%
1%
5%
10%
20%
50%
80%
90%
95%
99%
99.9%
Median for all hours
Median for Time Block 2
V(p,θ) in Decibels
θ in Milliradians
50
40
30
20
10
0
-10
-20
0
10
20
30
40
50
60
70
80
90
100

Figure 3

percentage of hours p and the path and equipment parameters, or an expression for the predetection hourly median RMS-signal-to-RMS-noise ratio available for p percent of all hours, using a fixed value of transmitter power P_o over the same path. Both results may be obtained for various values of carrier frequency, but for any particular carrier frequency value and a given path the calculated basic transmission loss value L_{bm} and the path antenna gain G_p are constants.

The auxiliary constant K_o is given by:

$$K_o = L_{bm} - G_p - 204 + F + B + L_t, \tag{3}$$

where the symbols on the right-hand side are the same as in (1) and have been defined above. Substituting (3) in (1), and changing notation slightly,

$$P_{tm} = K_o + R_m, \tag{4}$$

where P_{tm} is the transmitter power required to provide the grade of service R_m for the Time Block 2 median hour, as L_{bm} was used in (1) and (3). The relation between the transmitter power $P_t(p)$, exceeded for p percent of all hours and the required power P_{tm} for the Time Block 2 median hour is the same as the relation between the corresponding transmission loss values given in (2a). By a simple substitution,

$$P_t(p) = P_{tm} - V(p) = K_o + R_m - V(p), \tag{5}$$

is obtained, where $P_t(p)$ is the transmitter power required to provide a grade of service, R_m, or better, during p% of all hours.

If, on the other hand, the transmitter power is assumed fixed or predetermined at a value P_o, the predetection hourly median RMS-signal-to-RMS-noise ratio R will exceed R(p) for the percentage of hours or time availability which may be determined from:

$$R(p) = P_o - K_o + V(p) . \qquad (6)$$

Thus, (6) determines the grade of service as a function of time availability. Here the designer is able to determine the grade of service R(p) expected to be exceeded during a given percentage of all hours.

The term "expected" has been used here because of the empirical nature of the prediction formulas, especially of the time variability V(p). For a given set of path and equipment parameters, measurement results may vary substantially from path to path. Average, or statistically expected values are provided by (5) and (6), whereas prediction errors will be taken into account later on.

At this point it is advantageous to illustrate the procedure outlined so far by means of an example. This will also aid in the understanding of the remaining discussion and procedures.

The National Bureau of Standards, at the request of U. S. Air Force agencies, measured transmission loss over a 200-mile path between North Africa and southern Spain during January and February, 1957. This path lends itself well as an illustrative example because of the opportunity to compare the results of the measurements with the original predictions.

The terrain profile for this path is shown on Fig. 4, with the pertinent horizon distances and other important parameters [Rice, Longley, and Norton, 1959] indicated thereon. The communication requirements and applicable equipment specifications for this path are as follows:

System: Quadruple Diversity, Frequency Modulation

Carrier Frequency Range: Optimum between 400 and 2000 Mc/s.

Number of Channels and Modulation Requirements: 24-voice channels, each 4 kc/s wide including guard band. It is assumed that up to 25% of the channels are active simultaneously at any one time, and that two voice channels carry 16 teletype channels each, using standard multiplex methods. The teletype signal utilizes the 5-unit, start-stop code at the rate of 60 words per minute.

Grade of Service Required: Average short-term teletype character error rate of 0.01% or better (not more than 1 in 10,000 character errors), corresponding to an hourly median signal-to-noise ratio of 40 db per cycle of noise bandwidth in the output teletype channel. The corresponding signal-to-noise ratio in the output voice channel is taken as 70.5 db per cycle of noise bandwidth. Both figures apply to a Rayleigh-fading carrier under the assumption of quadruple diversity.

Transmitter Power: Up to 10 kw.

Antenna Sizes: Up to 60-ft. diameter for parabolic reflectors.

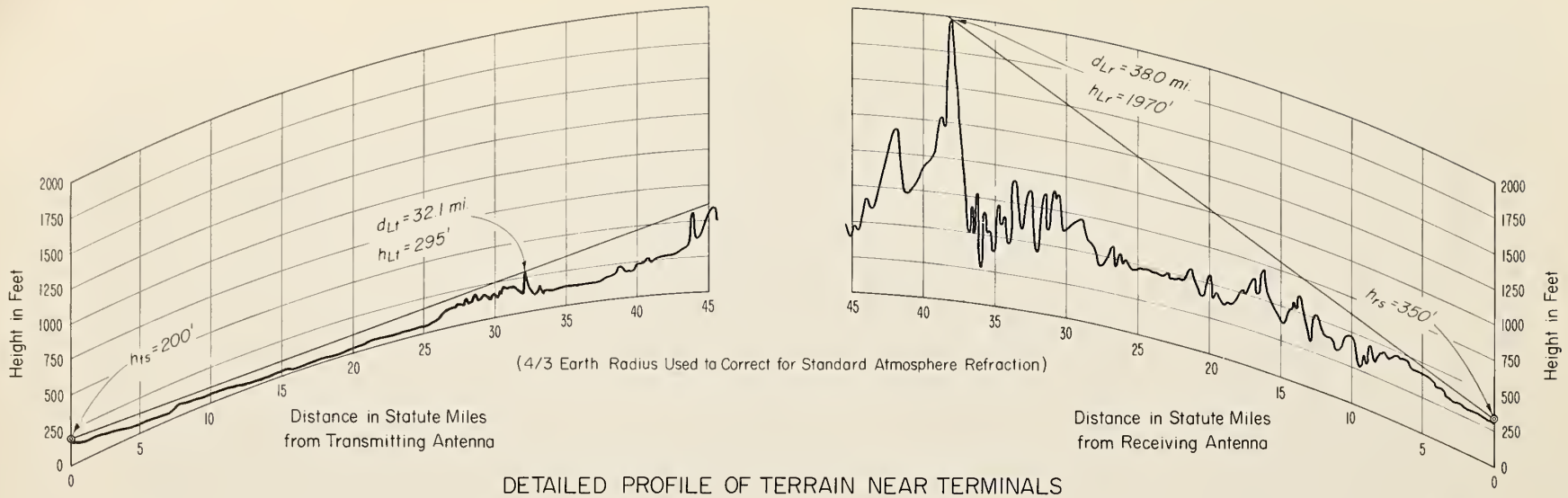

DETAILED PROFILE OF TERRAIN NEAR TERMINALS

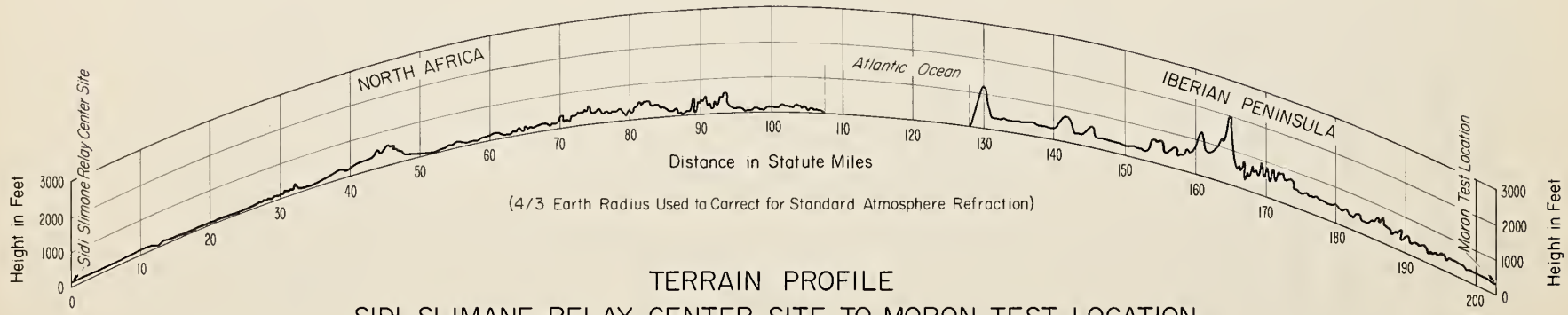

TERRAIN PROFILE
SIDI SLIMANE RELAY CENTER SITE TO MORON TEST LOCATION

Figure 4

Receiver Noise Figure: 2 db over the frequency range considered based on the use of parametric front-ends.

Transmission Line Losses: Based on the use of low-loss concentric lines or wave guide of appropriate dimensions for the frequency considered.

Typical values of line loss and noise figures are given in Table I, below.

TABLE I

Typical Line Loss and Noise Figure Values as Functions of Frequency

Carrier Frequency Mc/s	Effective System Noise Figure, F, db	Transmitting Antenna Line Losses L_t, db
400	3.5	1.5
600	3.8	1.8
800	4.0	2.0
1000	4.5	2.5
2000	4.0*	2.0*

*Assumes use of wave guide.

The effective system noise figure is discussed in Appendix III. For the frequency range considered, external noise contributions can be roughly approximated by setting $f_a = 1$ and if we further assume $f_c = 1$ and $t_t = t_o$, the effective system noise figure F simply exceeds the receiver noise figure F_r by the receiving antenna transmission line loss, $10 \log_{10} \ell_t$, if all quantities are expressed in decibels. For the parametric receiver front-ends specified here the receiver noise figure F_r may be assumed to be

2 db over the entire frequency range and the values of F in Table I were determined on the assumption that the transmission lines at the transmitting and receiving ends of the path introduce the same losses.

For the assumed loading conditions and the specified output signal-to-noise ratios, a functional dependence may be set up between the average short-term teletype error rate and the predetection hourly median RMS-signal-to-RMS-noise ratio R, using the methods given by Florman and Tary [1961]. The results for the specified system of 24-voice channels are shown on Fig. 5 for various assumptions of the deviation ratio. In all cases the width of the base band is assumed to be 108 kc/s. As each deviation ratio corresponds to a definite predetection radio or intermediate frequency channel bandwidth, several curves are shown, each labeled with the total radio frequency bandwidth B expressed in decibels. The possibility of trading off signal-to-noise ratio R for bandwidth B is thereby demonstrated.

The reference value L_{bm} of median basic transmission loss and the path antenna gain G_p have been calculated in this report in accordance with the methods of Rice, Longley, and Norton [1959], using the applicable path parameters and atmospheric constants. This reference value, L_{bm}, is shown as a function of carrier frequency for two given antenna heights on Fig. 6a.

Substitution of all known values including the reference value of basic transmission loss L_{bm} into (1) results in curves of transmitter power versus frequency. These curves are shown on Fig. 6b for two antenna sizes, and the values of R_m = 7.2 db and B = 60.3 db corresponding to a deviation ratio of 2.6 and the 0.01%

TELETYPE ERROR RATE VERSUS PRE-DETECTION CARRIER-TO-NOISE RATIO R FOR 24 VOICE CHANNEL QUADRUPLE DIVERSITY FREQUENCY MODULATION SYSTEMS

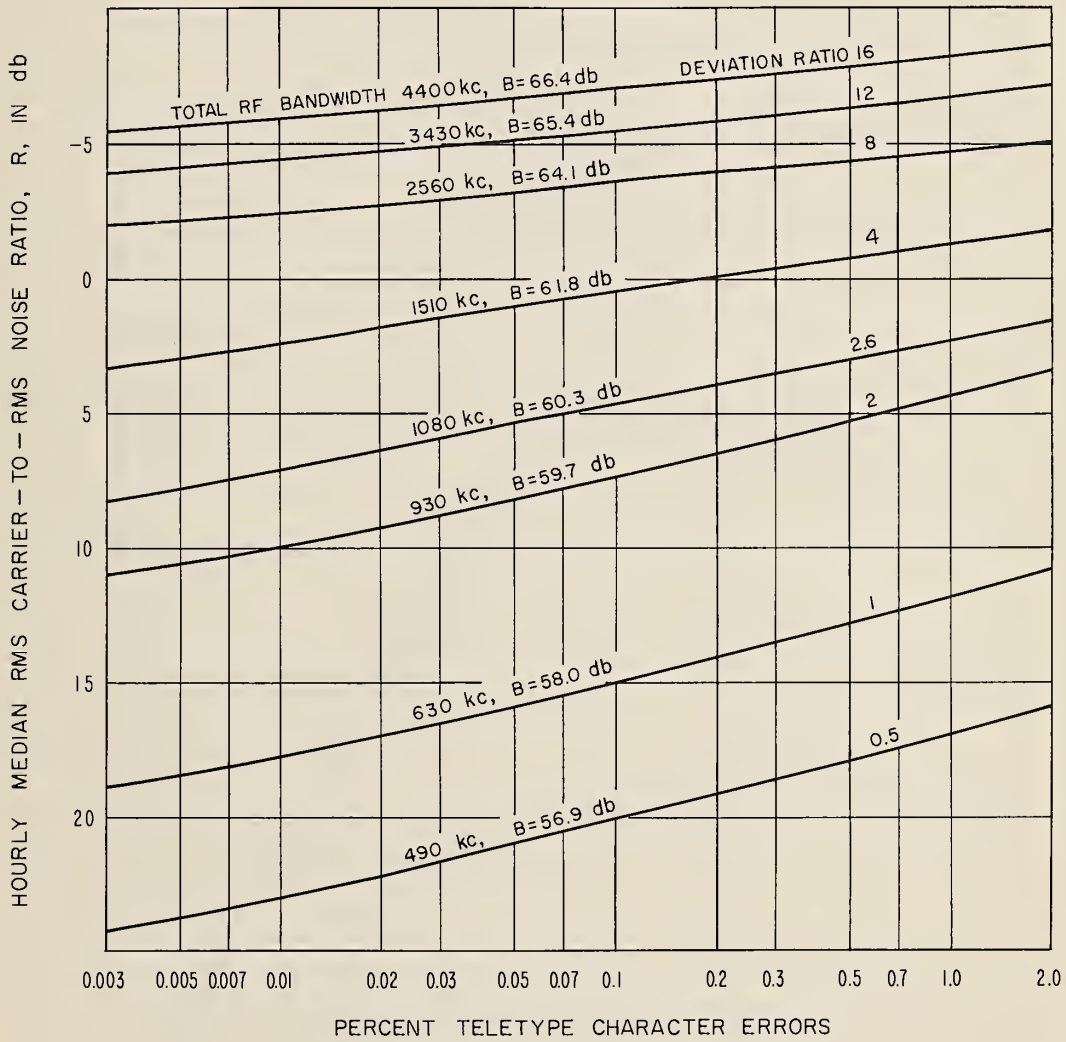

Figure 5

CALCULATED MEDIAN BASIC TRANSMISSION LOSS VERSUS FREQUENCY FOR AVERAGE WINTER AFTERNOON HOURS (TIME BLOCK 2 MEDIANS)

Sample Path Sidi Slimane to Moron

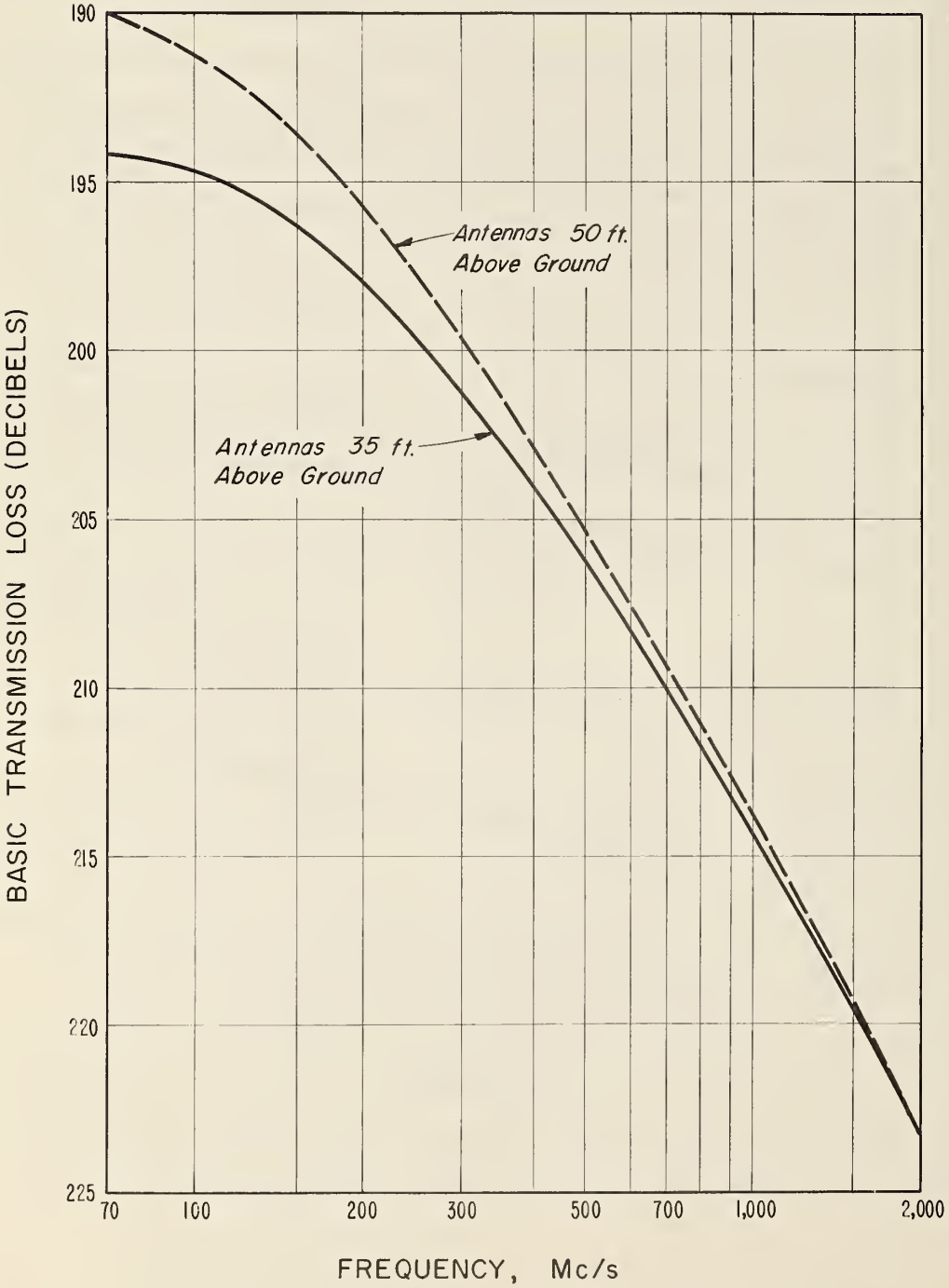

Figure 6a

REQUIRED TRANSMITTER POWER FOR
AVERAGE WINTER AFTERNOON HOURS
(TIME BLOCK 2 MEDIAN) 202.7 Mi. SAMPLE PATH

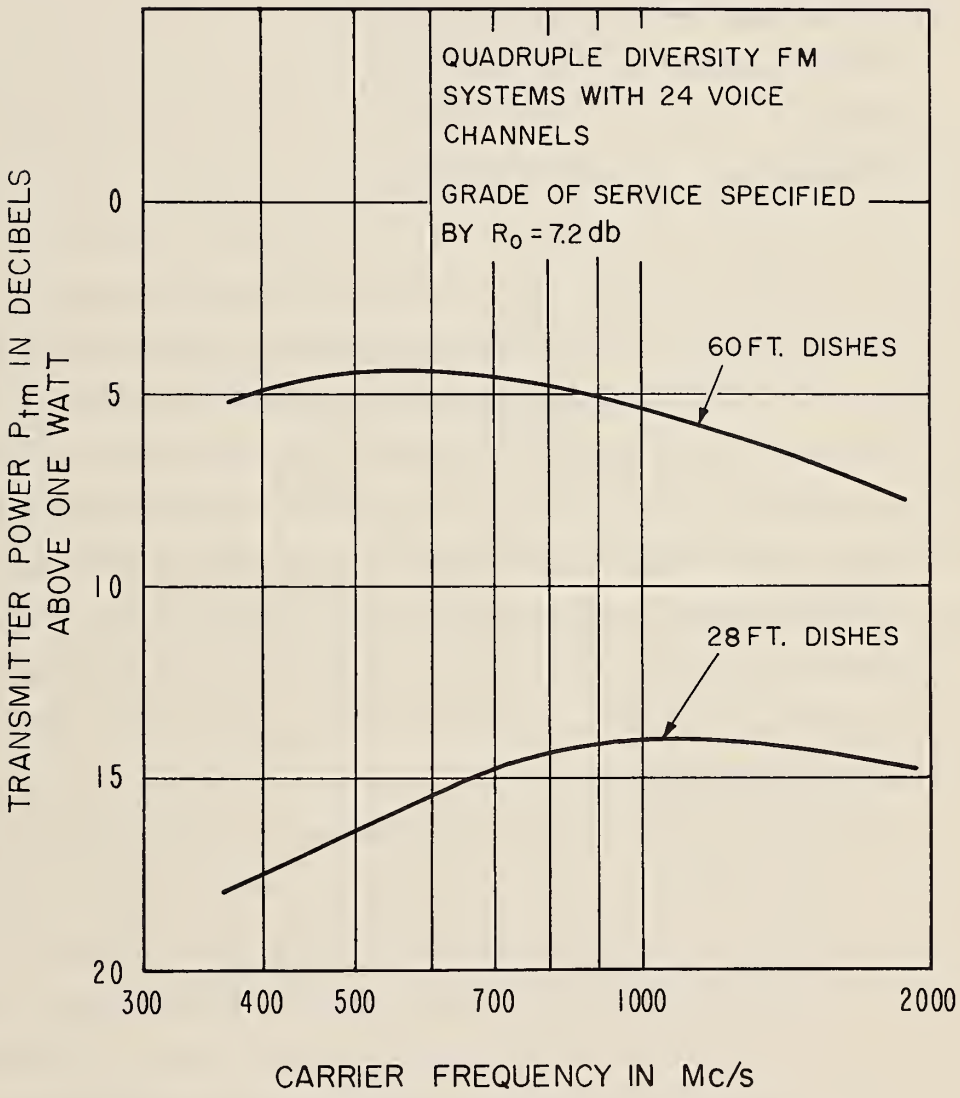

Figure 6b

short-term teletype error rate. The resulting transmitter power values P_{tm} correspond to the reference basic transmission loss value L_{bm}, and thus apply to the median of all Time Block 2 hourly medians; i.e., they are applicable to the average winter afternoon hour, and are not final results. They serve to demonstrate the frequency dependence of the required transmitter power for the given path geometry and equipment parameters.

In comparing Figs. 6a and 6b one should note that the frequency dependence of transmitter power is quite different from the frequency dependence of basic transmission loss alone. This is due to the effects of path antenna gain, and the frequency-dependent equipment parameters. The curves of Fig. 6b permit selection of an optimum frequency, or an optimum frequency range, where P_{tm} is a minimum. The optimum frequency is, of course, usually different for each equipment combination. For the sample path, the optimum frequency is 1050 Mc/s for 28-ft dishes and 550 Mc/s for 60-ft dishes. The example shows (and it is generally true) that the optimum frequency decreases with increasing antenna size. If conventional receiver front-ends are used the optimum frequency would be lowered, as in this case the receiver noise figure also increases with frequency.

In the calculations leading to Fig. 6b, no consideration has been given to the problem of selective fading as a function of carrier frequency. It may be assumed from available data and theoretical studies that the bandwidth of the medium is sufficiently large relative to the highest modulation frequency considered for a path of this type.

From the curves of Fig. 6b, values of transmitter power, P_{tm}, may be determined for any desired frequency range and equip-

ment combination. For the example, the following are chosen in order to conform to the design characteristics of available equipment.

TABLE II

Dish Size	Frequency or Range of Frequencies	Transmitter Power P_{tm}
28 ft	1000-1200 Mc/s	14.1 dbw
60 ft	500-600 Mc/s	4.4 dbw
60 ft	1000 Mc/s	5.4 dbw

It has already been shown, and should be restated here, that the transmitter power value P_{tm} was determined from the median of all Time Block 2 hourly median values; i.e., the value required for the average winter afternoon hour. The constant K_o, and the distribution of all P_{tm} values over the entire year may be obtained by (3) and (6a). The angular distance θ is accurately known (θ = 40.2 milliradians) and the $V(p, \theta)$ curves of Fig. 1 are used to determine the all-day, all-year variability of the hourly medians. The resulting cumulative distributions curves of transmitter power or predetection signal-to-noise ratio are shown on Fig. 7 for the 28-ft antenna size operating in the 1000-1200 Mc/s frequency range.

Fig. 7a indicates the expected value of transmitter power $P_t(p, \theta)$ necessary to provide the specified grade of service (or better) given by R_m = 7.2 db during a given percentage, p, of all hours of the year. Similarly, Fig. 7b shows the expected distribution of the predetection hourly RMS-signal-to-RMS-noise ratio $R(p)$ if the

EXPECTED TIME AVAILABILITY FOR SAMPLE COMMUNICATION CIRCUIT

d = 202.7 mi., θ = 40.2 MILLIRADIANS

QUADRUPLE DIVERSITY FM SYSTEMS ON 1,000-1,200 Mc/s WITH 28 ft. DISHES

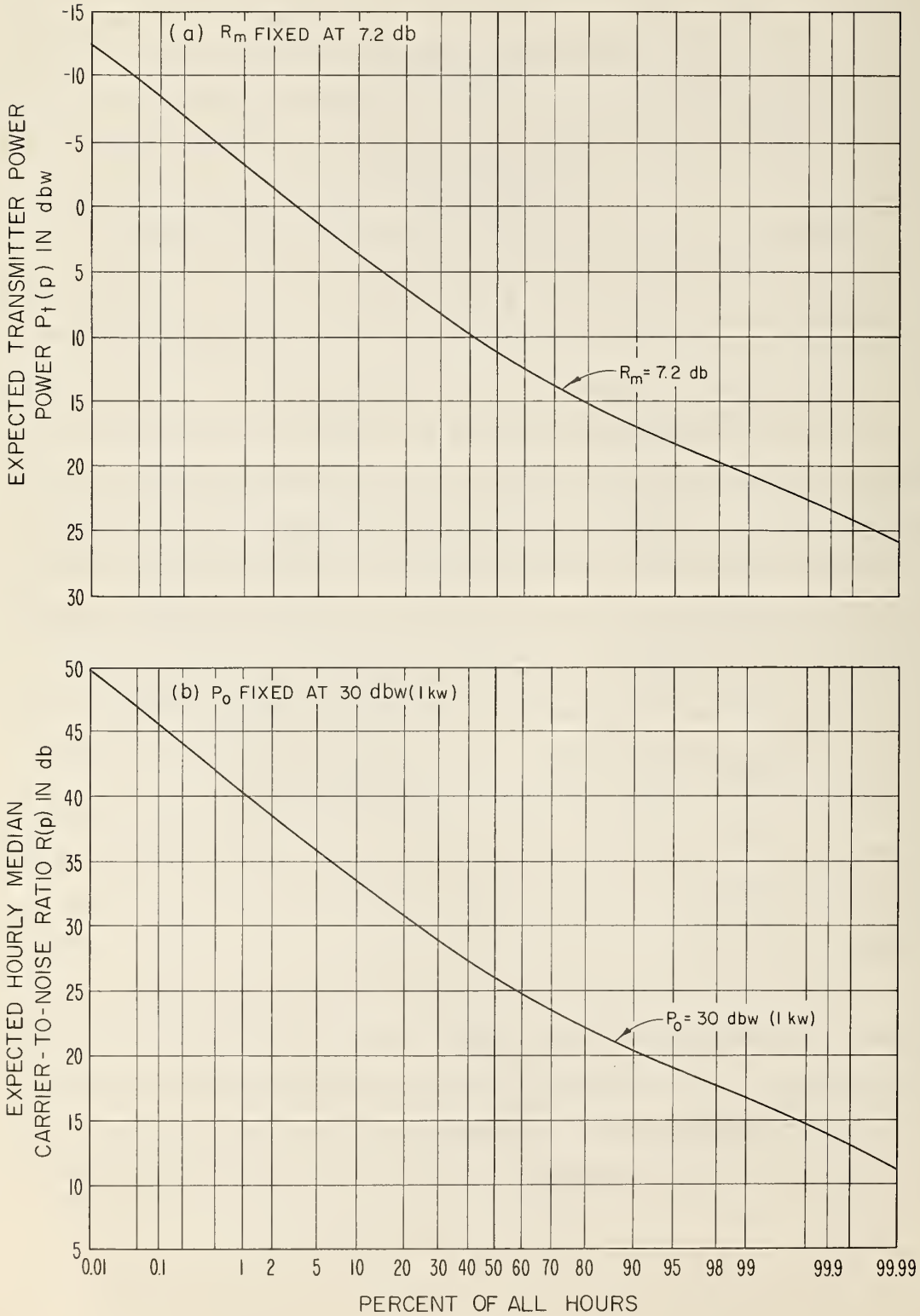

Figure 7

transmitter power is fixed at P_o = 30 dbw (1 kw). The ordinate values on Fig. 7 are clearly labeled "expected values", because they are based, in part, on empirical terms in the prediction formula, and there may be appreciable deviation of predicted from observed values in many cases. It will be shown in the next section how these prediction errors are accounted for in systems design.

3. THE CONCEPT OF SERVICE PROBABILITY

Although Fig. 7a is a graph of time availability versus transmitter power for a specified grade of service, the design problem is still not completely solved. The prediction formula for the hourly median basic transmission loss has empirical terms in it, and its comparison with data shows appreciable deviations of predicted from observed values. There are factors influencing the transmission loss and thus the required transmitter power which are not taken into account by the prediction formula, because it is impractical to allow in more detail for the actual characteristics of the terrain and the atmosphere and because of uncertainty in the estimate of equipment performance terms, especially the predetection hourly median signal-to-noise ratio R_m, which defines the grade of service. Therefore, if a number of tropospheric propagation paths are considered which have identical geometrical and meteorological parameters entering the prediction formula, and result in the same predicted all-day, all-year distribution of hourly median basic transmission loss (or required transmitter power, similar to Fig. 7a), an extensive long-term measurement program of transmission loss, or performance factors, for all those similar paths would result in a range of all-day, all-year distributions as well as in a range for the long-term overall medians rather than in a single result.

Fig. 8 illustrates the concept of service probability. The heavy dashed curve shows the calculated value $L_{bc}(p)$ of basic transmission loss expected to be exceeded by (100 - p) per cent of observed hourly median values L_{bo}. For the same set of values of prediction parameters such as angular distance and frequency, the lighter solid curves show "true" infinite-time cumulative distributions $L_{bo}(p)$ versus p for six randomly different paths. It is assumed that values $L_{bo}(p)$ are normally distributed with a variance $\sigma_c^2(p)$, which depends upon p, about the calculated value $L_{bc}(p)$, as explained in Appendix I. It is shown, there, for instance, that the prediction uncertainty for winter afternoon median values may be characterized by a standard deviation $\sigma_c = 3.57$ db, independent of the angular distance, θ.

In order to obtain values of standard deviation which are applicable to all hours of the year, and for percentage points other than the median, a substantial number of available field strength measurements have been analyzed, as described in more detail in Appendix I. This analysis constitutes a first estimate in the evaluation of a difficult statistical problem and results in standard deviation values $\sigma_c(p)$ which characterize the prediction uncertainty for p% of all hours of the year. Curves of $\sigma_c(p)$ versus p are shown by the dashed curve on Fig. 9. The estimation of $\sigma_c(p)$ is based upon predictions using the time availability functions $V(p, \theta)$, depending on the angular distance θ; the values of $\sigma_c(p)$ so obtained, however, are also considered to be applicable to predictions based upon the time availability functions $V(p, d)$.

The uncertainty in estimating the equipment performance parameters F (effective noise figure) and R_m (predetection hourly

TYPICAL PATH-TO-PATH VARIATION OF INFINITE-TIME DISTRIBUTIONS
FOR A SINGLE SET OF VALUES OF THE PREDICTION PARAMETERS

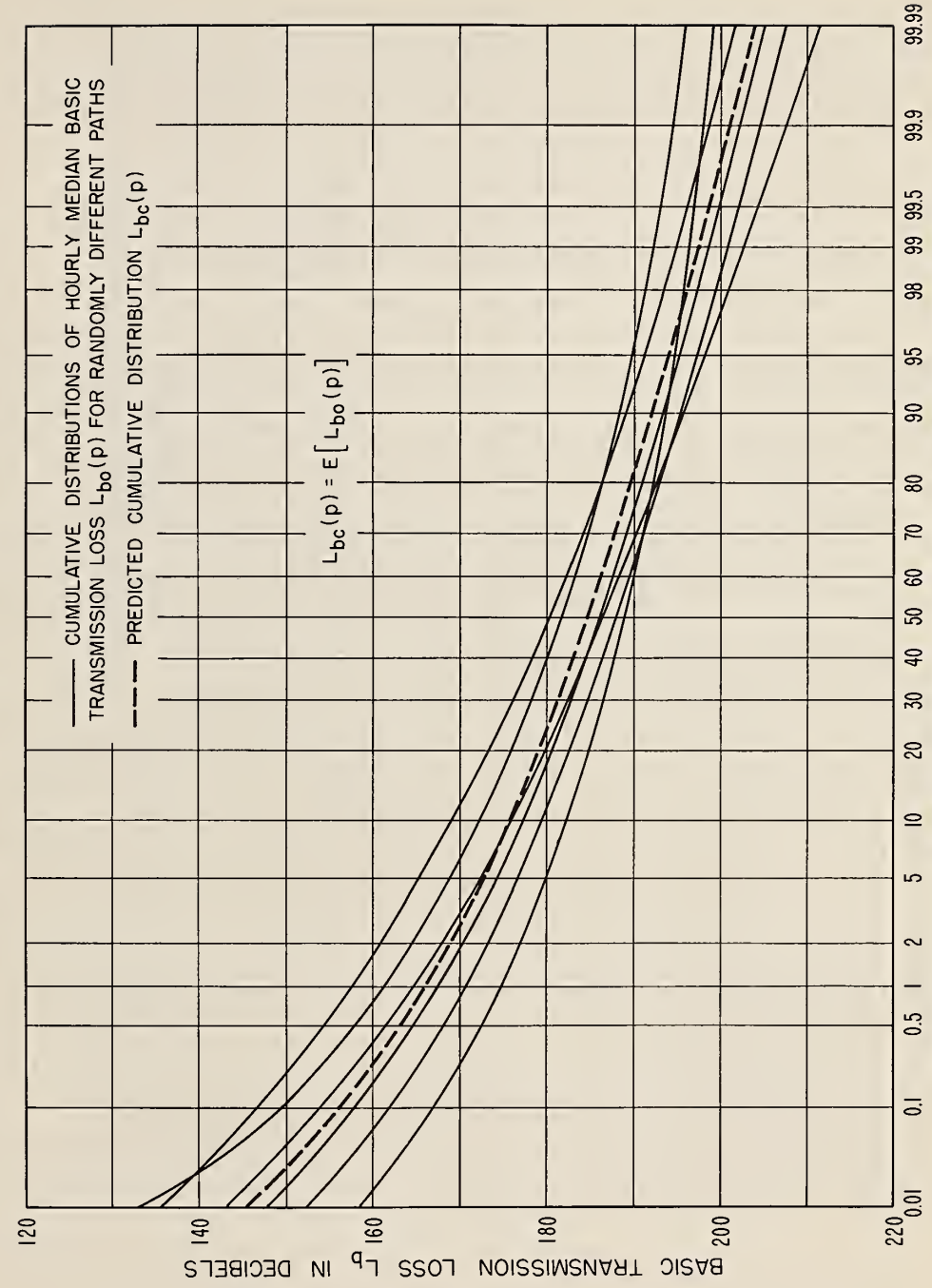

Fig. 8

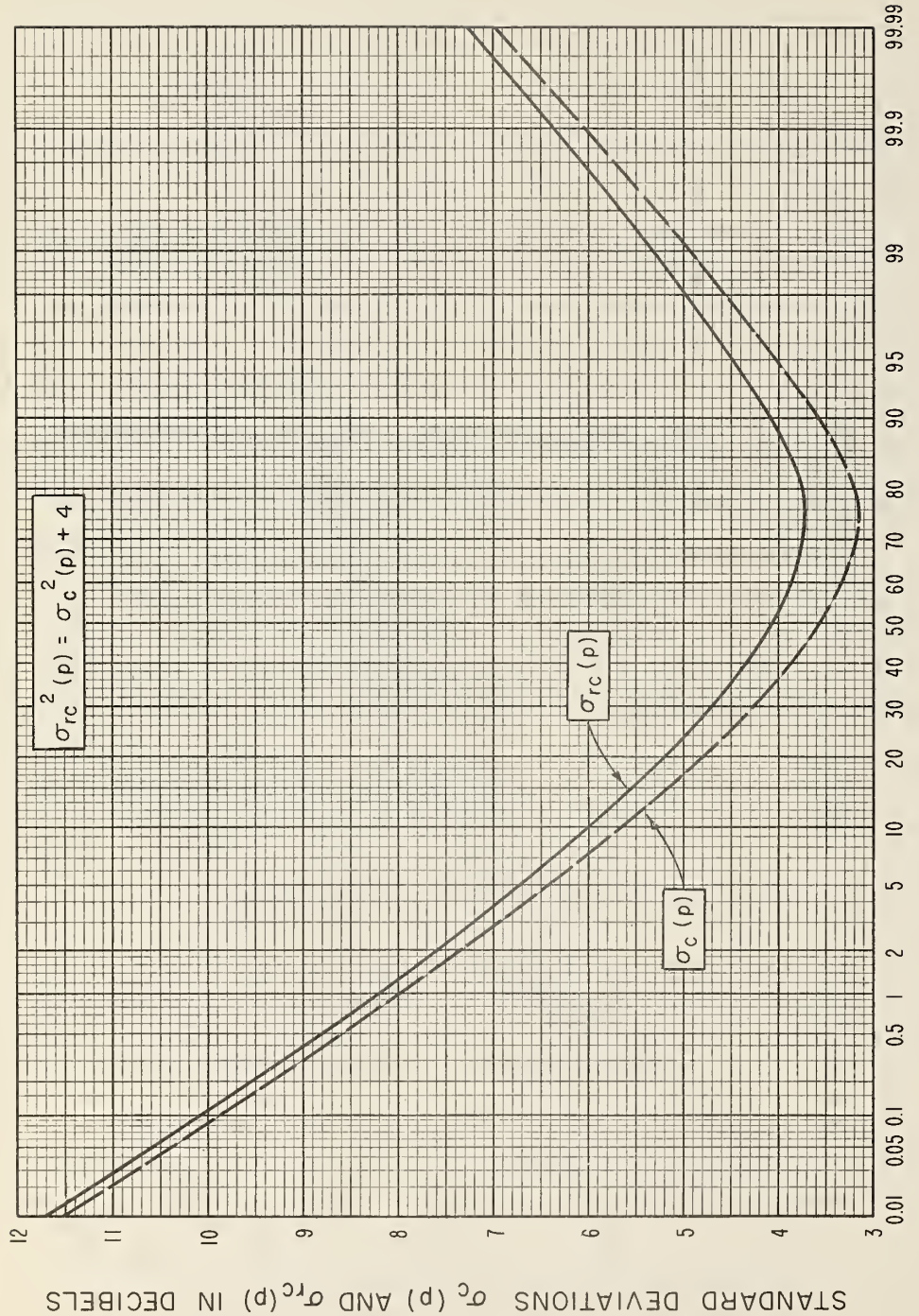
$\sigma_{rc}^2(p) = \sigma_c^2(p) + 4$
$\sigma_{rc}(p)$
$\sigma_c(p)$
STANDARD DEVIATIONS $\sigma_c(p)$ AND $\sigma_{rc}(p)$ IN DECIBELS
PERCENT OF ALL HOURS OF THE YEAR
12
11
10
9
8
7
6
5
4
3
0.01
.005
0.1
0.5
1
2
5
10
20
30
40
50
60
70
80
90
95
99
99.9
99.99

Figure 9

median RMS-signal-to-median-RMS-noise ratio required) is expressed by a standard deviation σ_r which has somewhat arbitrarily been taken to be equal to 2 db in the absence of sufficient test data. The total prediction uncertainty for p% of all hours may thus be characterized by a standard deviation $\sigma_{rc}(p)$, which is given by

$$\sigma_{rc}^2(p) = \sigma_c^2(p) + \sigma_r^2 \qquad (7)$$

under the reasonable assumption that the variables concerned are uncorrelated. See Fig. 9.

Prediction uncertainty is defined in terms of the probability of obtaining a specified grade of service or better for a given percentage of time. This is a measure of the chance of success for a particular path, and is termed "service probability". Values of service probability are obtained by combining the all-day, all-year distribution of expected transmitter power or carrier-to-noise ratio values (Fig. 7) with the standard deviation $\sigma_{rc}(p)$ as shown below. The method is based on the assumption that the errors are normally distributed. Service probability $F(t)$ lies between zero and one; an "expected value" $E[L_o(p)] = L_c(p)$ corresponds to $F(t) = 0.5$, and a normally satisfactory allowance for errors will be made by setting $F(t) = 0.95$.

For a fixed R_m, the system power $P[F(t), p]$ required to provide the specified grade of service or better during p% of all hours with the probability $F(t)$ may now be related to the expected value of system power $P[0.5, p] \equiv P_t(p)$ by

$$P[\,F(t),p\,] = P[\,0.5,p\,] + t \cdot \sigma_{rc}(p) \qquad (8)$$

where

$$F(t) = \frac{1}{\sqrt{2\pi}} \int_{-\infty}^{t} \exp(-z^2/2)\, dz \qquad (9)$$

$F(t)$, as stated above, is the service probability, t is the standard normal deviate, while $\sigma_{rc}(p)$ is defined by (7). The time distribution of the expected transmitter power $P[0.5,p\,] \equiv P_t(p)$ is determined by the $V(p,\theta)$ curves of Figs. 1, 2, and 3.

As service probability calculations usually are made for a specific path, the parameter θ is not necessary any more for identification, and has been dropped in (8). However, a new parameter, namely $F(t)$, has been added in order to identify clearly the value of service probability considered. A value of the service probability $F(t) = 0.5$ corresponds to the statistically expected value, which has formed the basis for calculations up to now. For $F(t) = 0.5$, the standard normal deviate t is zero, and (8) reduces to an identity, as it should.

Depending on whether R_m or P_o is considered fixed, (5) and (6) may now be generalized to include the prediction uncertainty term $t \cdot \sigma_{rc}(p)$ as follows:

$$P[\,F(t),p\,] = R_m + K_o - V(p,\theta) + t \cdot \sigma_{rc}(p) \qquad (10a)$$

$$R[\,F(t),p] = P_o - K_o + V(p,\theta) - t \cdot \sigma_{rc}(p) \qquad (10b)$$

These equations are now complete expressions either for the required transmitter power with a given R_m or for the predetection hourly median RMS-signal-to-RMS-noise ratio with a given P_o, taking into account the prediction uncertainty associated with a given percentage of hours, or time availability, p.

4. SERVICE PROBABILITY CALCULATIONS

For purpose of illustration, the sample path data will be used again. Let it be required to calculate the power P(0.95, 99%) for the same equipment parameters as were used for drawing Fig. 7a (28-ft dishes on 1000-1200 Mc/s). This amount of power would provide the specified grade of service (with R_m = 7.2 db) during 99% of all hours with a 0.95 probability of success. This number, 0.95, means that out of, say, 100 paths all having the same parameters, 95 would be expected to provide the specified grade of service or better during 99% of all hours, and 5 would probably fail to do so. In other words, the designer takes a risk corresponding to the probability that 5 out of 100 (or 1 out of 20) similar paths might fail to perform as required.

The power P(0.95, 99%) is determined from (8) by reading the value P(0.5, 99%) = 20.5 db from the curve of Fig. 7a, and adding to it the term $t \cdot \sigma_{rc}(99\%)$ which, in this case, is the product $1.645 \times 5.35 = 8.8$ db. The value $\sigma_{rc}(99\%)$ is read from Fig. 9 while $t = 1.645$ for $F(t) = 0.95$ is obtained from probability tables [Bennett and Franklin, 1954]. The result, in this case, is 29.3 dbw for the transmitter power P(0.95, 99%).

Table III, below, shows additional values of t for various service probabilities F(t), as taken from probability tables in Bennett and Franklin [1954].

TABLE III

F(t)	t
0.50	0
0.70	0.524
0.90	1.282
0.95	1.645
0.98	2.054
0.99	2.326
0.995	2.576
0.998	2.878
0.999	3.090

For service probabilities less than 50%, t is negative and

$$F(-t) = 1 - F(t) \tag{11}$$

By choosing several values for F(t), the time availability graphs of Fig. 7 may be augmented. The curves drawn originally were for F(t) = 0.50, or t = 0. New curves for any desired value of F(t) may be obtained by substitution into (10a) or (10b). Fig. 10 shows the results for the sample path with the values for F(t) = 0.90, 0.95, and 0.99, added to the original curves of Fig. 7. It is seen from the upper graph (a) that more power is needed if values of service probability F(t) > 0.5 are taken into account. Similarly, from the lower graph (b), the hourly median predetection RMS-signal-to-RMS-noise ratio R expected to be exceeded with the probability F(t) for a fixed transmitter power P_o is substantially reduced when values of F(t) > 0.5 are considered.

TIME AVAILABILITY FOR SAMPLE COMMUNICATION CIRCUIT
AT VARIOUS VALUES OF SERVICE PROBABILITY

d = 202.7 mi., θ = 40.2 MILLIRADIANS

QUADRUPLE DIVERSITY FM SYSTEMS ON 1,000-1,200 Mc/s WITH 28 ft. DISHES

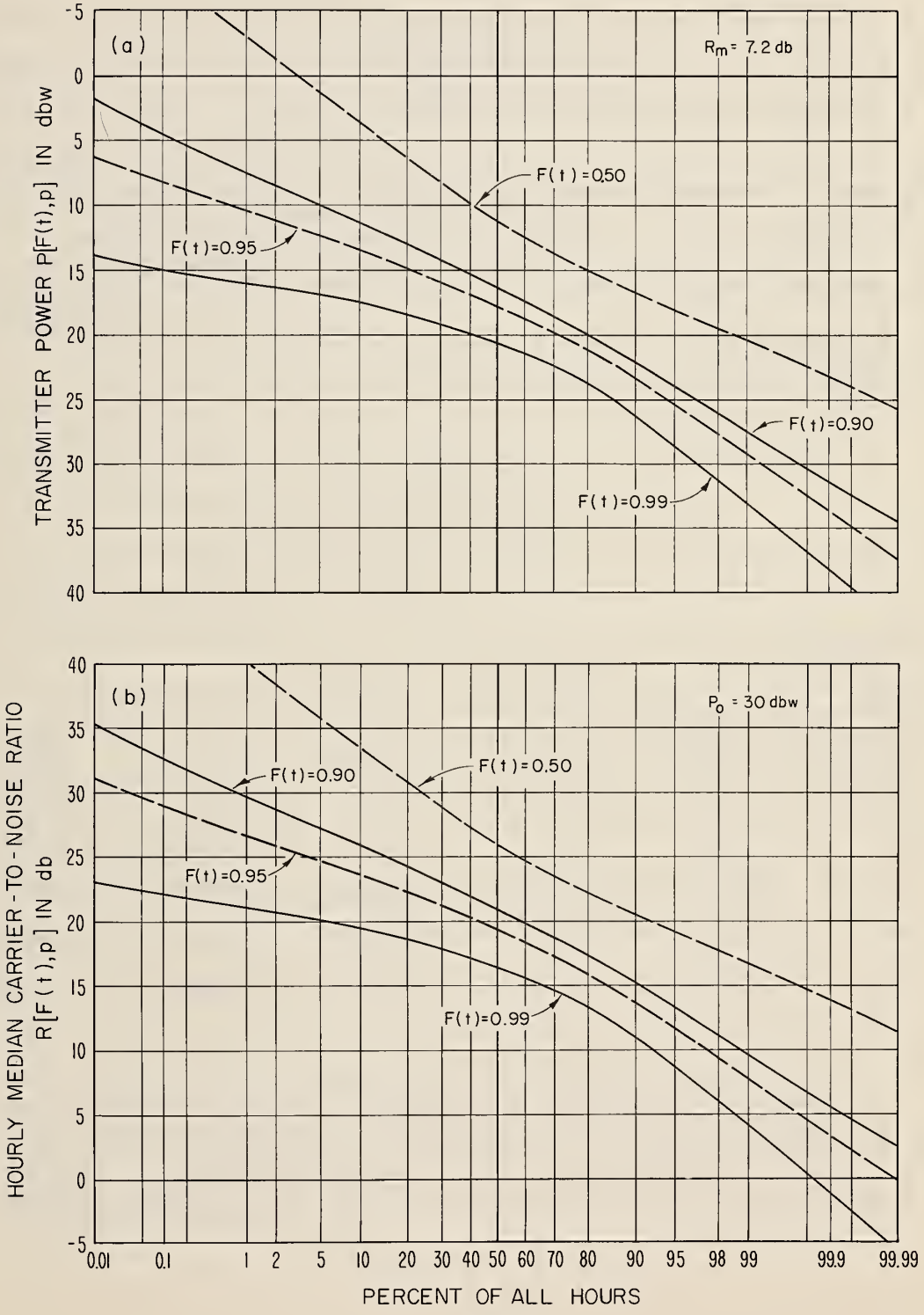

FIGURE 10

It is also possible to determine the service probability F(t) as a function of p for fixed values of both R_m and P_o by setting $P[F(t), p] = P_o$ in (8) and solving for t:

$$t = \frac{P_o - P(0.5, p)}{\sigma_{rc}(p)} \tag{12}$$

Note that t is simply a function of p and $\sigma_{rc}(p)$ and that F(t) can be determined from t using the appropriate probability tables [Bennett and Franklin, 1954]. As an example, Table IV gives the calculations of F(t) versus p for P_o = 30 dbw with 28-ft dishes at 1000-1200 Mc/s, using the sample path.

TABLE IV

Service Probability Calculations

(1)	(2)	(3)	(4)	(5)	(6)
Time Availability, p, in percent of all hours	P(0.5,p) in db	P_o-P(0.5,p) in db	$\sigma_{rc}(p)$ in db	t	F(t)
99.99	25.7	4.3	7.28	0.590	0.722
99.9	23.3	6.7	6.35	1.056	0.854
99	20.5	9.5	5.35	1.776	0.962
95	18.1	11.9	4.49	2.65	0.9960
90	16.1	13.4	4.09	3.28	0.99948

The values in Column (2) of Table IV were determined from Fig. 7a, while the values in Column (4) were determined from Fig. 9. Column (5) is obtained by dividing (4) into (3), and (6) is obtained

from (5) by the use of the table of standard normal deviates. The resulting values of $F(t)$ may now be plotted as abscissa values to the ordinates p on a double probability display, and the points connected by a smooth curve, as shown on Fig. 11. This is an additional way of presenting the service probability-time availability relation, using a fixed value of transmitter power and a fixed value of hourly median carrier-to-RMS-noise ratio in addition to the other fixed parameters of the path and the system. This form of presentation shows how time availability and service probability may be traded off.

If the term $P_o - P(0.5, p)$ is negative, t will be negative and the corresponding values of $F(t)$ will be less than 0.5. Using Bennett and Franklin [1954], the values in the column headed $1 - F(t)$ are applicable in this case, as shown by (11).

The smooth curves drawn on Fig. 11 are the final results of the study and represent the relationship between service probability and the time availability for the specified grade of service. Besides the system used for the example, calculations were made for other system combinations and the resulting service probability curves are also shown on Fig. 11. The intersection of the curve marked 60 ft dishes - 1000 Mc/s - 1 kw with the 99.9% ordinate, for example, determines an abscissa service probability value of 0.990. This is the probability that the specified grade of service or better will be obtained during 99.9% of all hours by the use of the 1000 Mc/s-60 ft dishes 1 kw transmitter power combination. It may also be seen that by lowering the carrier frequency to the 600 Mc/s range and for the same 1 kw value of transmitter power the probability of obtaining the specified grade of service or better during 99.9% of all hours is increased to 0.9955.

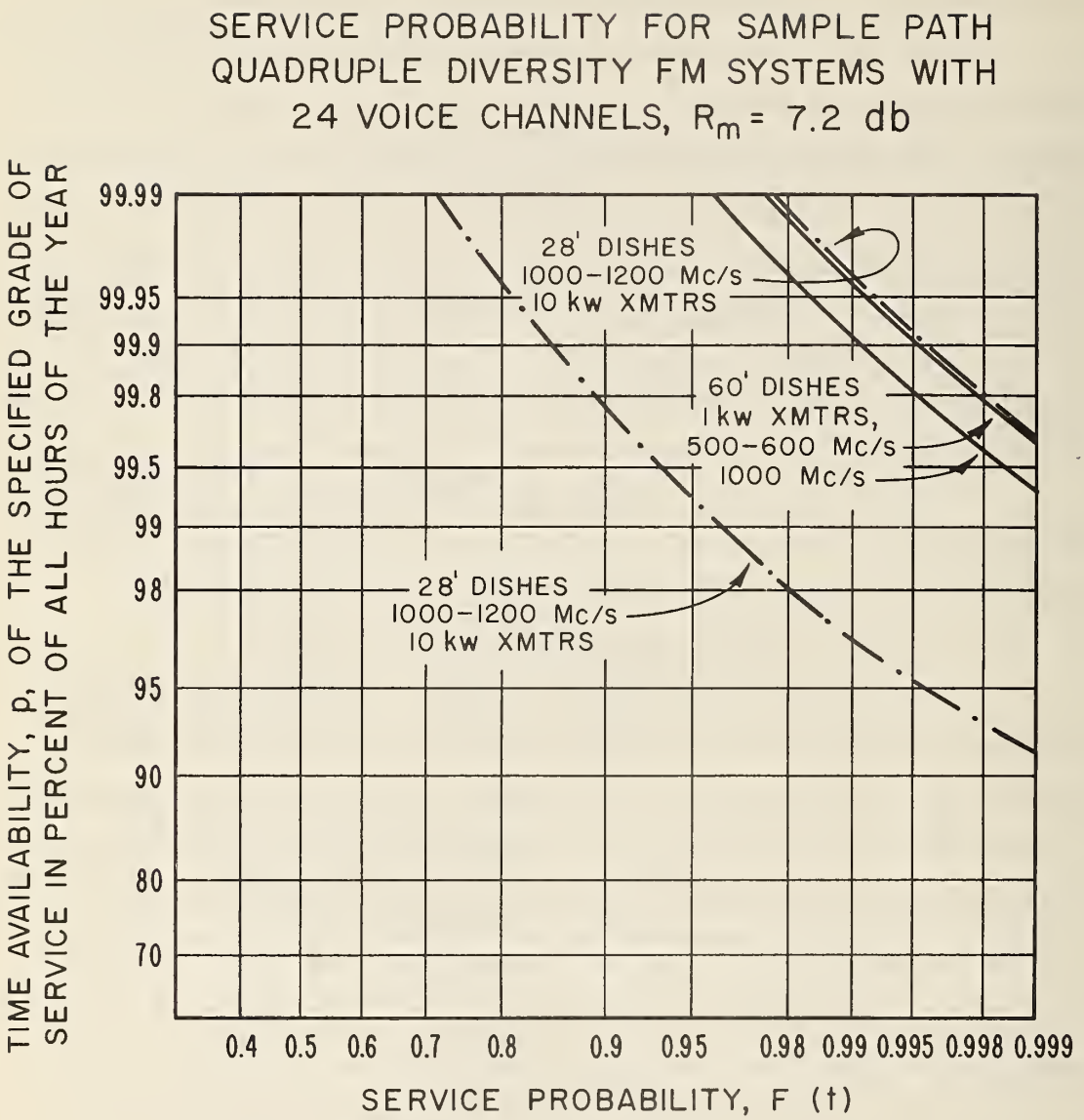
SERVICE PROBABILITY FOR SAMPLE PATH
QUADRUPLE DIVERSITY FM SYSTEMS WITH
24 VOICE CHANNELS, R_m = 7.2 db
TIME AVAILABILITY, p, OF THE SPECIFIED GRADE OF SERVICE IN PERCENT OF ALL HOURS OF THE YEAR
99.99
99.95
99.9
99.8
99.5
99
98
95
90
80
70
28' DISHES
1000–1200 Mc/s
10 kw XMTRS
60' DISHES
1 kw XMTRS,
500–600 Mc/s
1000 Mc/s
28' DISHES
1000–1200 Mc/s
10 kw XMTRS
0.4 0.5 0.6 0.7 0.8 0.9 0.95 0.98 0.99 0.995 0.998 0.999
SERVICE PROBABILITY, F (t)

Figure 11

Each of the curves on Fig. 11 may be labeled with a dollar tag denoting cost of installation, operation, and maintenance; thus an estimate may be made of the additional cost necessary to obtain a greater probability of success; i.e., an increase from a 0.854 to a 0.9955 probability shown for 28-ft dishes at 99.9% time availability is obtained by increasing the transmitter power from 1 to 10 kw. This means that the additional installation and operational expenses "buy" a better chance of obtaining the desired results. Fig. 11 shows also that for this particular path an increase in antenna size to 60 ft provides essentially the same probability value as a transmitter power increase from 1 to 10 kw with 28-ft dishes; thus the costs for the two possibilities may be compared on the basis of the service probability values read from the curves.

The entire risk versus cost picture is provided by diagrams such as Fig. 11 and this makes possible an intelligent determination of the best system to employ. For example, in some cases it may be desirable to install a lower powered system with the knowledge that inadequate performance which might occur by chance with this lower power can later be improved by the addition of a power amplifier.

5. PERFORMANCE OF A CHAIN OF SYSTEMS OPERATING IN TANDEM

In this section consideration will be given to the method of calculation of the performance expected when two or more systems are operated in tandem. Under these circumstances teletype or other errors tend to add as the signal is transmitted via the successive links in the chain, and, as a consequence, the performance of

the chain will always be somewhat inferior to the performance over the poorest of its individual links. It would be possible to determine the error rate over the chain at a particular time, e.g., for a period of one hour, by an appropriate combination of the error rates of the individual links for that hour. Then the final performance would have to be determined by an appropriate statistical combination of each of these hourly values, making appropriate allowance for the fact that the fading would occur more or less independently on the separate links. Fortunately the performance can be evaluated adequately and much more directly in terms of the concept of the time availabilities on the several links, and this will be the approach adopted here.

It will be convenient to express the time availability, p_i, on the i^{th} link in terms of a probability $p_i' \equiv (100 - p_i)/100$ of not obtaining a given grade of service R_m, or better, over that link for a specified long period of time; this is usually taken to be all hours of the year. The value of p_i may be determined for the i^{th} link from the equation:

$$V(p_i, \theta_i) = K_{oi} + R_m - P_{ti} \qquad (13)$$

where K_{oi} denotes the value of K_o, as given by (3), for the i^{th} link and P_{ti} denotes the transmitter power for the i^{th} link. The value of p_i is determined, for the given value of $V(p_i, \theta_i)$, by interpolation from the appropriate graphs on Figs. 1, 2, or 3. In carrying out this interpolation it will be desirable to plot $V(p_i, \theta_i)$ vs. p_i' for the angular distance θ_i corresponding to the i^{th} link; for example, see Fig. 12.

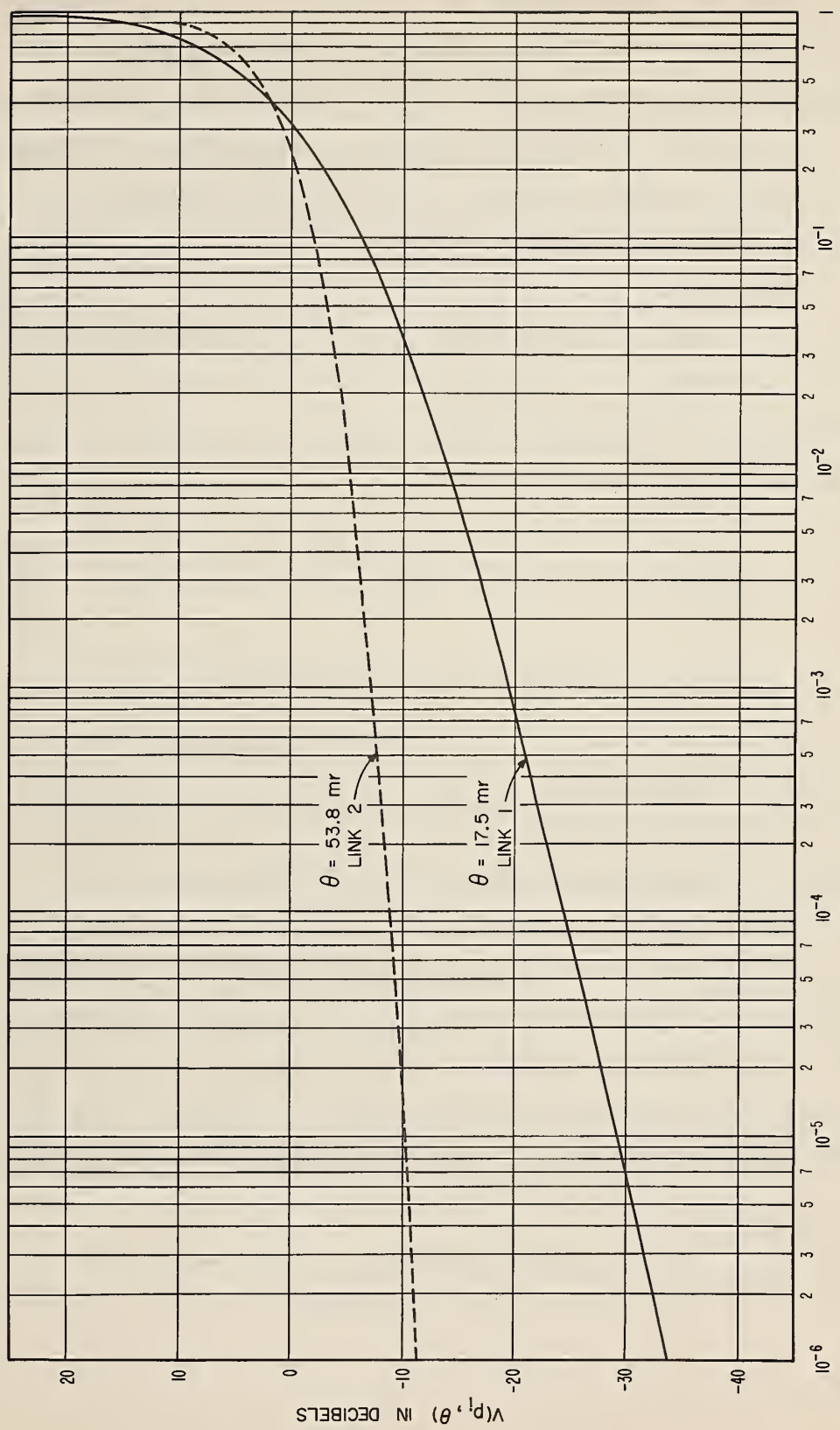
EXAMPLE OF CALCULATING TANDEM SERVICE PROBABILITY:
TIME AVAILABILITY CURVES FOR INDIVIDUAL LINKS
V(p_i', θ) IN DECIBELS
20
10
0
-10
-20
-30
-40
θ = 53.8 mr
LINK 2
θ = 17.5 mr
LINK 1
10^-6
10^-5
10^-4
10^-3
10^-2
10^-1
1
p_i' = (100 - p_i)/100

Figure 12

First the case of two links operating in tandem will be considered. Let p_1' and p_2' denote the probabilities of not obtaining the grade of service, R_m, or better, over each of these links considered separately. The general theory of probabilities of combined events [Feller, 1950, page 13] may be used for obtaining the probability p_c' of not obtaining the grade of service R_m, or better, over the chain of two links in tandem. Let A_1 and A_2 denote the events of not obtaining the grade of service R_m, or better, over the first and second links, respectively. Now the probability $P(A_1 \text{ or } A_2)$ of not obtaining the grade of service R_m, or better, over the chain of two links is given by:

$$P(A_1 \text{ or } A_2) = P(A_1) + P(A_2) - P(A_1 \text{ and } A_2) \qquad (14)$$

$P(A_1 \text{ or } A_2)$, $P(A_1)$ and $P(A_2)$ may be readily identified with p_c', p_1', and p_2', respectively,* and it remains to discuss $P(A_1 \text{ and } A_2)$. It will be convenient to think of $P(A_1 \text{ and } A_2)$ now as the fraction of the time that the grade of service is worse than R_m on both links at the same time. Without loss of generality, we will assume that $P(A_2) \leq P(A_1)$; now it follows that the maximum value of $P(A_1 \text{ and } A_2)$ is equal to $P(A_2)$, and the minimum value of $P(A_1 \text{ and } A_2)$ is the larger of the two values $[P(A_1) + P(A_2) - 1]$ or zero. If the fading is well correlated on the two paths, service failures A_1 and A_2 will tend to occur at the same times, and $P(A_1 \text{ and } A_2)$ will then approach the value $P(A_2)$. On the other hand, if enhanced signals occur on the

*The identification of p_c' with $P(A_1 \text{ or } A_2)$ is only approximate, but, as will be discussed below, introduces negligible error in practice.

first link whenever fades occur on the second link, $P(A_1 \text{ and } A_2)$ approaches $[P(A_1) + P(A_2) - 1]$ or zero, whichever is the larger. Thus, regardless of the nature of the fading, the following inequality is obtained:

$$p'_1 \leq p'_c \leq \text{The smaller of } p'_1 + p'_2 \text{ or } 1 \quad (\text{where } p'_2 \leq p'_1) \qquad (15)$$

In terms of time availabilities, the above may be written:

$$\text{The larger of } 0 \text{ or } (p_1 + p_2 - 100) \leq p_c \leq p_1 \quad (\text{where } p_1 \leq p_2) \qquad (16)$$

The above results may easily be generalized to n links:

$$\text{The larger of } 0 \text{ or } \sum_{i=1}^{n} p_i - 100(n-1) \leq p_c \leq p_s \qquad (17)$$

Here p_s denotes the smallest of the n time availabilities. Note that the inequality (17) contains a quantitative formulation of the conclusion, stated without proof at the beginning of this section, that the performance p_c of the chain will be at best somewhat worse than the performance of its poorest link. As an example of the use of the above general formula, a chain of four links will be assumed with time availabilities, as determined by (13), equal to $p_1 = 99\%$, $p_2 = 98\%$, $p_3 = 97\%$ and $p_4 = 98\%$. It follows from (17) that the expected time availability, p_c, of service of grade R_m, or better, at the end of the chain of these four links will satisfy the following inequality:

$$92\% \leq p_c \leq 97\% \qquad (18)$$

The above inequality is valid for any possible correlations between the occurrences of the fading on the four links; if the fading tended to occur simultaneously on the four links, i.e., with large positive correlations between the transmission losses on these links, then p_c would be nearer to 97% whereas, if there were no overlap in the long-term fading on the four links, i.e., with large negative correlation between the transmission losses on these links, then p_c would be nearer to 92%. In most cases in practice the correlation in the fading on the several links would be expected to be somewhat positive. However, in the case of a line-of-sight link and an adjacent beyond-the-horizon link, the correlation between the variations in the transmission losses on the two links might well be found to be negative.

It seems most likely that the correlations in the transmission losses on the several links would not be very large, either positive or negative, and thus we are led to examine the case of zero correlation, i.e., the assumption that the long-term variations occur independently on the several links. Consider first the case of a chain of only two links. In this case of independent long-term variations in the hourly medians:

$$P(A_1 \text{ and } A_2) = P(A_1) \cdot P(A_2) \tag{19}$$

Using the above, the following expression is obtained from (14):

$$p'_c = p'_1 + p'_2 - p'_1 p'_2 \tag{20}$$

Note that the assumption of independence in the long-term variations yields an explicit formula for p'_c rather than an inequality. Since the long-term variations would be expected to occur more or less independently on the several links of a chain, (20) will be adopted as the best readily available estimate of the probability, p'_c of not obtaining a given grade of service R_m, or better, over a chain of two links; the corresponding best estimate of the time availability is given by $p_c = 100\,(1 - p'_c)$.

In order to generalize (20) to a chain of n links, the following product will be used which is applicable to the case of independent fading:

$$P(A_1 \text{ and } A_2 \text{ and } \ldots A_i \ldots \text{and } A_n) = P(A_1) \cdot P(A_2) \ldots P(A_i) \ldots P(A_n) \tag{21}$$

Using (21) in a general formula for combining events given by Feller [1950, page 61], the following expression is obtained for a chain of n links:

$$p'_c = S_1 - S_2 + S_3 - S_4 + - \ldots \pm S_n \tag{22}$$

$$S_1 = \Sigma p'_i,\ S_2 = \Sigma p'_i p'_j,\ S_3 = \Sigma p'_i p'_j p'_k,\ \ldots \tag{23}$$

The S_i given above refer only to the case of independent events. Here $i < j < k \ldots \leq n$, so that in the sums each combination appears once and only once; hence S_r has $\{n(n-1)\ldots(n-r+1)\}$ / $\{1.2\ldots(r-1)\cdot r\}$ terms. The last sum S_n reduces to the

single term $p'_1 \cdot p'_2 \ldots p'_n$ which is the probability of the simultaneous realization of all n independent events. As an example, the above formula will be applied to the same chain of four links discussed above. For this chain $p'_1 = 0.01$, $p'_2 = 0.02$, $p'_3 = 0.03$, and $p'_4 = 0.02$; $S_1 = 0.08$, $S_2 = 0.0023$, $S_3 = 0.000028$, and $S_4 = 0.00000012$, and thus:

$$p'_c = 0.08 - 0.0023 + 0.000028 - 0.00000012 = 0.07772788 \quad (24)$$

From this it follows that the best estimate of the time availability at the end of this particular chain of four links is expected to be $p_c = 100(1 - p'_c) = 92.227212\%$. As discussed above, it is more likely that the correlation of the fading on the several links will be somewhat positive rather than negative, and this would lead to a slightly larger value of p_c; thus the use of (24) normally leads to a slightly conservative estimate of the time availability for the chain.

If it is found that the time availability for the chain is too small, then it will be necessary to improve one or more or all of the individual links in order to increase p_c to a satisfactory level. In general it will be best to improve the poorest of the n links first, since this will usually yield the largest increase in p_c for a given expenditure.

It was indicated that A_1 and A_2 denote the events of not obtaining the grade of service R_m, or better, over the first and second links, respectively, and then $P(A_1 \text{ or } A_2)$ was identified with the probability p'_c of not obtaining the grade of service R_m, or better, over the chain of two links in tandem, i.e., it was assumed in effect that the grade of service R_c for the chain is exactly the

same as the grade of service R_m achieved on each link independently. This is an extremely good approximation, but is not quite exact for the following reason. Suppose that the required grade of service R_m corresponds to an 0.01% teletype error rate. As the received signals fade up and down on the two links, the hourly median signal-to-noise ratios R_1 and R_2 on these two links will also vary. Now the error rate for the chain for any given hour is approximately the sum of the error rates corresponding to R_1 and R_2; since the short-term fading will be independent, the chain error rate would be given by $100\epsilon_c = 100(\epsilon_1 + \epsilon_2 - \epsilon_1 \cdot \epsilon_2)$ and, for small error probabilities ϵ_1 and ϵ_2, the term $\epsilon_1\epsilon_2$ is negligible. It is seen that $100\epsilon_c$ can deviate from the larger of the two link error rates at most by a factor of two, i.e., when $R_1 = R_2$. Thus for a particular hour such that $R_1 = R_2 = R_m$, the error rate for the chain would be 0.019999% rather than the design value of 0.01%. Reference to Fig. 5 shows that a change of error rate from 0.01% to 0.02% corresponds to a change in R_m of the order of one decibel so that R_c should be about one decibel greater than R_o if R_1 and R_2 were not varying. However, since R_1 will nearly always be substantially different from R_2, because of the fading, the net error in identifying $P(A_1 \text{ or } A_2)$ with p'_c will be a very small fraction of one decibel, depending on the magnitudes of the long-term fading ranges on the two links, and may be neglected for all practical purposes. To the degree that one may neglect the above-described small correction, it follows that this analysis concerns only the variability of the hourly transmission loss medians rather than the variability of signal-to-noise ratios. Consequently, to this same degree, it is immaterial in estimating the time availability for the chain whether the noise is

removed at a relay station (as in the case of teletype transmissions), or the entire modulation of signal plus noise is re-transmitted.

The time availability $p_c = 100\,(1 - p'_c)$ determined for the chain of n links in tandem from the value of p'_c given by (22) is the expected value corresponding to $F(t) = 0.5$, and it is still necessary to consider the influence of the errors of estimation as measured by the variances $\sigma^2_{rc}(p_i)$ for the n separate links, and thus to determine p_c for various values of the service probability $F(t)$. A precise formulation of this problem will be given showing how a solution may be obtained in practice. However, the solution obtained is somewhat tedious to use, and the reader may well decide to forego the luxury of such a solution and to settle instead for the expected time availability p_c for the chain of n links in tandem, together with the graphs of time availability versus service probability for the n individual links.

It will now be shown how the cumulative distribution of the time availability, p_c, versus service probability is determined for a chain of n links in tandem. In what follows it will be assumed that the errors of estimation for the individual paths, as measured by the variances $\sigma^2_{rc}(p_i)$, are independent from one link to the next. We first determine p'_i versus $F(t)$ for each of the n links separately and then determine for each link m different values of p'_{ik} corresponding to $F(t_k) = (2k - 1)/2m$, $k = 1$ to m. These values p'_{ik} may be read off the graphs of p'_i versus $F(t)$ or may be determined by the inverse solution of the equation:

$$t_k = \{V(p_{ik}, \theta_i) - V(p_i, \theta_i)\} / \sigma_{rc}(p_{ik}), \qquad (25)$$

where $V(p_i, \theta_i)$ is the expected value of $V(p, \theta)$ for path i. For this expected value, $F(t_k) = 0.5$ and $t_k = 0$.

Next the p'_{ik}, k = 1 to m, are reordered at random for each value of i from i = 2 to n. This reordering can be accomplished by using (n - 1) sets of random numbers [Rand Corporation, 1955]. For each value of k, p'_{ck} may be calculated by means of (22). The corresponding values of p_{ck} are finally rearranged in order of decreasing magnitude so that $p_{c_1} \geq p_{c_2} \geq \ldots p_{cj} \ldots \geq p_{cm}$ and plotted versus

$$F_j(t) = (2j - 1)/2m. \tag{26}$$

This is the desired approximate relation between p_c and F(t), and should be reasonably reliable for j less than m-4 or m-5. For instance, for m = 100, the time availability p_c corresponding to a tandem service probability $F_{95}(t) = 0.945$ is the smallest value of p_c for which a good estimate of service probability is provided by this method.

In order to illustrate the calculation of tandem service probability for two links, an example is chosen for which values of θ, K_o, P_o, and R_m are listed in Table V.

TABLE V

Circuit Parameters		Link 1	Link 2
Angular distance, θ	:	17.5 mr	53.8 mr
Auxiliary constant, K_o	:	-5.7 db	16.1 db
Transmitter power, P_o	:	30 dbw	47 dbw
Signal-to-noise ratio, R_m	:	8.0 db	13.5 db
$V(p_i, \theta_i)$ for $F(t) = 0.5$	:	-27.7 db	-17.4 db

Fig. 12 shows $V(p_i, \theta_i)$ for the two links, $i = 1$ and $i = 2$, plotted versus $p'_i \equiv (100 - p_i)/100$. The calculation scheme is set up in Table VI as follows: Column 2 shows 100 values of $F(t_k)$ evenly spaced between 0 and 1, and Column 3 shows the corresponding values of the standard normal deviate t_k, determined from probability tables such as those given by Bennett and Franklin [1954]. The curves on Fig. 13 show $p_{1k} = 100\,(1 - p'_{1k})$ plotted versus $F(t_{1k})$ and $p_{2k} = 100\,(1 - p'_{2k})$ plotted versus $F(t_{2k})$; these curves are simply the service probability curves for the individual links, similar to those shown for a different path on Fig. 11. Now, columns 4 and 5 of Table VI list values of p'_{1k} and p'_{2k} corresponding to the values of $F(t_k)$ from Column 2 and corresponding to the curves of Fig. 13.

Next it is necessary for p'_{1k} and p'_{2k} to be placed in a random relative order. The order of p'_{1k} as given in Column 4 is left unchanged. The index k from Column 1 is reordered, using a table of randomly ordered two-digit numbers [Rand Corporation, 1955], uniformly distributed between 00 and 99 with no repetitions. Column 6 shows the corresponding randomly reordered values p'_{2k} from Column 5. The randomly ordered values of p_{ck} in Column 7 are obtained as $p_{ck} = 100\,(1 - p'_{ck})$, where p'_{ck} is given by (20), the special case of (22) appropriate for $n = 2$. Arranging these same values p_{ck} in descending order, they were relabeled p_{cj} in Column 8 of Table VI and plotted versus $F(t_k)$ in Fig. 13. The circled dots in Fig. 13 show the tandem service probability corresponding to the random ordering shown in Column 6 of Table VI, and the x's in Fig. 13 represent a second estimate obtained by the same

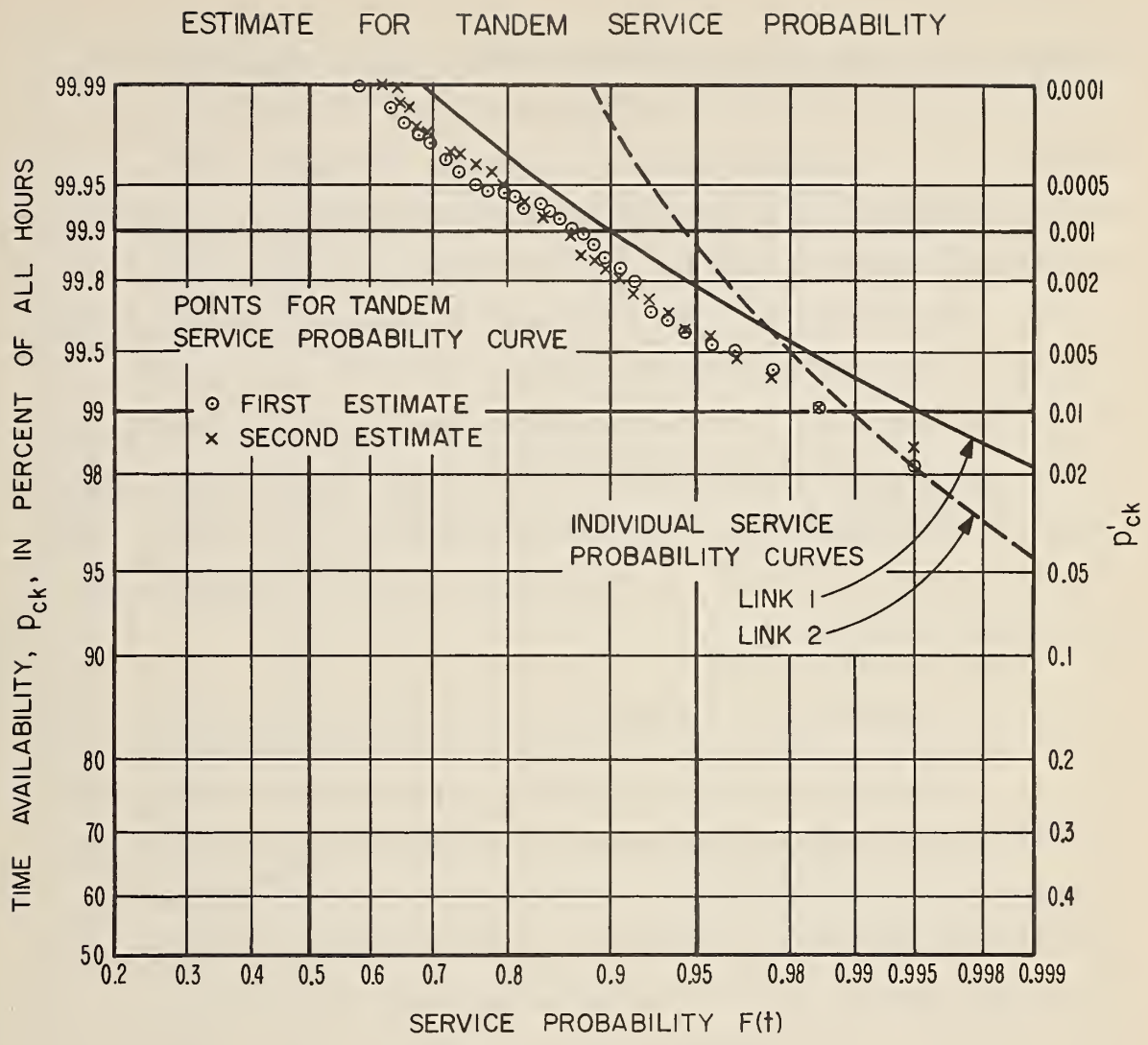
ESTIMATE FOR TANDEM SERVICE PROBABILITY
TIME AVAILABILITY, p_{ck}, IN PERCENT OF ALL HOURS
99.99
99.95
99.9
99.8
99.5
99
98
95
90
80
70
60
50
0.0001
0.0005
0.001
0.002
0.005
0.01
0.02
0.05
0.1
0.2
0.3
0.4
p'_{ck}
POINTS FOR TANDEM SERVICE PROBABILITY CURVE
⊙ FIRST ESTIMATE
× SECOND ESTIMATE
INDIVIDUAL SERVICE PROBABILITY CURVES
LINK 1
LINK 2
0.2
0.3
0.4
0.5
0.6
0.7
0.8
0.9
0.95
0.98
0.99
0.995
0.998
0.999
SERVICE PROBABILITY F(t)

Figure 13

method with another set of random numbers used to reorder the p'_{2k} values. Note that, for all values of F(t), p_{ck} must be less than p_{ik} (i = 1 to n) and, as a consequence, the one x and one o at F(t) = 0.995 are clearly in error. The p'_{ck} ordinate scale corresponding to the tandem time availability values p_{ck} is indicated on the right hand side of Fig. 13.

As noted before, the tandem service probability estimates of Fig. 13 are reliable only for values of F(t) less than about 0.945. An increase in m would extend the range of reliability. The example given corresponded to n = 2; the extension to n links involves the addition of m randomly reordered values of p'_{ik} for each value of i = 3 to n and then the use of (22) to calculate the m values of p'_{ck}.

6. PREDICTION IMPROVEMENT BY MEASUREMENTS

In preceding sections a method was presented enabling the engineer to evaluate his performance predictions for a tropospheric communication circuit in terms of the service probability concept. Service probability has been defined as the probability of obtaining a specified grade of service or better during a given percentage of hours within a specified time period, usually taken to be all the hours of the year. Basically, the service probability concept takes into account the uncertainties contained in the prediction process. These uncertainties are represented by the standard deviation $\sigma_{rc}(p)$ of a normal distribution of prediction errors. The standard deviation, $\sigma_{rc}(p)$, includes a term $\sigma_c(p)$ for errors in the estimate of transmission loss, as well as a term σ_r which allows for uncertainties in estimating equipment characteristics such as the noise figure F

Table VI

Tabulations of the Numerical Values Required to Determine Chain Reliability p_c vs Service Probability F(t) for Two Links in Tandem

k	$F(t_k)$	Increasing Order t_k	Increasing Order p'_{1k}	Increasing Order p'_{2k}	Randomly Reordered p'_{2k}	Random Order p_{ck}	Decreasing Order p_{cj}
1	0.005	-2.576	0	0	0	100	100
2	0.015	-2.170	0	0	0	100	100
3	0.025	-1.960	0	0	0	100	100
4	0.035	-1.812	0	0	0	100	100
5	0.045	-1.695	0	0	0	100	100
6	0.055	-1.598	0	0	2.7 (-7)	100	100
7	0.065	-1.514	0	0	1.0 (-7)	100	100
8	0.075	-1.440	0	0	0	100	100
9	0.085	-1.372	1.7 (-8)	0	0	100	100
10	0.095	-1.311	2.6 (-8)	0	0	100	100
11	0.105	-1.254	3.8 (-8)	0	0	100	100
12	0.115	-1.200	5.2 (-8)	0	0	100	100
13	0.125	-1.150	7.4 (-8)	0	0	100	100
14	0.135	-1.103	9.4 (-8)	0	0	100	100
15	0.145	-1.058	1.3 (-7)	0	0	100	100
16	0.155	-1.015	1.7 (-7)	0	4.6 (-5)*	100	100
17	0.165	-0.974	2.1 (-7)	0	0	100	100

* 4.6 (-5) is the same as 4.6×10^{-5}.

Table VI (cont'd)

k	$F(t_k)$	Increasing Order t_k	Increasing Order p'_{1k}	Increasing Order p'_{2k}	Randomly Reordered p'_{2k}	Random Order p_{ck}	Decreasing Order p_{cj}
18	0.175	-0.935	2.8 (-7)	0	0	100	100
19	0.185	-0.896	3.3 (-7)	0	1.8 (-2)	98.200	100
20	0.195	-0.860	4.1 (-7)	0	0	100	100
21	0.205	-0.824	5.0 (-7)	0	0	100	100
22	0.215	-0.789	6.0 (-7)	0	0	100	100
23	0.225	-0.755	7.2 (-7)	0	0	100	100
24	0.235	-0.722	8.4 (-7)	0	0	100	100
25	0.245	-0.690	9.6 (-7)	0	0	100	100
26	0.255	-0.659	1.1 (-6)	0	0	100	100
27	0.265	-0.628	1.3 (-6)	0	1.8 (-6)	100	100
28	0.275	-0.598	1.5 (-6)	0	6.6 (-4)	99.934	100
29	0.285	-0.568	1.7 (-6)	0	0	100	100
30	0.295	-0.539	2 (-6)	0	7.6 (-6)	99.999	100
31	0.305	-0.510	2.3 (-6)	0	0	100	100
32	0.315	-0.482	2.6 (-6)	0	0	100	99.999
33	0.325	-0.454	3 (-6)	0	0	100	99.999
34	0.335	-0.426	3.3 (-6)	0	0	100	99.999
35	0.345	-0.399	3.8 (-6)	0	2.2 (-4)	99.978	99.999
36	0.355	-0.372	4.7 (-6)	0	0	99.999	99.999
37	0.365	-0.345	5 (-6)	0	0	99.999	99.999

Table VI (cont'd)

k	$F(t_k)$	Increasing Order t_k	Increasing Order p'_{1k}	Increasing Order p'_{2k}	Randomly Reordered p'_{2k}	Random Order p_{ck}	Decreasing Order p_{cj}
38	0.375	-0.319	5.4 (-6)	0	7.1 (-3)	99.290	99.999
39	0.385	-0.292	6.2 (-6)	0	0	99.999	99.999
40	0.395	-0.266	7 (-6)	0	0	99.999	99.999
41	0.405	-0.240	7.7 (-6)	0	0	99.999	99.999
42	0.415	-0.215	8.6 (-6)	0	1.3 (-4)	99.999	99.999
43	0.425	-0.189	9.6 (-6)	0	0	99.999	99.999
44	0.435	-0.164	1.1 (-5)	0	0	99.999	99.998
45	0.445	-0.138	1.2 (-5)	0	0	99.999	99.998
46	0.455	-0.113	1.4 (-5)	0	0	99.999	99.998
47	0.465	-0.088	1.5 (-5)	0	0	99.999	99.997
48	0.475	-0.062	1.6 (-5)	0	3.7 (-3)	99.628	99.997
49	0.485	-0.038	1.8 (-5)	0	1.7 (-7)	99.998	99.997
50	0.495	-0.013	1.9 (-5)	0	0	99.998	99.997
51	0.505	0.013	2.2 (-5)	0	5.3 (-6)	99.997	99.996
52	0.515	0.038	2.4 (-5)	0	0	99.998	99.996
53	0.525	0.063	2.6 (-5)	0	4 (-7)	99.997	99.995
54	0.535	0.088	2.9 (-5)	0	0	99.997	99.993
55	0.545	0.113	3.2 (-5)	0	1.6 (-8)	99.997	99.993
56	0.555	0.138	3.5 (-5)	0	0	99.996	99.992
57	0.565	0.164	3.8 (-5)	0	0	99.996	99.990

Table VI (cont'd)

k	$F(t_k)$	Increasing Order t_k	Increasing Order p'_{1k}	Increasing Order p'_{2k}	Randomly Reordered p'_{2k}	Random Order p_{ck}	Decreasing Order p_{cj}
58	0.575	0.189	4.2 (-5)	0	3.4 (-5)	99.992	99.989
59	0.585	0.215	4.6 (-5)	0	0	99.995	99.988
60	0.595	0.240	5 (-5)	0	6.6 (-5)	99.988	99.988
61	0.605	0.266	5.6 (-5)	0	1.6 (-5)	99.993	99.988
62	0.615	0.292	6.2 (-5)	0	6.1 (-5)	99.988	99.987
63	0.625	0.319	6.6 (-5)	0	0	99.993	99.986
64	0.635	0.345	7.4 (-5)	0	1.6 (-4)	99.977	99.984
65	0.645	0.372	8 (-5)	0	0	99.992	99.981
66	0.655	0.399	8.8 (-5)	0	2.2 (-5)	99.989	99.978
67	0.665	0.426	9.6 (-5)	1.6 (-8)	4.5 (-4)	99.945	99.977
68	0.675	0.454	1.0 (-4)	3.1 (-8)	0	99.990	99.977
69	0.685	0.482	1.2 (-4)	6.4 (-8)	0	99.988	99.975
70	0.695	0.510	1.3 (-4)	1.0 (-7)	0	99.987	99.973
71	0.705	0.539	1.4 (-4)	1.7 (-7)	5.6 (-7)	99.986	99.970
72	0.715	0.568	1.5 (-4)	2.7 (-7)	1.1 (-5)	99.984	99.967
73	0.725	0.598	1.7 (-4)	4.0 (-7)	1.5 (-3)	99.833	99.963
74	0.735	0.628	1.9 (-4)	5.6 (-7)	1.3 (-6)	99.981	99.958
75	0.745	0.659	2.0 (-4)	8.2 (-7)	3.1 (-4)	99.949	99.955
76	0.755	0.690	2.3 (-4)	1.3 (-6)	0	99.977	99.950
77	0.765	0.722	2.5 (-4)	1.8 (-6)	9.8 (-4)	99.976	99.949
78	0.775	0.755	2.7 (-4)	2.5 (-6)	0	99.973	99.945

Table VI (cont'd)

k	$F(t_k)$	Increasing Order t_k	Increasing Order p'_{1k}	Increasing Order p'_{2k}	Randomly Reordered p'_{2k}	Random Order p_{ck}	Decreasing Order p_{cj}
79	0.785	0.789	3.0 (-4)	3.6 (-6)	0	99.970	99.945
80	0.795	0.824	3.3 (-4)	5.3 (-6)	8.2 (-7)	99.967	99.945
81	0.805	0.860	3.7 (-4)	7.6 (-6)	0	99.963	99.938
82	0.815	0.896	4.2 (-4)	1.1 (-5)	2.5 (-6)	99.958	99.934
83	0.825	0.935	4.5 (-4)	1.6 (-5)	6.4 (-8)	99.955	99.933
84	0.835	0.974	5.0 (-4)	2.2 (-5)	0	99.950	99.931
85	0.845	1.015	5.5 (-4)	3.4 (-5)	0	99.945	99.923
86	0.855	1.058	6.2 (-4)	4.6 (-5)	0	99.938	99.914
87	0.865	1.103	6.9 (-4)	6.1 (-5)	3.1 (-8)	99.931	99.903
88	0.875	1.150	7.7 (-4)	6.6 (-5)	0	99.923	99.890
89	0.885	1.200	8.6 (-4)	1.1 (-4)	0	99.914	99.876
90	0.895	1.254	9.7 (-4)	1.6 (-4)	0	99.903	99.857
91	0.905	1.311	1.1 (-3)	2.2 (-4)	0	99.890	99.832
92	0.915	1.372	1.2 (-3)	3.1 (-4)	3.6 (-6)	99.876	99.800
93	0.925	1.440	1.4 (-3)	4.5 (-4)	0	99.857	99.700
94	0.935	1.514	1.7 (-3)	6.6 (-4)	0	99.832	99.628
95	0.945	1.598	2.0 (-3)	9.8 (-4)	0	99.800	99.620
96	0.955	1.695	2.4 (-3)	1.5 (-3)	2.3 (-3)	99.532	99.532
97	0.965	1.812	3.0 (-3)	2.3 (-3)	0	99.700	99.509
98	0.975	1.960	3.8 (-3)	3.7 (-3)	0	99.620	99.470
99	0.985	2.170	5.3 (-3)	7.1 (-3)	0	99.470	99.040
100	0.995	2.576	9.6 (-3)	1.8 (-2)	0	99.040	98.200

and the signal-to-noise ratio R_m required for a specific grade of service. If $\sigma_{rc}(p)$ can be reduced below the values given on Fig. 9, the estimate of the power required for high service probabilities such as $F(t) = 0.95$ will be reduced accordingly. Also, service probability curves determined by these methods will be less steep, and the expected value of the time availability p, for $F(t) = 0.5$, would constitute a much better estimate since it would not differ as much from the estimates for higher and lower values of service probability. The question is how much the standard deviation of the prediction error can be decreased by taking into account the results of transmission loss measurements made for various periods of time. The uncertainty in the assumption of the required predetection median-RMS-signal-to-median-RMS-noise ratio R_m and of the effective noise figure F, which has been expressed by the standard deviation σ_r, will not be affected by the availability of transmission loss or field strength measurements, and only the $\sigma_c(p)$ portion of the standard deviation $\sigma_{rc}(p)$ can be reduced.

Analogous to the prediction uncertainty $\sigma_c(p)$ which is assigned to calculated field strength or transmission loss values, an equivalent prediction uncertainty, again expressed by a standard deviation, may be assigned to observed field strength or transmission loss values. This standard deviation has been designated $\sigma_{oe}(p, n)$, as it is a function of the percentage of the hours p for which the improved prediction is desired, a function of the number of days n in the period for which measurements are available, and it contains a component σ_e to take into account calibration and reading errors inherent in the measurement methods. If now, in conformance with statistical practice, weights are defined as the reciprocals of

variances (or squared standard deviations), the improved prediction may be obtained by calculating weighted averages of predicted and measured values, usually for a number of percentage values.

The statistical basis for prediction improvement, and the detailed derivations of the expressions used are given in Appendices I and II. The results of these derivations are used here to obtain the proper weights and other parameters for any specific problem. The procedure will be described in what follows.

The general problem considered here is the improvement of predictions made for a specific tropospheric propagation path, using measurements obtained over the same or a slightly different path. It will often be the case that measurements are made only during a few weeks or months, while the improved prediction should be applicable to all hours of the year.

As the calculations for tropospheric communication systems are usually in terms of basic transmission loss, L_b, the method of prediction improvement will also be treated in these terms. It should be remembered, however, that the two quantities, field strength and basic transmission loss, are directly related, and an hourly median value of field strength $E(p)$ exceeded during at least p percent of all hours is equivalent to a basic transmission loss value $L_b(p)$ not exceeded during at least p percent of all hours. In the following discussion, all L values are hourly medians of basic transmission loss and the p-dependence is implied, although the symbol p and the subscript b may be dropped for convenience.

If an observed transmission loss value L_o and a calculated value L_c, both in decibels, are available for a path, the improved prediction L_t is given by:

$$L_t(p) = \frac{w_o(p)\, L_o(p) + w_c(p)\, L_c(p)}{w_o(p) + w_c(p)} \qquad (27)$$

where w_o and w_c are weights assigned to the observed and calculated values for the path, and L_t constitutes a weighted average. In order to simplify notation, the transmission loss $L_o(p, T)$ exceeded for 100 - p percent of the hourly medians of a T-hour recording, is referred to in this section as either $L_o(p)$ or L_o. In Appendix I, however, $L_o(p)$ is used only to denote a "true" infinite time value which does not include the effect of random measurement errors or a finite recording period.

The weight $w_c(p)$ is the reciprocal of the squared standard deviation $\sigma_c^2(p)$ assigned to a calculated transmission loss value L_c. It does not contain the component σ_r due to errors in estimating equipment characteristics of the ultimate communication circuit, as in this analysis only field strength or transmission loss values are compared:

$$w_c(p) = \frac{1}{\sigma_c^2(p)} \qquad (28)$$

The standard deviation $\sigma_c(p)$ is the lower (dashed) curve on Fig. 9, and the corresponding weight $w_c(p)$ may be readily calculated from (28).

The weight $w_o(p)$ assigned to the observed transmission loss value $L_o(p)$ is the reciprocal of the sum of the variances

$$w_o(p) = \frac{1}{\sigma^2_{oe}(p,n)} = \frac{1}{\sigma^2_o(p,n) + \sigma^2_e} \tag{29}$$

The variance σ^2_e due to equipment and reading errors caused by the measurement method may in most cases be assumed to be equal to 2 db^2. The variance $\sigma^2_o(p,n)$ is derived in Appendix I. It is given by

$$\sigma^2_o(p,n) = 0.0786\ g(n,H)\ f(\theta)\ \sigma^2_c(p) \tag{30}$$

The significance of the various terms will be explained below.

The weight $w_t(p)$ assigned to the improved prediction $L_t(p)$ is the denominator of (27), namely the sum of the weights assigned to the calculated and the measured values, respectively. It is evident that this new weight is greater than either of the individual weights from which it is obtained; thus its reciprocal, the variance $\sigma^2_t(p)$ associated with the improved prediction, is smaller than either of the original component variances representing the prediction and measurement uncertainties. The following expressions may be written:

$$w_t(p) = w_o(p) + w_c(p) \tag{31}$$

$$\sigma^2_t(p) = \frac{1}{w_t(p)} = \frac{1}{w_o(p) + w_c(p)} = \frac{\sigma^2_{oe}(p,n) \cdot \sigma^2_c(p)}{\sigma^2_{oe}(p,n) + \sigma^2_c(p)} \tag{32}$$

It is seen that an improved prediction with less uncertainty than the original prediction is obtained for any value of p, the percentage of hours.

Equation (29) shows that the variance $\sigma_o^2(p, n)$ is a function of the percentage of hours, p, the angular distance, θ^*, and the number of days of measurements, n. The parameter H in (30) is the number of hours per day as explained in Appendix I. For the purpose of application it is only necessary to select that curve of the variance ratio g(n, H), which corresponds to the number of consecutive days, n, and the number of hours per day, H, for which measurements were made. The year-to-year variation $f(\theta)$ is shown on Fig. 14, and curves for g(n, H) are shown on Fig. 15 for all hours of the year and for various time block combinations, depending on whether there are 5 hours, or 6 or more hours in a time block.

Recapitulating the results obtained so far, the improved prediction $L_t(p)$ of the distribution of basic transmission loss as a function of the percentage of hours is given by (27), and the remaining prediction uncertainty $\sigma_t(p)$ assigned to it is given by (32). This corresponds exactly to the assignment of the original prediction uncertainty $\sigma_c(p)$ to the calculated value $L_c(p)$. If it is desired to obtain system power requirements, the term σ_r^2 has to be added to $\sigma_t^2(p)$ in order to obtain a measure of the total prediction uncertainty taking into account the uncertainty in estimating the system parameters

---

* In cases where parameters other than the angular distance are used to describe the time availability V(p), it is permissible to use an equivalent angular distance value corresponding to the V(p) distribution. This value may be determined from inspection of Fig. 1. For paths within the radio horizon ($\theta < 0$), the angular distance θ may be assumed equal to zero for the purpose of estimating $\sigma^2(p, n)$.

THE YEAR-TO-YEAR VARIANCE $f(\theta)$

$$f(\theta) = E\left[(L_y - L_c - \delta)^2\right]$$

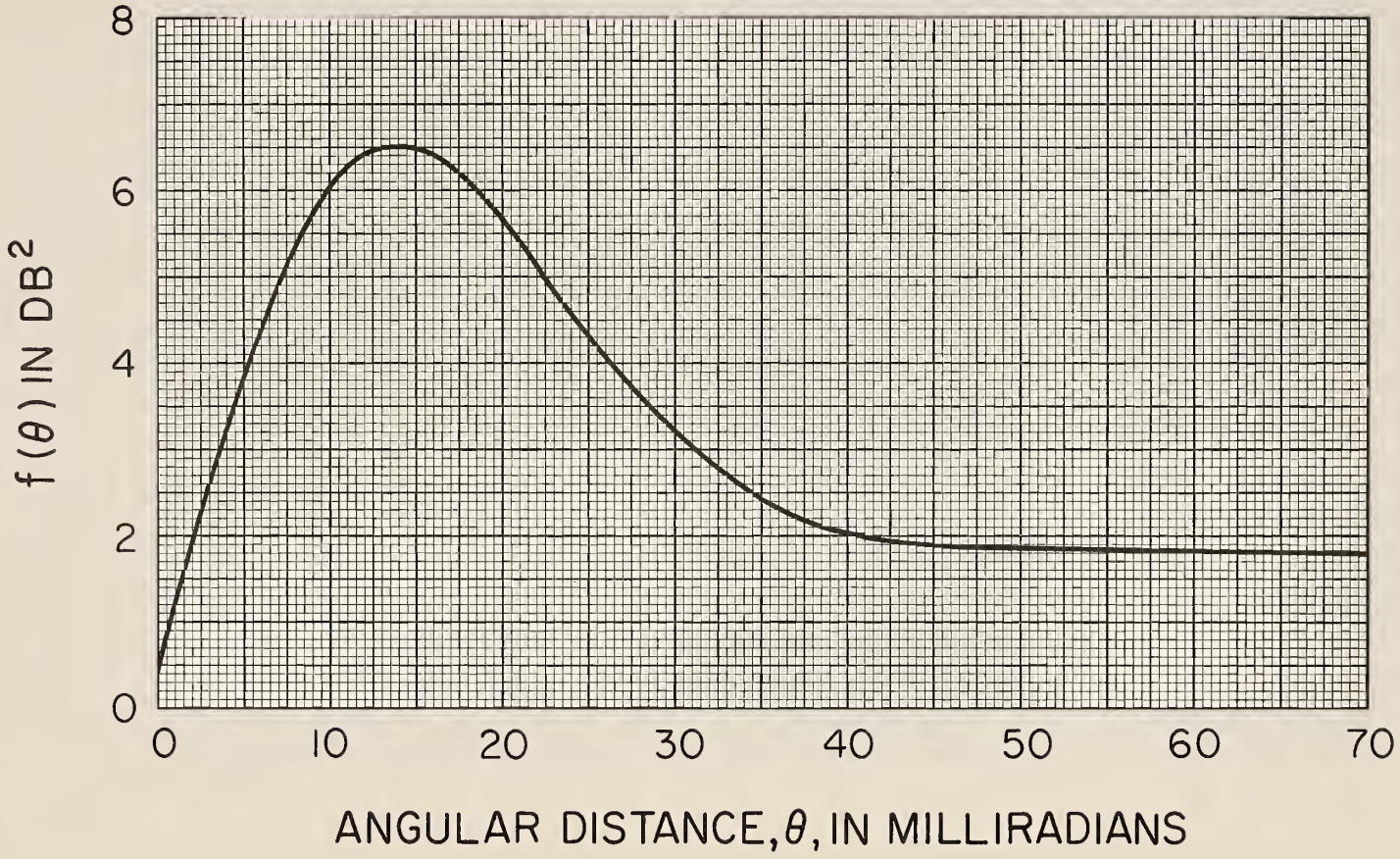

Figure 14

RATIO OF THE VARIANCE OF A n-DAY MEAN TO THE VARIANCE OF A YEARLY MEAN

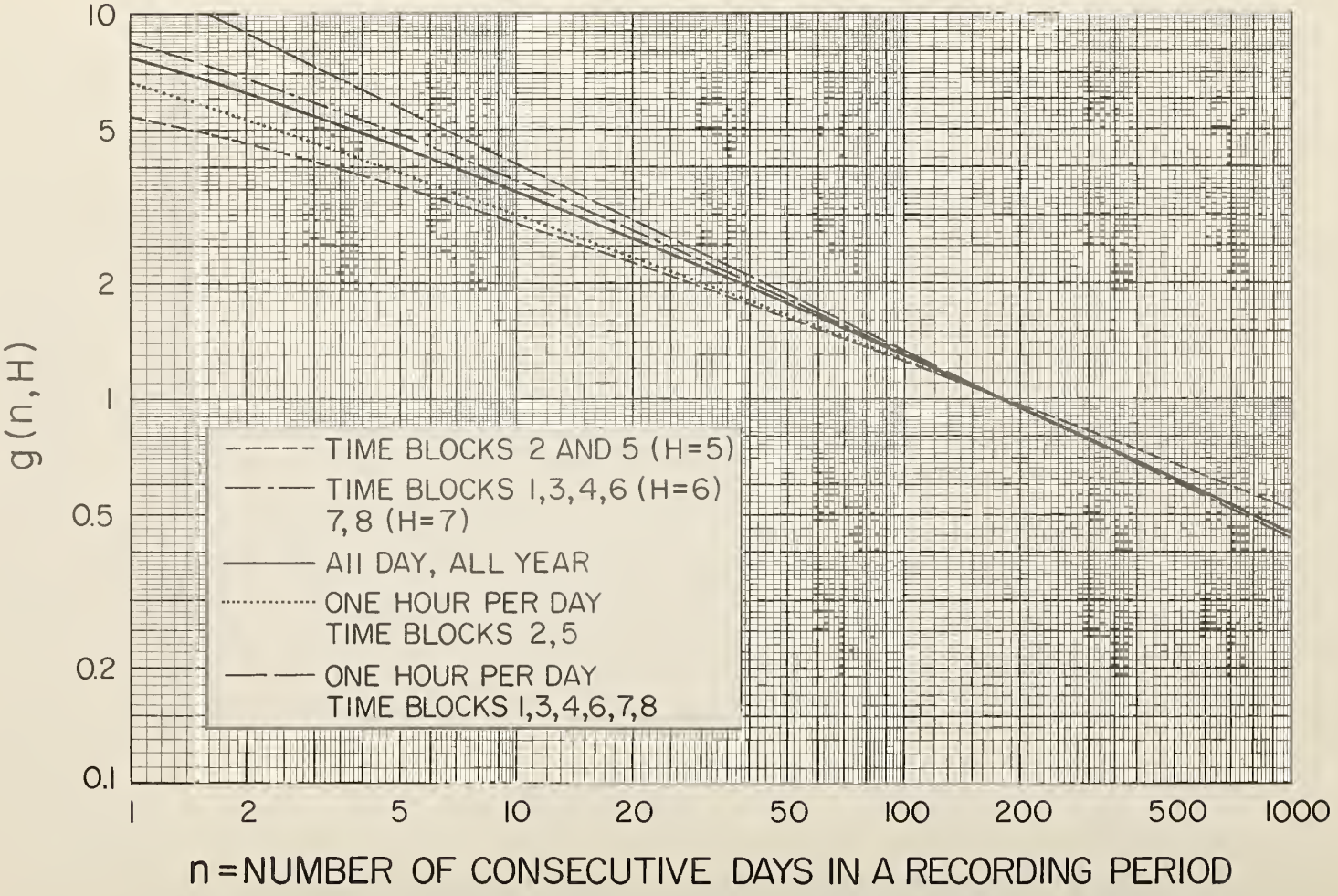

Figure 15

F and R_o as discussed in Section 2. Thus, the prediction uncertainty is characterized by a standard deviation $\sigma_t(p)$ as a function of p, if one deals with transmission loss or field strength values, or by a standard deviation $\sigma_{tr}(p)$, if predictions are to be made for the performance of a complete system including the uncertainties inherent in estimating equipment parameters. $\sigma_{tr}(p)$ is given by

$$\sigma_{tr}^2(p) = \sigma_t^2(p) + \sigma_r^2 \tag{33}$$

The preceding discussion dealt with prediction improvement by taking into account measurements over exactly the same path for which the prediction is made. There might be cases, however, where an improved prediction is desired for a path "b", whereas measurements are available only for a different path "a", which might be in the same region, or have similar parameters and characteristics.* Calculated values of hourly median basic transmission loss, however, may be obtained for both paths. If these are denoted L_{ca} and L_{cb}, an estimate of the improved prediction L_{tb} for Path "b" may be made as follows:

$$L_{tb} = L_{ta} + (L_{cb} - L_{ca}) \tag{34}$$

where L_{ta} is the improved prediction for Path "a", obtained in the

* Considerations of antenna beam width and lobing effects lead to the conclusion that the use of two different frequencies over the same geometrical path may constitute a difference between paths in the sense used here, especially if very narrow beam antennas are used.

manner described above. All terms in (34) are of course functions of the percentage of hours p, as before, and p has been dropped for convenience. An estimate of the prediction error associated with L_{tb} is not only a function of the prediction errors associated with the terms on the right-hand side of (34), but also depends on the correlation between the values L_{ca} and L_{cb}. This matter is discussed in detail in Appendix II. The result obtained is an expression for the prediction uncertainty σ_{tb} assigned to the improved prediction L_{tb} which is a function of the prediction uncertainties σ_{ca}, σ_{cb}, and σ_{ta}, as well as the correlation coefficient ρ_{ab}.

$$\sigma_{tb}^2 = \sigma_{cb}^2 + \sigma_{ca}^2 - \sigma_{ta}^2 - 2\sigma_{ca}\sigma_{cb}\rho_{ab}(1 - \sigma_{ta}^2/\sigma_{ca}^2) \qquad (35)$$

If Path "a" is the same as Path "b", $L_{tb} = L_{ta}$, the variances σ_{ca}^2 and σ_{cb}^2 are equal, and $\rho_{ab} = 1$; in this case, (35) reduces to $\sigma_{tb}^2 = \sigma_{ta}^2$ as it should

It is shown in Appendix II that the correlation coefficient ρ_{ab} between estimates L_{ca} and L_{cb} over the two Paths "a" and "b" has to be at least 0.5 in order to reduce the standard error of estimating L_{tb} below the standard error of L_{cb}. In general, it will be quite difficult to make an accurate estimate of the correlation coefficient ρ_{ab}. The results of the same study show that ρ_{ab} has to be very close to unity in order to obtain a substantial improvement in the estimate of L_{tb} over the estimate L_{cb} obtained without any measurements. Available data which may be used to estimate ρ_{ab} are contained in papers by Kirby and Capps [1956] and Kirby [1957]. It is shown there that for a fixed transmitter location the correlation

coefficient between field strength values observed at adjacent measuring locations drops to 0.5 within a distance of one-half to one mile. On the other hand, Kirby, et al, [1956] have shown that there is sometimes relatively high correlation between different frequencies received over essentially the same paths using antennas of moderately wide beam widths. All these results were obtained on much shorter paths than are normally used for tropospheric scatter communication systems. However, to the extent that such measurements are applicable, it would appear that path-loss measurements made on paths with one or the other of their terminals separated by as much as one mile from the terminals of the path for which a prediction is required will be of little or no direct value, especially in rough terrain.

After having obtained the variance σ^2_{tb} assigned to L_{tb} from (35) using an appropriate assumption of the correlation coefficient ρ'_{ab}, the variance σ^2_r has to be added to σ^2_{tb} for the purpose of system design, just as in (33):

$$\sigma^2_{trb}(p) = \sigma^2_{tb}(p) + \sigma^2_r \qquad (36)$$

Having obtained $L_t(p)$ or $L_{tb}(p)$ and $\sigma_{tr}(p)$ or $\sigma_{trb}(p)$ as functions of p, service probability values may be calculated in the same way as was done in Section 4 for the theoretical prediction. The complete procedure will be demonstrated in the next section by means of an example.

7. COMPARISON OF PREDICTED AND MEASURED DATA AND AN EXAMPLE OF PREDICTION IMPROVEMENT.

Although the uncertainty of any percentage point of the predicted transmission loss curve is given by the $\sigma_c(p)$ curve of Fig. 9,

additional allowance has to be made for the departure of observed values from their true long-term medians. The departures of both the predicted and the observed values from the true values are independent random variables and are assumed to be normally distributed with standard deviations $\sigma_c(p)$ and $\sigma_{oe}(p,n)$, respectively. The difference between the predicted transmission loss and the observed system loss for a given time availability p will then be normally distributed with a standard deviation $\sigma(p)$ determined by:

$$\sigma^2(p) = \sigma_c^2(p) + \sigma_{oe}^2(p,n) \tag{37}$$

An example will now be given to illustrate how this analysis may be used to determine whether an observed distribution deviates significantly from the predicted distribution. For this purpose the observations on the 200-mile (θ = 40.2 milliradians) path described in Section 2 will be used. Transmission loss measurements were performed in February of 1957, using a 1046 Mc/s unmodulated horizontally polarized carrier. The transmitter power was approximately 15 watts, and ten-foot diameter dipole-fed parabolic antennas were used with their centers 26 feet above ground. The receiver bandwidth was approximately 1000 cps, and the carrier envelope was recorded both on strip charts and on time-totalizing equipment. Fig. 16a shows the distribution of the 378 measured hourly medians, together with the predicted all hours - winter distribution for this path.

In order to determine whether the observed and the predicted distributions are significantly different, confidence limits for

COMPARISON OF PREDICTED TRANSMISSION LOSS AND MEASURED SYSTEM LOSS FOR 1046 Mc/s SAMPLE PATH WITH EVALUATION OF THEIR DIFFERENCES

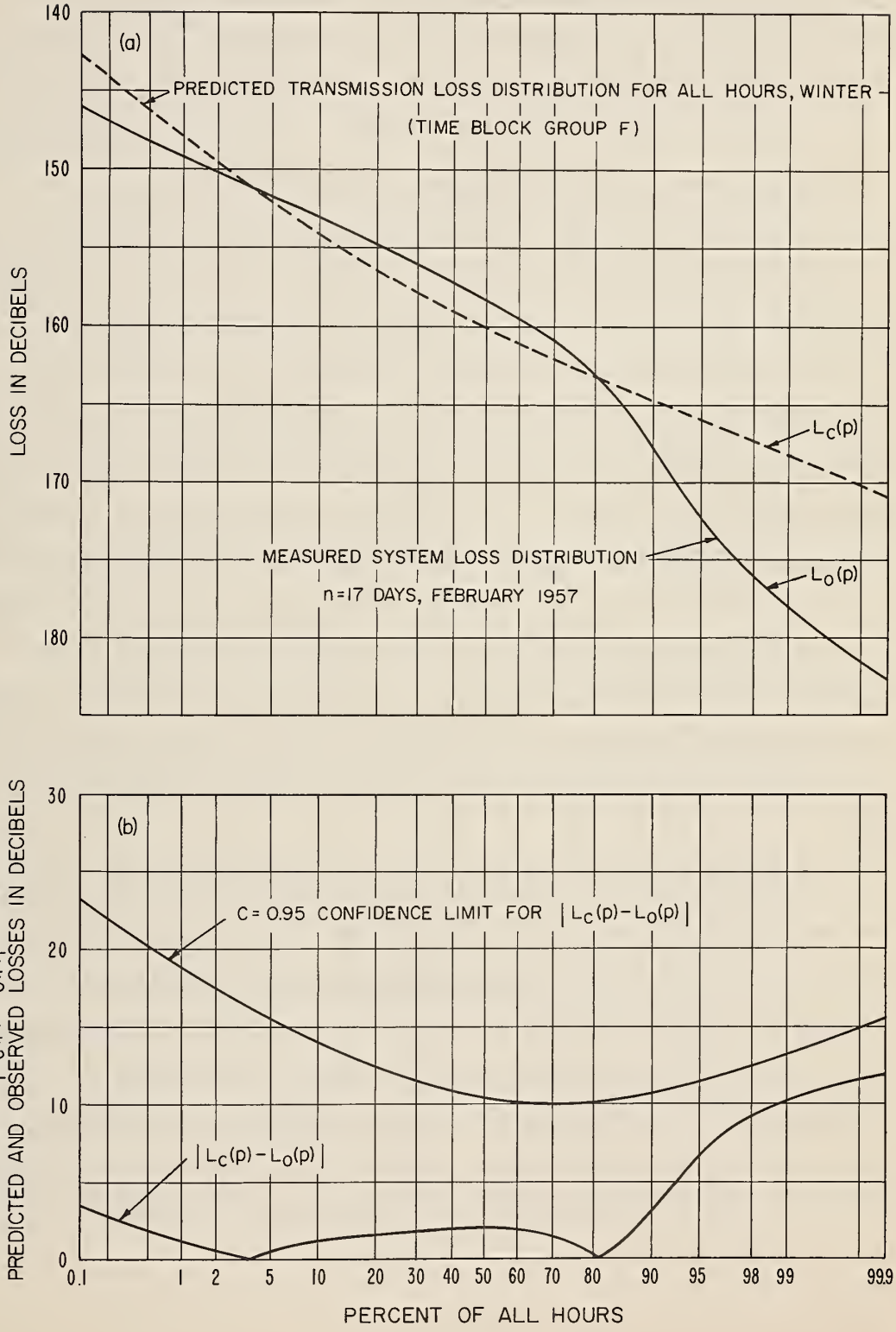

Figure 16

the difference between the observed and the predicted values are given on Fig. 16b. Since positive and negative differences are equally likely, differences less than $t \cdot \sigma(p)$ are expected with a probability $C = 2F(t) - 1$. It is evident on Figs. 16a and 16b that the observed and predicted values in this case do not differ significantly for any p at the confidence level $C = 0.95$. In general, if the differences $|L_c(p) - L_o(p)|$ for all values of p are less than $t \cdot \sigma(p)$ at a confidence level $C = 0.95$, it is desirable to use both the observed and calculated values for determining an improved prediction. If $|L_c(p) - L_o(p)|$ deviates by more than $t \cdot \sigma(p)$ at a confidence level $C = 0.95$ for some value of p, it is desirable to carefully re-examine the measurements to see whether they are reliable and to re-examine the nature of the path to see whether the calculated values might reasonably be expected to apply. For example, unusual ducting conditions which are sometimes encountered on paths over sea water might well be poorly predicted for the smaller values of p and even for values of $p > 50\%$ in cases where these ducts are almost always present. It should be noted that $V(p)$ and $\sigma_c(p)$ are based on a very large amount of transmission loss data but transmission paths may occasionally be found with true distributions which depart more than $\pm 2\sigma_c(p)$ from $L_c(p)$.

The terms "system loss" and "transmission loss" used in this analysis and appearing on Fig. 16 have been discussed by Norton [1959]. One calculates transmission loss as ten times the logarithm of the ratio of the power delivered to the transmitting antenna terminals to the power available at the receiving antenna terminals under the assumption of no circuit losses in the antennas. The measured system loss is the same power ratio, but includes antenna circuit losses. In the case of tropospheric propagation the antenna circuit

losses can usually be neglected, except when inherently lossy antennas like rhombics are involved. For the example used here, however, the approximation is applicable and transmission loss and system loss are considered to be nearly equal. Basic transmission loss L_b and transmission loss L differ only by the effective path antenna gain G_p.

Since the calculated and observed losses in this example were not found to differ significantly, they may be combined to obtain an improved prediction. Hourly medians of system loss shown on Fig. 16a are first converted to basic transmission loss by adding the calculated value of G_p, and their distribution is shown by the dotted line marked $L'_{bo}(p)$ on Fig. 17. In conformance with the analysis of long-time variability by time blocks already discussed in Section 2, the measurements represent the winter time-block group (designated by the subscript "F"), as they were performed during February and include all hours of the day.

The measured values are first adjusted to all-day, all-year values by subtracting a term $\Delta V_{AF}(p, \theta)$. This term is the difference between the $V(p, \theta)$ values for all-day, all-year (read from Fig. 1 at the path angular distance value $\theta = 40.2$ milliradians), and the $V(p, \theta)$ values for all hours, winter (read from Fig. 2 at the same $\theta = 40.2$ milliradians). It is assumed here that errors in $L_{bo}(50)$ and any $\Delta V(p, \theta)$ are uncorrelated, and that the variance assigned to a ΔV value is identical to a corresponding variance $\sigma_o^2(p, n) - \sigma_o^2(50, n)$ assigned to the difference of observed values. The adjusted values, $L_{bo}(p) \equiv L'_{bo}(p) - \Delta V_{AF}(p, \theta)$ are shown by the broken line on Fig. 17. This curve represents the observed values adjusted to represent all-day, all year values. The weight assigned to each value $L_{bo}(p)$

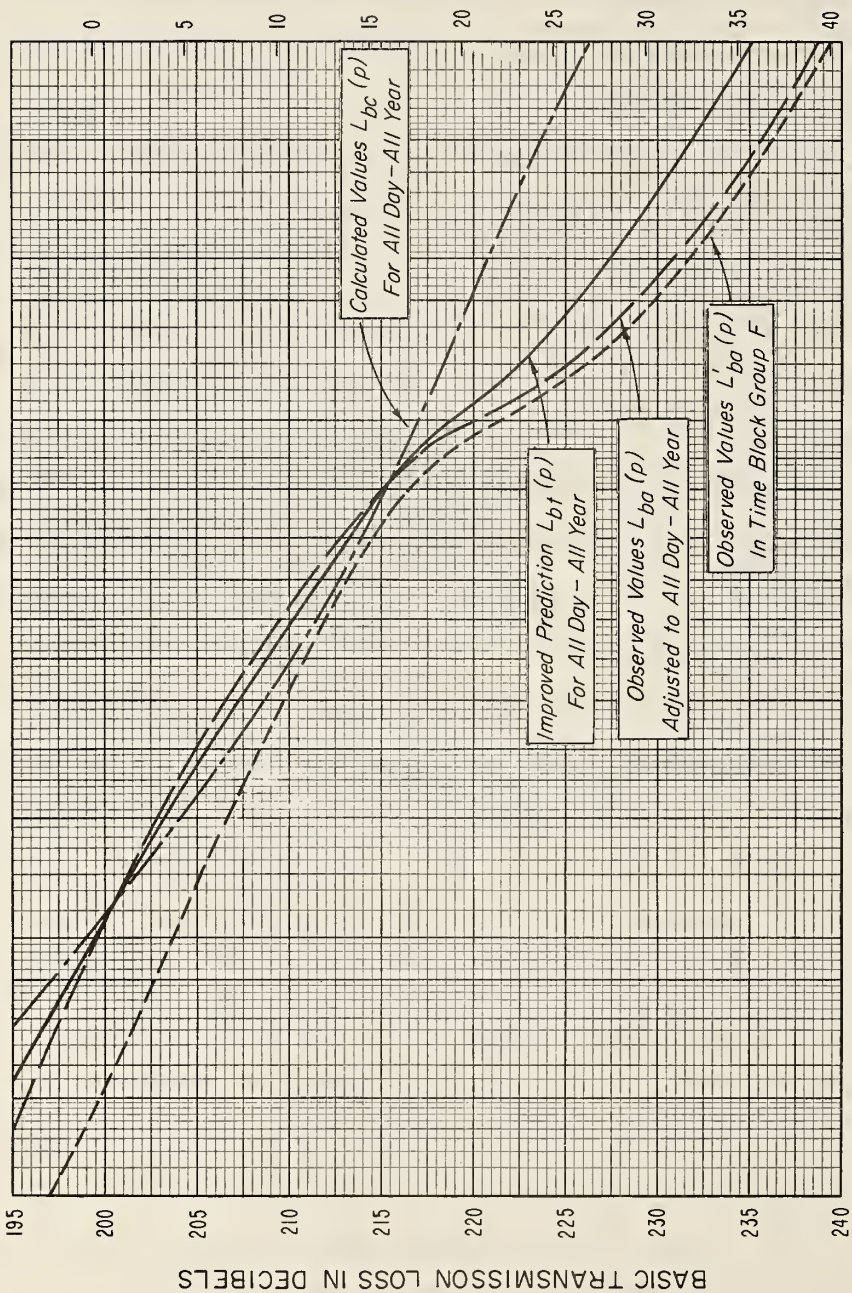
DISTRIBUTIONS OF HOURLY MEDIANS OF
BASIC TRANSMISSION LOSS ON 1046 Mc/s
FOR SAMPLE PATH
TRANSMITTER POWER P(0.5, p) FOR SAMPLE SYSTEM
IN dbw
0
5
10
15
20
25
30
35
40
BASIC TRANSMISSION LOSS IN DECIBELS
195
200
205
210
215
220
225
230
235
240
TIME AVAILABILITY, p, IN PERCENT OF ALL HOURS
0.01
0.05
0.1
0.2
0.5
1
2
5
10
20
30
40
50
60
70
80
90
95
98
99
99.8
99.9
99.99
Calculated Values L_{bc} (p)
For All Day - All Year
Improved Prediction L_{bf} (p)
For All Day - All Year
Observed Values L_{ba} (p)
Adjusted to All Day - All Year
Observed Values L'_{ba} (p)
In Time Block Group F

Figure 17

is obtained from (30) using Figs. 14 and 15. For $n = 17$ days, the all-day, all-year $g(n, H) = 2.8$ and for $\theta = 40.2$ milliradians, $f(\theta) = 2.02\,(db)^2$. Thus for the median ($p = 50\%$), $\sigma_o^2(50, 17)$ is determined to be $5.66\,(db)^2$. To each $\sigma_o^2(p, 17)$ a term $\sigma_e^2 = 2.0\,(db)^2$ is added in order to allow for path-to-path equipment (reading and calibration) errors. The resultant values $\sigma_{oe}(p, 17)$ represent the uncertainty assigned to each observed value $L_{bo}(p)$, as adjusted to all-day, all-year values. The weight $w_o(p)$ assigned to each value $L_{bo}(p)$ is the reciprocal of each $\sigma_{oe}^2(p, 17)$.

For the same 1046 Mc/s frequency, the Time Block 2 median basic transmission loss value is calculated using the methods of Rice, et al [1959]. It should be remembered that the sample calculations of Sections 2 and 4 refer to the same path. The calculated Time Block 2 median value, $L_{bm} = 214.7$ db, together with the $V(p, \theta)$ values of Fig. 1, produces the calculated distribution of hourly medians for all-day, all-year:

$$L_{bc}(p, \theta) = L_{bm} - V(p, \theta) \tag{38}$$

The calculated values $L_{bc}(p, \theta)$ are shown by the dash-dotted line on Fig. 17. They may be redesignated as $L_{bc}(p)$, as the angular distance θ does not enter any more. The prediction uncertainty $\sigma_c(p)$ associated with each $L_{bc}(p)$ is given by the dashed curve of Fig. 9. Prior to combining predictions and measurements, the system error σ_r (representing principally the uncertainties in estimating the system parameters F and R) does not enter. The weights $w_c(p)$ are the reciprocals of the squared $\sigma_c(p)$ values read from Fig. 9.

Now the weighted average of $L_{bc}(p)$ and $L_{bo}(p)$ may be obtained in accordance with (27), resulting in the distribution of hourly medians $L_{bt}(p)$, the improved prediction. This is the solid curve on Fig. 17 and the corresponding weights $w_t(p)$ are obtained by adding $w_c(p)$ and $w_o(p)$.

The performance of a communication system utilizing this path may now be predicted on the basis of three methods: first, using the calculated values along; second, using only observed values; and third, using the weighted average of the two, which constitutes the improved prediction. Prediction uncertainties for all three cases are shown on Fig. 18. It is necessary here to keep in mind that the desired communication system utilizes a path slightly different from the one applicable to the measurements, as larger antennas (28 ft. versus 10 ft.) at a higher elevation (50 ft. versus 26 ft.) are involved. However, in order to permit the use of this example, this difference is neglected here so that the assumption $\rho_{ab} = 1$ can be made in the sense of the discussions of the preceding section.

The first case has already been discussed in Section 4. For this case the distribution $L_{bc}(p)$ of Fig. 17 is used with the prediction uncertainty given by the dash-dotted $\sigma_{rc}(p)$ curve of Fig. 18, which is the same curve as the solid curve of Fig. 9. The system error σ_r is included in $\sigma_{rc}(p)$, as explained in Section 4.

$$\sigma^2_{rc}(p) = \sigma^2_c(p) + \sigma^2_r \qquad (7)$$

For the second case the observed distribution (adjusted to all-day, all-year) $L_{bo}(p)$ of Fig. 17 is used, together with the prediction uncertainty $\sigma_{or}(p,n)$ shown by the dashed curve on Fig. 18.

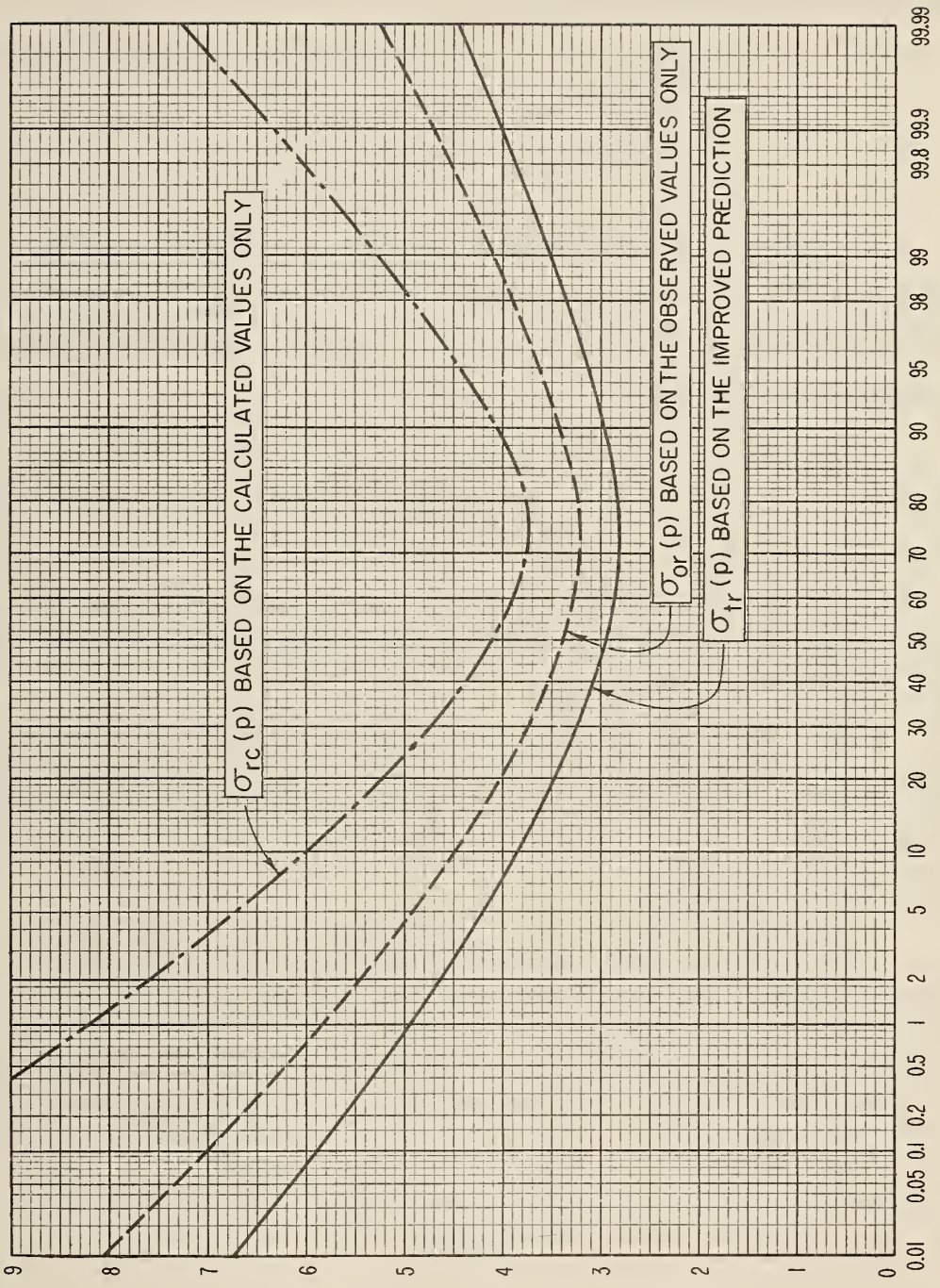
PREDICTION UNCERTAINTY FOR SAMPLE PATH
PREDICTION UNCERTAINTY, DECIBELS
PERCENT OF ALL HOURS
$\sigma_{rc}(p)$ BASED ON THE CALCULATED VALUES ONLY
$\sigma_{or}(p)$ BASED ON THE OBSERVED VALUES ONLY
$\sigma_{tr}(p)$ BASED ON THE IMPROVED PREDICTION
0
1
2
3
4
5
6
7
8
9
0.01
0.05
0.1
0.2
0.5
1
2
5
10
20
30
40
50
60
70
80
90
95
98
99
99.8
99.9
99.99

Figure 18

As the prediction applies to a complete system, $\sigma_{or}(p,n)$ also contains the system errors σ_r:

$$\sigma^2_{or}(p,n) = \sigma^2_{oe}(p,n) + \sigma^2_r \tag{39}$$

Finally, the improved prediction curve $L_{bt}(p)$ of Fig. 17 is used together with the prediction uncertainty $\sigma_{tr}(p)$ shown by the solid curve on Fig. 18. Again, $\sigma_{tr}(p)$ contains the system error σ_r, and is given by

$$\sigma^2_{tr}(p) = \sigma^2_t(p) + \sigma^2_r \tag{40}$$

where $\sigma^2_t(p)$ is the reciprocal of the sum of the weights $w_o(p)$ and $w_e(p)$ in accordance with (32).

Fig. 18 shows that the prediction uncertainty is appreciably reduced by the use of these measurements, based, of course, on the somewhat questionable assumption of perfect correlation between "paths" represented by $\rho_{ab} = 1$.

As the last step, service probability curves will be calculated in accordance with the method first outlined in Section 4. In this particular case, the effects of higher transmission loss and lower prediction uncertainty values tend to balance each other, as will be seen by the final comparison of service probabilities for 99 or 99.9 percent of all hours of the three cases, using both 1 kw and 10 kw transmitter power.

Briefly repeating the steps already explained in Sections 3 and 4, the relation between the system power $P[F(t), p]$ required

to provide the specified grade of service or better during p% of all hours with the probability F(t) and the expected value of system power P(0.5, p) is given by:

$$P[\,F(t), p\,] = P(0.5, p) + t \cdot \sigma(p) \qquad (8)$$

where P(0.5, p) here is related to the three curves of basic transmission loss values $L_{bc}(p)$, $L_{bo}(p)$, and $L_{bt}(p)$, and for $\sigma(p)$ either $\sigma_{rc}(p)$, $\sigma_{or}(p, n)$ or $\sigma_{tr}(p)$ are substituted, depending on the three cases considered. For the same system as used in Section 4 (28-ft. parabolic reflectors, parametric receiver front-ends, quadruple diversity FM, 1000-1200 Mc/s carrier frequency), and the same specified grade of service (24-voice channels, several of which are loaded with standard frequency-shift teletype signals), which has been assumed equivalent to $R_m = 7.2$ db, it can be shown by substitution into (1) that the required transmitter power P_t in decibels above one watt is given by the hourly median basic transmission loss L_b minus 199.4 db. Thus a fixed transmitter power P_o = 1 kw (30 dbw) corresponds to 229.4 db basic transmission loss on the curves of Fig. 17 for this system. A corresponding scale of power versus transmission loss may now be set up on Fig. 17 for this system and values of P(0.5, p) read for substitution into (8). Now, (8) is solved for t:

$$t = \frac{P_o - P(0.5, p)}{\sigma(p)} \,, \qquad (12)$$

and from t, the service probability F(t) may be found from appropriate probability tables [Bennett and Franklin, 1954].

For each of the three cases, F(t) may be now determined as a function of p, with P(0.5,p) determined from the right hand ordinate scale and the appropriate L_b curve of Fig. 17 and $\sigma(p)$ read from the corresponding curve of Fig. 18. P_o is fixed at 1 kw and 10 kw. The resultant curves of service probability are shown on Fig. 19.

On the basis of the observed values alone, and assuming a transmitter power of 1 kw, Fig. 19 would predict a time availability greater than 99% for only 36 installations out of 100 over this type of path. On the basis of the calculated values alone, Fig. 19 would predict a time availability greater than 99% for 96 installations out of 100. The improved prediction curve, which is based on both the observed values $L_{bo}(p)$ and the calculated values $L_{bc}(p)$, indicates that the time availability would exceed 99% for 71 installations out of 100. Increasing the transmitter power to 10 kw will provide a time availability greater than 99% for 999 installations out of 1000, if either the theoretical curve or the one corresponding to the improved prediction is used.

For any path of system, measurements add to the information gained from theoretical considerations alone. The relative positions of the "calculated" and the "improved prediction" curve on Fig. 19 are due to the discrepancy between calculated and measured values at the high end of the time availability scale (see Fig. 17). An example of much better agreement between calculated and measured values is shown in a recent paper by Barghausen and Peterson [1960]. There the "improved prediction" curves are generally above the

SERVICE PROBABILITY FOR SAMPLE PATH QUADRUPLE DIVERSITY FM SYSTEMS, 1000-1200 MC/S, 24 VOICE CHANNELS, 28 ft. DISHES, R_m = 7.2 db

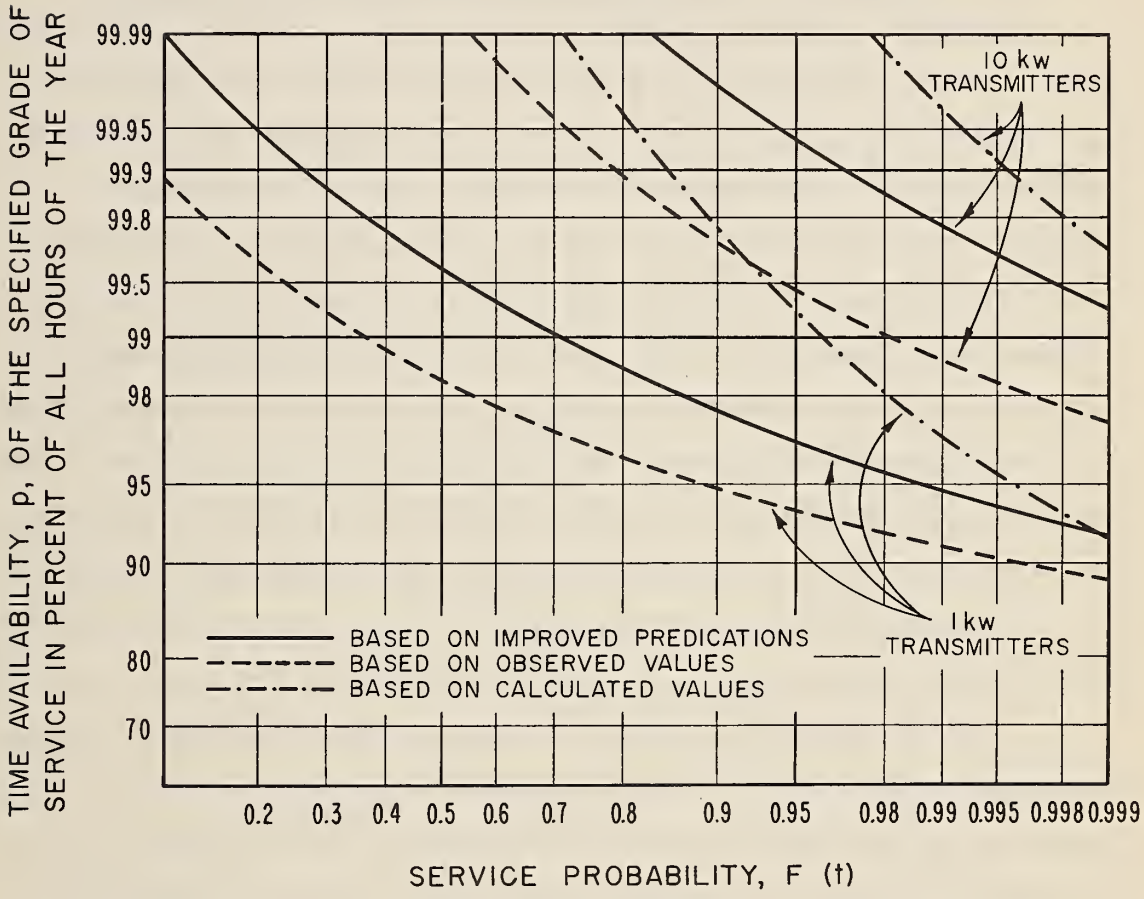

Figure 19

"calculated" curves, resulting in greater values of time availability for the "improved prediction" over the entire range of service probability values shown.

8. ADDITIONAL CONSIDERATIONS AND CONCLUSIONS

It has been shown first how the performance of a communication system may be predicted, and how the probability of its success may be evaluated by the introduction of the "service probability" concept. Thus the accuracy of the prediction depends on the magnitude of the standard error values $\sigma_{rc}(p)$ as functions of the time availability p in percent of all hours, and of the equipment error σ_r. The standard error values $\sigma_{rc}(p)$ were obtained from an extensive and very general measurement program. As an extension of this method, and based on data from the same measurement program, it has been shown how this prediction method may be modified to take into account transmission loss measurements over exactly the same path or a path similar to the one for which the final system is intended.

The "improved prediction" obtained from forming a weighted average of calculated and observed values will always result in a reduction of the prediction uncertainty because the resultant weight is greater than each of the individual weights assigned to either the calculated or the observed values.

In some cases it may be of interest to determine the expected number of days of measurement necessary to result in a prediction uncertainty substantially less than the prediction uncertainty associated with the calculated value. In terms of the preceding discussions, this means setting (30) equal to an appropriate fraction of $\sigma^2_{rc}(p)$ as given on Fig. 9 and solving for n, the number of days of measure-

ments, as a function of the angular distance θ, and the time availability p in percent of all hours.

Before deriving a solution, one has to consider that a certain minimum number of days is necessary to define a given percentage value for a distribution of hourly medians. While one single hourly median may be considered a 50% value, it is necessary to have at least 50 hourly medians in order to define a value exceeded for 99% or 1% of all hours, and 500 hours to define a value exceeded for 99.9% or 0.1% of all hours. This is based on the method customarily used in obtaining cumulative distributions of hourly medians. It is also important to know how many and which hours per day were measured in order to use the appropriate $g(n, H)$ curve of Fig. 15.

The model which has been used specifies a strong dependence of the variance of a limited number of observed hourly medians on angular path distance, but no such dependence appears to exist for the variance associated with calculated hourly medians.

Let it be desired that the variance $\sigma^2_{tr}(p)$ characterizing the uncertainty of an improved transmission loss prediction $L_{bt}(p)$ be reduced to a fraction a^2 of the variance $\sigma^2_{rc}(p)$ characterizing the uncertainty associated with the transmitter power obtained from a calculated transmission loss value $L_{bc}(p)$. As actual systems are considered here, both variances contain the equipment uncertainty term σ^2_r, which allows for errors in estimating equipment parameters, especially the required carrier-to-noise ratio R_o and the noise figure F. This may be written as

$$\sigma^2_{tr}(p) = a^2 \sigma^2_{rc}(p) \tag{41}$$

where $\sigma^2_{tr}(p) = \sigma^2_t(p) + \sigma^2_r$, and $\sigma^2_{rc}(p) = \sigma^2_c(p) + \sigma^2_r$, as before. Also, (32) may be written in the following form:

$$\frac{1}{\sigma^2_t(p)} = \frac{1}{\sigma^2_{oe}(p)} + \frac{1}{\sigma^2_c(p)} = \frac{1}{\sigma^2_o(p,n) + \sigma^2_e} + \frac{1}{\sigma^2_c(p)} \qquad (42)$$

Solving (42) for $\sigma^2_{oe}(p)$ and substituting (30) for $\sigma^2_o(p,n)$,

$$\sigma^2_{oe}(p) = 0.0786\, g(n,H)\, f(\theta)\, \sigma^2_c(p) + \sigma^2_e = \frac{\sigma^2_t(p)\, \sigma^2_c(p)}{\sigma^2_c(p) - \sigma^2_t(p)} \qquad (43)$$

is obtained.

The usual assumptions of $\sigma^2_r = 4$ and $\sigma^2_e = 2$ are now made, and (43) is solved for $g(n,H)$, using $\sigma^2_{tr}(p) = \sigma^2_t(p) + 4$, $\sigma^2_{rc}(p) = \sigma^2_c(p) + 4$:

$$g(n,H) = \frac{12.73\, \{a^2\, \sigma^4_c(p) - 6\sigma^2_c(p)\, [\,1 - a^2\,] - 8[\,1 - a^2\,]\,\}}{f(\theta)\, \sigma^2_c(p)\, \sigma^2_{rc}(p)\, [\,1 - a^2\,]} \qquad (44)$$

For any desired value of $a < 1$, and any desired percentage point p, $g(n,H)$ may now be calculated, using the $\sigma_c(p)$ and the $\sigma_{rc}(p)$ curves of Fig. 9. Having obtained $g(n,H)$, corresponding values of n may be determined from Fig. 15, using the curve appropriate to the time block or time block combination, or number of hours per day for which measurements are available. The result is n, the number of days of measurements necessary to reduce the

standard deviation $\sigma_{tr}(p)$ associated with an improved prediction to a fraction "a" times the standard deviation $\sigma_{rc}(p)$ associated with the calculated values; all applicable to p% of all hours.

Depending on the desired reduction a and the percentage p, (44) may break down, as in some instances a value of g(n, H) less than zero results. This is to be interpreted in this manner: due to the fixed component variances σ_r^2 and σ_e^2 it is not possible to reduce $\sigma_{rc}^2(p)$ by any arbitrary amount. In other words, there is a lower limit for the factor a. A relation between p and a may be established by setting the curly bracket in (44) equal to zero, and solving for $\sigma_c^2(p)$ as a function of a. For a = 0.5, the limit $\sigma_c^2(p)$ for which g(n, H) equals zero is found to be 19.25, or $\sigma_c(p) \cong 4.4$. This means that the prediction uncertainty cannot be reduced by one-half unless the original $\sigma_c(p)$ is at least 4.4 db. From Fig. 9, this corresponds to a percentage value p less than 27%, or greater than 97.5%. For percentages between these two values, the prediction uncertainty cannot be reduced by one-half, because of the assumed fixed component calibration and equipment errors.

Results of the preceding analysis are shown on Figs. 20 and 21. The number of days, n, of measurements is shown which is necessary to obtain an improved prediction uncertainty $\sigma_{tr}(p)$ equal to 0.5 $\sigma_{rc}(p)$ (on Fig. 20), or equal to 0.707 $\sigma_{rc}(p)$ (on Fig. 21). The resulting curves were calculated for all-day, all-year measurements using the solid g(n, H) curve of Fig. 15. They are functions of the angular path distance θ, and assume a shape similar to the $f(\theta)$ curve on Fig. 14. This means that more measurements are necessary for paths with intermediate lengths ($10 < \theta < 20$) than for a long path ($\theta > 50$) or for a short path ($\theta < 2$). On Fig. 20, curves

LENGTH OF MEASUREMENT PERIOD NECESSARY
TO OBTAIN AN IMPROVED PREDICTION UNCERTAINTY
EQUAL TO 0.5 $\sigma_{rc}(p)$

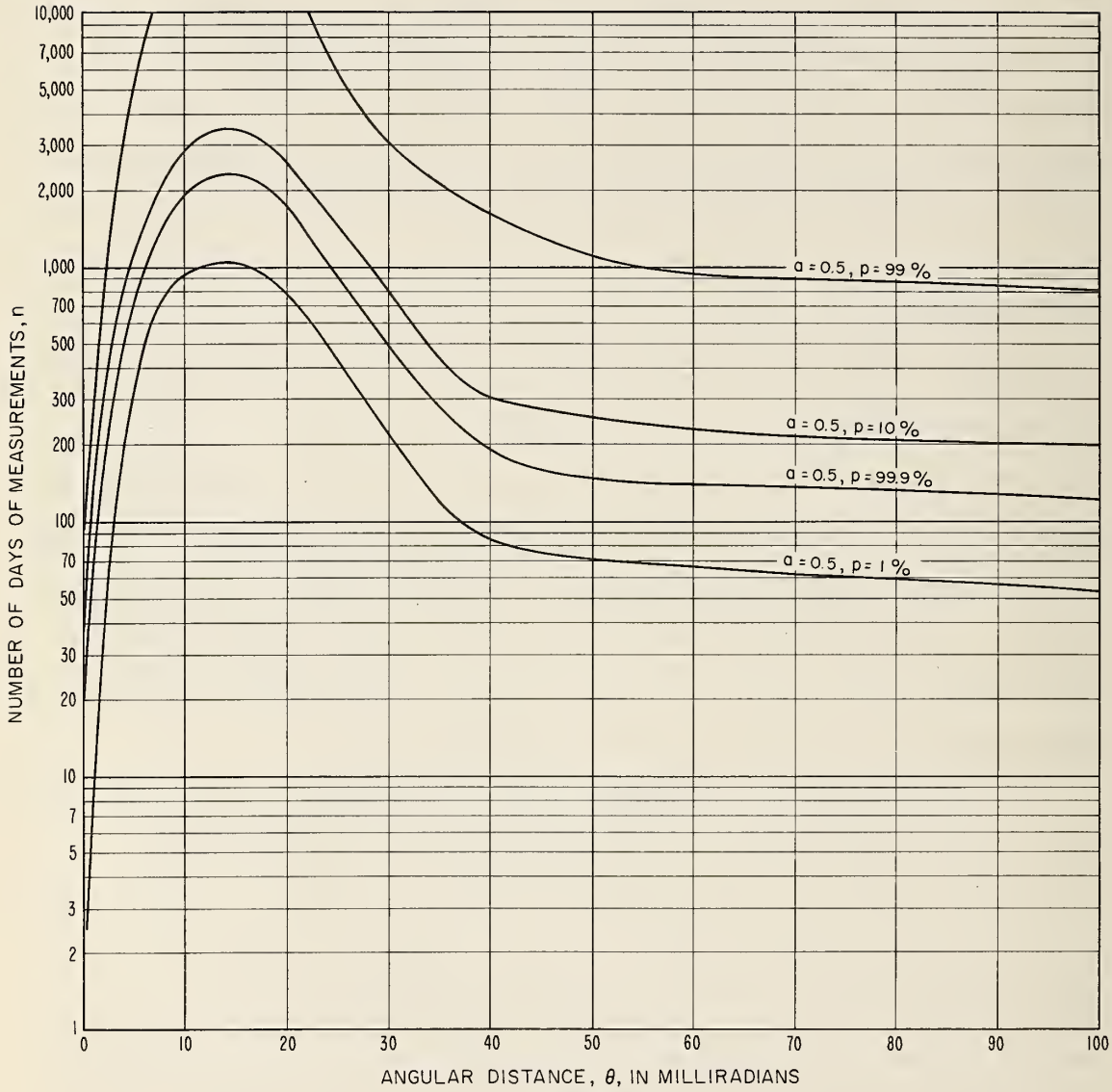

Figure 20

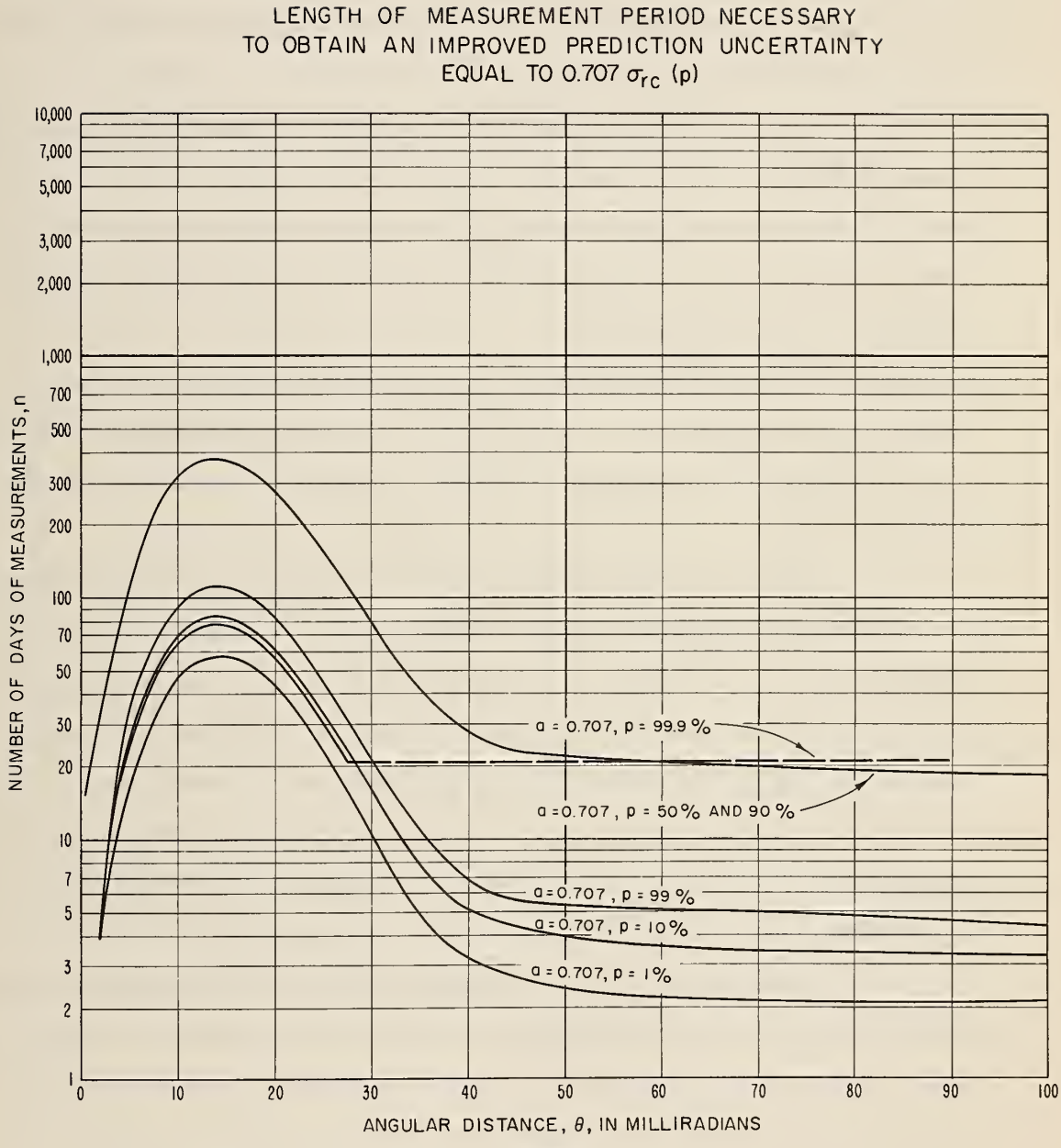
LENGTH OF MEASUREMENT PERIOD NECESSARY
TO OBTAIN AN IMPROVED PREDICTION UNCERTAINTY
EQUAL TO 0.707 σ_{rc} (p)
NUMBER OF DAYS OF MEASUREMENTS, n
10,000
7,000
5,000
3,000
2,000
1,000
700
500
300
200
100
70
50
30
20
10
7
5
3
2
1
0
10
20
30
40
50
60
70
80
90
100
ANGULAR DISTANCE, θ, IN MILLIRADIANS
a = 0.707, p = 99.9 %
a = 0.707, p = 50% AND 90 %
a = 0.707, p = 99 %
a = 0.707, p = 10%
a = 0.707, p = 1%

Figure 21

for $a = 0.5$, and $p = 50$ and 90% are missing, as a result of the limitations explained in the preceding paragraph. Similar reasoning also explains the seeming paradox: that it required less extensive measurements to reduce the prediction uncertainty to a fixed fraction for the extreme percentage point values. At 99.9% or 1% the calculated prediction uncertainty $\sigma_{rc}(p)$ is substantially larger than its component σ_r; therefore, $\sigma_{tr}(p)$ can easily be reduced to a given fraction of $\sigma_{rc}(p)$. For percentage points closer to the minimum between 50 and 90%, $\sigma_{rc}(p)$ is already small, and $\sigma_{tr}(p)$ cannot easily be reduced.

On Fig. 21, the 99.9% curve for $a = 0.707$ has been broken off at the limit $n = 20.8$ days, which here corresponds to the minimum number of hourly medians necessary to obtain a 99.9% value.

As an example, Fig. 20 shows that for a path characterized by an angular distance $\theta = 40$ milliradians, 190 days of measurements (more than half a year) are necessary to reduce the prediction uncertainty associated with 99.9% of all hours to one-half of the value, $\sigma_{rc}(99.9\%) = 6.35$ db. In the study of interference fields, it would take 300 days of measurement to reduce the prediction uncertainty associated with 10% of all hours to one-half of the value $\sigma_{rc}(10\%) = 6.0$ db.

In some applications, it might be desired to reduce the prediction uncertainty to some fixed value, say K decibels. In this case (41) may be written as

$$K = a\,\sigma_{rc}(p)\,, \tag{45}$$

and "a" determined first, before substituting in (44). In this case, "a" will be a function of the desired percentage value p.

Curves for K = 3 db are shown on Fig. 22. There is no real paradox in this approach, as it obviously takes more hours of measurements to reduce a large prediction uncertainty to a fixed value than to a very small one. This graph, however, illustrates the substantially greater prediction uncertainty associated with low-percentage fields which are important for jamming or interference studies. While it takes 145 days of measurements to reduce the prediction uncertainty associated with 99% of all hours (service fields) to 3 db, it would take more than 10,000 days (27 years) of measurements to reduce the prediction uncertainty of 1%-of-all hours interference fields to the same 3 db value.

Figs. 20, 21, and 22 should not be interpreted as indicating where and for how long measurements should be made. This question still depends on the relative cost of measurements versus, say, the cost of more transmitter power or larger antennas. If, for instance, the calculations for a particular path result in the requirement of 10 kw transmitter power and 60-ft parabolic reflectors, which would provide the specified grade of service or better with a probability of 0.95 during 99% of all hours, and if two weeks of measurements might be expected to show that 28-ft antennas would provide a similar service probability, the designer will have to balance the cost of the measurements against the cost of installing and maintaining the larger antennas with due regard to the fact that the larger antennas would, in any case, provide a better service. Of course, there is always a possibility that measurements will show that more power, or larger antennas are required, as indicated

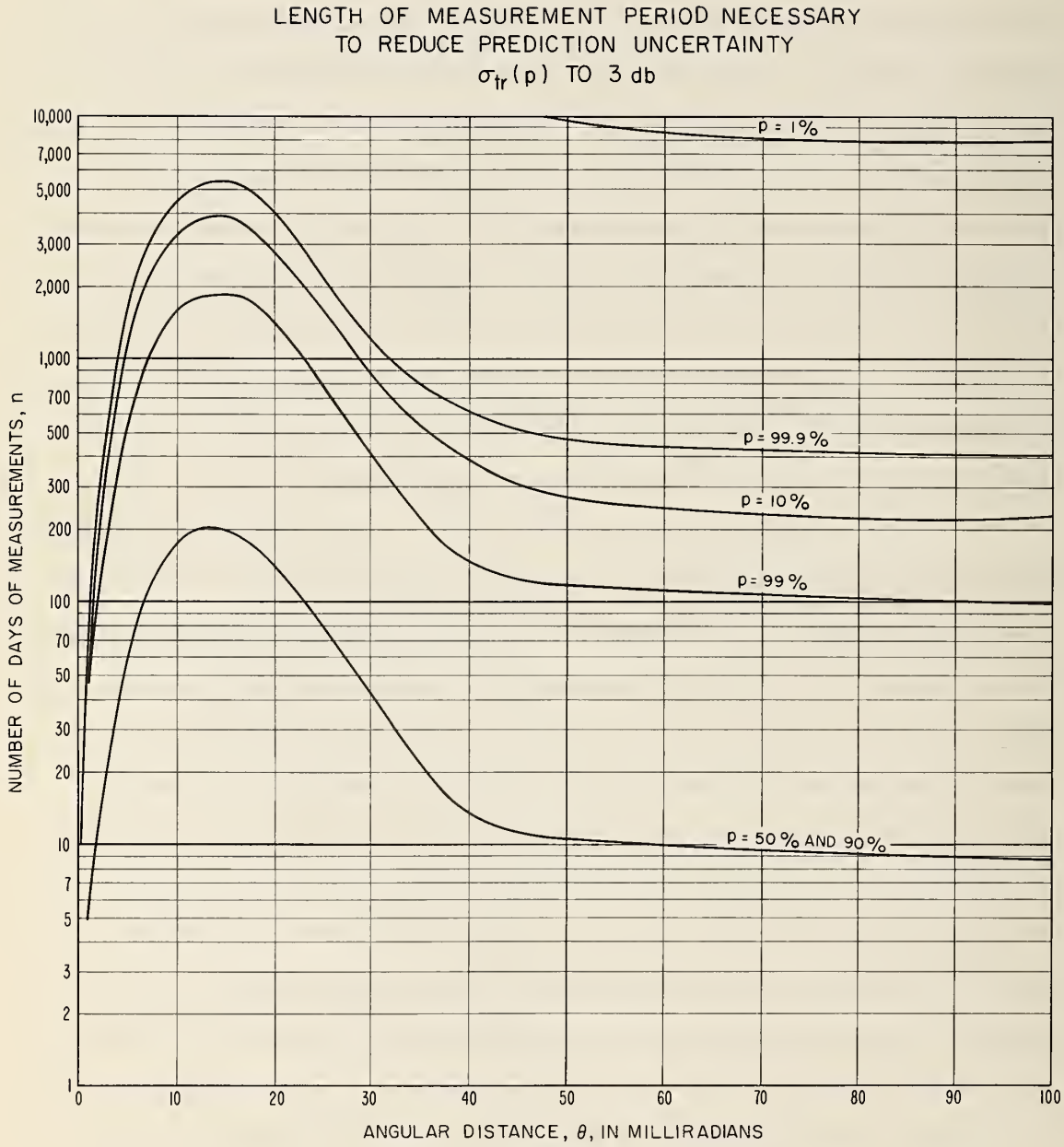
LENGTH OF MEASUREMENT PERIOD NECESSARY
TO REDUCE PREDICTION UNCERTAINTY
$\sigma_{tr}(p)$ TO 3 db
NUMBER OF DAYS OF MEASUREMENTS, n
10,000
7,000
5,000
3,000
2,000
1,000
700
500
300
200
100
70
50
30
20
10
7
5
3
2
1
0
10
20
30
40
50
60
70
80
90
100
ANGULAR DISTANCE, θ, IN MILLIRADIANS
p = 1%
p = 99.9%
p = 10%
p = 99%
p = 50% AND 90%

Figure 22

by the example in the previous section. In general, it is quite likely that measurements over a particular path will only serve to confirm the estimates made solely on the basis of calculations.

The methods outlined in this section may also be used as a basis for specifying acceptance tests for a completed communications link. This could be done by specifying a range of values of hourly basic transmission loss medians calculated on the basis of (43) and graphs similar to Figs. 20 and 21. Measured values may then be expected to lie within this range, which is a function of angular path distance and the number of days of testing required. It is intended to study this matter further and to publish results at a later date.

The basic concept of service probability and the methods for making predictions and for determining prediction uncertainty are expected to be valid in spite of possible changes in the detailed procedures. It has already been pointed out that the estimates of the prediction uncertainty for percentage values other than the median are based on an approximate statistical analysis. The fundamental problems involved are under study now, and their solution will possibly provide a slightly different curve of $\sigma_c(p)$, replacing the one shown on Fig. 9. Re-evaluation of available data, and the addition of new data may also affect the curve. Final results in any particular case may also be affected by the estimate of the calibration error σ_e, and the equipment error σ_r. The data and constants used in this paper, however, constitute the best available estimates to date, and may be used without serious reservation in the prediction of the performance of long-distance tropospheric communication circuits.

9. ACKNOWLEDGEMENTS

The authors are indebted to Messrs. R. S. Kirby and J. W. Herbstreit for their careful review of the original material, and for their suggestions. Drafting work on the figures was done by Mr. J. C. Harman and his group. Personnel of the Propagation-Terrain Effects Section participated in the measurement program and data evaluation used for the examples. The manuscript was typed by Mrs. D. J. Hunt, Mrs. R. H. Rotherham, Mrs. L. A. Charles, Mrs. J. L. Nadgwick, and Miss S. J. Bush. The studies leading to this paper were in part sponsored by the U. S. Air Force Ground Electronics Engineering Installation Agency and by U. S. Air Force Project 480-L in connection with the establishment of telecommunication performance standards for tropospheric communication circuits.

APPENDIX I

ANALYSIS OF VARIANCE OF LONG-TERM MEDIAN TROPOSPHERIC TRANSMISSION LOSS DATA

I.1 Introduction

It will be recalled from Section 6 that it is desired to assign a standard deviation $\sigma_{oe}(p, n)$ to observed field strength or transmission loss values, analogous to the standard deviation $\sigma_c(p)$ assigned to theoretical values. The standard deviation $\sigma_{oe}(p, n)$ is a function of the number of days of measurements n, and the percentage p of the hours within a given time block for which an improved prediction is desired. Weights are defined as the reciprocals of squared standard deviations or variances, and the improved prediction is obtained as a weighted average of predicted and measured values.

Variations in transmission loss are classified arbitrarily as short-term and long-term, with the hourly median value of observed transmission loss the basic unit for studying long-term variations. Seven hundred thousand values of hourly median transmission loss for 300 propagation paths and for frequencies between 40 and 4000 megacycles per second were grouped into eight "time blocks", defined in Table I-1, in order to allow for observed seasonal and diurnal trends. This appendix assumes then that data recorded within a single time block are statistically homogeneous. Transmission loss is less in summer than in winter on the average, and diurnal trends are usually most pronounced between May and October in the temperate latitudes of the northern hemisphere, with maximum transmission loss occurring in the afternoon.

Table I-1

Time Blocks

	Months			Hours
1.	Nov.	-	Apr.	0600 - 1300
2.	Nov.	-	Apr.	1300 - 1800
3.	Nov.	-	Apr.	1800 - 2400
4.	May	-	Oct.	0600 - 1300
5.	May	-	Oct.	1300 - 1800
6.	May	-	Oct.	1800 - 2400
7.	May	-	Oct.	0000 - 0600
8.	Nov.	-	Apr.	0000 - 0600

The hours in Table I-1 refer to local standard time at the receiver.

Methods for examining the statistical behavior of data within these groups or any other time blocks similarly defined are developed in this appendix. The following sections explain the theory for a statistical model, describe the data used to obtain variances and correlation functions, and explain how the data were analyzed.

Estimates of the path-to-path variance have been obtained by analyzing deviations of observed time block medians from predicted values obtained by the methods of Rice, et al [1959]. A total of 223 full time blocks representing 53 different propagation paths shows a mean square deviation of observed from predicted time block medians equal to 19.35 db^2 and a mean square value for the year-to-year variance of time block medians equal to 4.62 db^2. The difference of these variances, 14.73 db^2, is taken as the best available estimate of path-to-path variance, and 2 db^2 of this variance is attributed to equipment and reading errors which vary from path to path. The remaining variance, $\sigma_c^2 = 12.73\ db^2$ is the error assigned to the prediction of an infinite-time median value for a given path. The

corresponding standard error, $\sigma_c(p = 50\%) = 3.57$ db, represents the standard error of prediction of any time block median.

In order to evaluate the effect of the length of a recording period on the reliability of measured long-term median values, data samples recorded over six months to several years are first broken down into smaller samples, and the variance of the medians of these shorter periods about their mean is analyzed in Section I.4.

Section I.5 of this appendix shows how $\sigma_c^2(p)$ is estimated for values of time availability other than 50 per cent, and Section I.6 describes the effect of the length of a recording period on the variance of percentiles $L_o(p)$ other than the long-term median transmission loss, $L_o(50)$.

I.2 A Statistical Model

Let L_t denote a single hourly median value of radio transmission loss as observed over a given propagation path during a given time block:

$$L_t = L_c + b + \delta + \xi_t , \qquad (I\text{-}1)$$

where b is the unknown fixed bias of the calculated value L_c, while δ is a random variable with mean zero and variance σ_δ^2 associated with the particular path being considered, and ξ_t is a random variable with mean zero and variance σ_ξ^2 associated both with the hour of recording and with the path; δ does not vary with time, but only from path to path, while ξ_t varies from hour to hour and from path to path.

The random variables δ and ξ_t are defined for all paths and for all possible atmospheric conditions that might be associated with each path, assuming a given set of values of the parameters used by Rice et al [1959] for predicting transmission loss.

Since the mean square deviation between the observed and predicted time block medians for 223 nearly full time blocks was found to be equal to 19.35 db^2, it follows that the mean square bias $b^2 < (19.35/223) = 0.087\ db^2$ which is small compared to either σ_δ^2 or σ_ξ^2. Consequently we may neglect b and write (I-1) as:

$$L_t = L_c + \delta + \xi_t \tag{I-2}$$

For a given hour, t, the average of any random variable such as L_t over the ensemble of all paths is referred to as the conditional expected value $E_r(L_t)$. The unconditional expected value of L_t over the total ensemble of all paths and all atmospheres is $E(L_t)$.

In a very complex fashion, L_c is determined by propagation theory and data including those whose variance is analyzed here. To a first approximation, each calculated value depends on an average of all available data, using propagation theory to normalize data to a single set of values of the prediction parameters.

The path-to-path deviation, δ, is assumed equal to the sum of a random error, δ_c, which allows for random propagation phenomena, and a reading and equipment error, δ_e. Each of these random variables is fixed for a given path and varies from path to path, but not from hour to hour:

$$\delta = \delta_c + \delta_e \ . \tag{I-3}$$

It is assumed that

$$E(\delta_c) = E_r(\delta_c) = 0, \qquad E(\delta_e) = E_r(\delta_e) = 0, \tag{I-4}$$

and that prediction errors, δ_c, are not correlated with reading and equipment errors, δ_e. Variances of these quantities are

$$E(\delta^2) = \sigma_\delta^2 = \sigma_c^2 + \sigma_e^2, \ \sigma_c^2 = E(\delta_c^2), \ \sigma_e^2 = E(\delta_e^2) \tag{I-5}$$

The error ξ_t in (I-2) allows mainly for random propagation phenomena, as well as for equipment and reading errors not allowed for by δ_e. It is assumed that

$$E(\xi_t) = E_r(\xi_t) = E_t(\xi_t) = \lim_{T\to\infty} \frac{1}{T} \sum_{t=1}^{T} \xi_t = 0 \qquad \text{(I-6)}$$

With these assumptions, (I-2) implies that

$$E(L_t) = E_r(L_t) = L_c \,, \qquad \text{(I-7)}$$

It also follows that

$$E_t(L_t) = \lim_{T\to\infty} \frac{1}{T} \sum_{t=1}^{T} L_t = (L_c + \delta_c) + \delta_e \qquad \text{(I-8)}$$

Thus an ergodic hypothesis is made that the average of L_t over all time equals the conditional expected value $E_t(L_t)$ over the infinite ensemble of all possible atmospheres that might be associated with a particular path, r. It is also assumed that the process which produces random values of ξ_t from hour to hour within a given time block over path r is stationary, or, in this case, that the expected statistical distribution and serial correlation of T successive values of ξ_t does not depend on t. The expected distribution in time of ξ_t does depend on the path, r.

The engineer proposing to install a communication link over a given path is usually interested in the "true value", $(L_c + \delta_c)$, for this path. The true value is never known; it is a random variable with a variance about the predicted value equal to σ_c^2, as defined by (I-5) and estimated to be 12.73 db^2.

There is assumed to be no correlation between any pair of the variables δ_c, δ_e, and ξ_t:

$$E(\delta_c \delta_e) = E(\delta_c \xi_t) = E(\delta_e \xi_t) = 0, \tag{I-9}$$

so that the variance of all hourly medians, L_t, over the total ensemble of paths and atmospheres is

$$E[(L_t - L_c)^2] = \sigma_c^2 + \sigma_e^2 + \sigma_\xi^2 \tag{I-10}$$

where the variance of ξ_t over the total ensemble is

$$\sigma_\xi^2 = E(\xi_t^2). \tag{I-11}$$

The conditional variance of ξ_t for all possible atmospheres and a single given path, r, is

$$\sigma_r^2 = E_t(\xi_t^2), \tag{I-12}$$

another random variable whose expected value $E(\sigma_r^2)$ is σ_ξ^2. The conditional variance of $L_t - L_c$ over all possible atmospheres that might be associated with a given path is

$$E_t[(L_t - L_c)^2] = \delta^2 + \sigma_r^2. \tag{I-13}$$

The sample hour-to-hour variance s_ξ^2 of ξ_t for a sequence $\xi_1, \xi_2, \ldots, \xi_t, \ldots, \xi_T$ differs somewhat from σ_r^2, as may be seen in what follows:

$$s_\xi^2(T) = \frac{1}{T-1} \sum_{t=1}^{T} (\xi_t - \bar{\xi})^2 = (\overline{\xi^2} - \bar{\xi}^2)\left(\frac{T}{T-1}\right), \tag{I-14}$$

where sample mean-square and sample mean values of ξ_t for a given path are

$$\overline{\xi^2} = \frac{1}{T} \sum_{t=1}^{T} \xi_t^2, \quad \bar{\xi} = \frac{1}{T} \sum_{t=1}^{T} \xi_t. \tag{I-15}$$

Consecutive hourly medians recorded over a given path are serially correlated in time. The random process which selects values of ξ_t from all possible atmospheres introduces a covariance with respect to time of hourly medians separated by $|t_1 - t_2|$ hours. It is assumed that

$$E_t(\xi_{t1}\,\xi_{t2}) = \sigma_r^2\,\rho_h(q), \qquad q = |t_1 - t_2|, \tag{I-16}$$

and that the normalized hour-to-hour autocorrelation function $\rho_n(q)$ is not a random variable, but is the same for every path. It follows that

$$E(\xi_{t1}\xi_{t2}) = \sigma_\xi^2\,\rho_h(q)\ . \tag{I-17}$$

From (I-14) and (I-16):

$$E_t(s_\xi^2) = \left[\frac{1}{T}\sum_{t=1}^{T} E_t(\xi_t^2) - \frac{1}{T^2}\sum_{\substack{t_1=1\\ t_2=1}}^{T} E_t(\xi_{t1}\xi_{t2})\right]\left(\frac{T}{T-1}\right) \tag{I-18}$$

The double summation in (I-18), may be expressed as

$$\sigma_r^2\,z_h(T) = \sigma_r^2\left[\frac{1}{T} + \frac{2}{T^2}\sum_{q=1}^{T-1}(T-q)\,\rho_h(q)\right], \tag{I-19}$$

so that

$$E_t(s_\xi^2) = \sigma_r^2\left[1 - z_h(T)\right]\left(\frac{T}{T-1}\right) \tag{I-20}$$

$$E(s_\xi^2) = \sigma_\xi^2\left[1 - z_h(T)\right]\left(\frac{T}{T-1}\right)\ . \tag{I-21}$$

If hourly medians ξ_t were not correlated, $z_h(T)$ would equal $1/T$; in such a case $E_t(s_\xi^2) = \sigma_r^2$ and $E(s_\xi^2) = \sigma_\xi^2$. If hourly medians were perfectly correlated for all values of q, $z_h(T)$ would be unity and s_ξ^2 would be zero, regardless of the values of σ_r^2 and σ_ξ^2.

If consecutive hourly medians were not correlated, the variance among estimates of the long-term medians obtained from several samples of the same size would be inversely proportional to the number of hourly medians in each sample. With tropospheric transmission loss data, there is a high degree of correlation of observations obtained from hour to hour, less from day to day, and almost no measurable correlation from year to year.

As a general rule, $\rho_h(q)$ may be set equal to zero for all q greater than some fixed value, and then T may be chosen sufficiently large so that $z_h(T)$ is approximately equal to $1/T$. The sample variance $s_\xi^2(T)$ is in such a case a fairly good estimator of σ_r^2, and the average of σ_r^2 over a large number of paths is a good estimator of σ_ξ^2.

Section I.4 shows how data are used to analyze the effect of sample length on the variability of long-term medians, obtaining estimates of the expected variance of the median of a sample recording of any length. The form of the hour-to-hour autocorrelation function $\rho_h(q)$ required by the statistical model described in this section is determined indirectly.

Let $L_k(\tau)$ be the mean of the k^{th} consecutive τ-hour sample in a total period of T hours:

$$L_k(\tau) = \frac{1}{\tau} \sum_{t=1+\tau(k-1)}^{\tau k} L_t, \qquad \text{(I-22)}$$

where $k = 1, 2, 3, \ldots$, and $k = T/\tau$.

The index t used in this appendix numbers hours chronologically from t = 1 to t = T for the year y = 1, from t = T + 1 to 2T for y = 2, and so on; t goes from 1 + T(y - 1) to Ty in any given year, where y = 1, 2, 3, ..., Y. L_c is the "expected value" $E[L_t]$ of transmission loss for an ensemble which includes an infinity of paths having identical prediction parameters, and $L_c + \delta$ is the time average for an infinite ordered set of hours, t, including H hours per day, N days per year, and an infinite number of years.

Besides the hour index t and year index y, a day index, ν, is defined. Each of the indices t, ν, and y may range from one to infinity, or for finite recording periods they may range from one to T, N, and Y, respectively. For simplicity it is assumed that the total number of days in a year, N, always equals 180 for any of the time blocks of Table I-1. T = HN equals 900 for Time Blocks 2 and 5 where the number of hours H per day is 5. For Time Blocks 1, 3, 4, and 6, H = 6 and T = 1080, and for Time Blocks 7 and 8, H = 7 and T = 1260. Note that as day follows day, in Time Block 2, for instance, the gap between 1800 hours one day and 1300 hours the next day is considered no greater than the gap between consecutive hours of a single day; and similarly, April 30 is followed immediately not by May 1, but by November 1. Each of the eight time blocks of Table I-1 is considered to be a homogeneous statistical sample, for which Rice et al [1959] estimate the expected cumulative distribution, $L_c(p)$, of hourly median transmission loss values.

Let L_ν represent the mean value for a single day of the H hourly median values recorded during that day, and let L_y represent a yearly mean of hourly medians. Symbols λ_ν and γ_y are introduced to denote the error of the daily mean and yearly mean, respectively, assuming that these values are used to estimate $L_c + \delta$:

$$L_t = L_c + \delta + \xi_t, \tag{I-2}$$

$$L_\nu = \frac{1}{H} \sum_{t=1+H(\nu-1)}^{H\nu} L_t = L_c + \delta + \lambda_\nu \tag{I-23}$$

$$L_y = \frac{1}{HN} \sum_{t=1+HN(y-1)}^{HNy} L_t = L_c + \delta + \gamma_y, \tag{I-24}$$

where from (I-6) it follows that mean values of λ and γ are zero over all paths, all atmospheres, or all hours.

If it were known how many independent observations n' are represented by a sample of n days, the theory for assigning weights to long-term medians obtained with short samples would be quite simple; the weights would be directly proportional to n'. There is so much more correlation from hour to hour during a single day than there is from day to day that it was decided to use the number of days in a sample rather than the number of hours as a first estimate of the number of observations upon which the weight of a sample should be based.

If each τ-hour period in (I-22) includes $n = \tau/H$ days, then

$$L_k(n) = \frac{1}{n} \sum_{\nu=1+n(k-1)}^{nk} L_\nu \tag{I-25}$$

as defined originally by (I-22), is also the mean of the k^{th} n-day sample in a total period of T hours, where $T = K\tau$ and $\tau = nH$.

The mathematics used to evaluate (I-18) is used here to write expressions for the conditional variances $E_t(\lambda_\nu^2)$ and $E_t(\gamma_y^2)$ of λ_ν and γ_y in terms of the function z_h defined by (I-19):

$$\sigma_\lambda^2 = E_t(\lambda_\nu^2) = \sigma_r^2 z_h(H), \quad E(\sigma_\lambda^2) = \sigma_\xi^2 z_h(H) , \tag{I-26}$$

$$\sigma_\gamma^2 = E_t(\gamma_y^2) = \sigma_r^2 z_h(T), \quad E(\sigma_y^2) = \sigma_\xi^2 z_h(T) \tag{I-27}$$

Defining a day-to-day autocorrelation function $\rho(s)$ as well as the hour-to-hour autocorrelation function, $\rho_h(q)$ defined by (I-16):

$$E_t(\lambda_{\nu_1} \lambda_{\nu_2}) = \sigma_\lambda^2 \rho(s), \quad s = |\nu_1 - \nu_2| \tag{I-28}$$

$$\rho(s) = \frac{1}{H^2 \sigma_\lambda^2} \sum_{t_1=1}^{H} E_t \left[\xi_{t_1} + H(\nu_1 - 1)\ \xi_{t_2} + H(\nu_2 - 1)\right]$$

$$= \frac{1}{z_h(H)} \left\{\frac{\rho_h(sH)}{H} + \frac{1}{H^2} \sum_{q=1}^{H-1} (H - q) \left[\rho_h(sH + q) + \rho_h(sH - q)\right]\right\} \tag{I-29}$$

Section I.4 evaluates $\rho_h(q)$ for H = 5 and H = 6 and uses these estimates and (I-29) to derive $\rho(s)$ for H = 5 and H = 6. A function, z(n) which depends on $\rho(s)$ is defined in the same way as $z_h(T)$, which depends on $\rho_h(q)$:

$$z(n) = \frac{1}{n} + \frac{2}{n^2} \sum_{s=1}^{n-1} (n - s)\ \rho(s) \tag{I-30}$$

In standard texts dealing with continuous functions and with integrals instead of summations,

$$z(n) = \frac{2}{n} \int_0^n dx(1 - x/n)\, \rho(x).$$

It is seen that the time variance σ_y^2 of yearly mean values for a fixed path r, given by (I-27), may also be written

$$\sigma_y^2 = \sigma_\lambda^2\, z(180) \tag{I-31}$$

assuming 180 days in every time-block year.

The expected variance in time of observed n-day mean values $L_k(n)$ relative to the true value $L_c + \delta$ for path r is

$$\hat{\sigma}_o^2(n) = E_t\{[L_k(n) - (L_c + \delta)]^2\} = \sigma_\lambda^2\, z(n) = \sigma_r^2\, z_h(\tau) \tag{I-32}$$

where $\tau = Hn$, and H = 5, 6, or 7, as may be seen from Table I-1. Section I. 4 uses (I-32) with other relationships to define $\rho_h(q)$, defines $\rho(s)$ in terms of $\rho_h(q)$ for H = 5 and H = 6, using (I-29), and finally estimates $\sigma_o^2(n) = E[\hat{\sigma}_o^2(n)]$, an average over all paths of the conditional variance $\hat{\sigma}_o^2(n)$ defined by (I-32). The desired weight for the mean or median of an n-day sample is taken to be $1/\sigma_{oe}^2(n)$, where

$$\sigma_{oe}^2(n) = E\{[L_k(n) - (L_c + \delta_c)]^2\} = \sigma_e^2 + \sigma_\xi^2\, z_h(n) \tag{I-33}$$

and σ_ξ^2 is approximated by fitting curves through estimates of σ_r^2 as obtained from data for 73 time blocks representing 29 different paths. Each path corresponds to different values of the prediction parameters, so it is assumed that the statistical model outlined in this section is the same for each of the 73 double ensembles. Values for some of the

parameters depend on the time block involved, so Section I. 4 refers to $\sigma_{\xi}^{2}(H)$, $\rho_{h}(q, H)$, $z_{h}(q, H)$, $\rho(n, H)$, $z(n, H)$, $\hat{\sigma}_{o}^{2}(h, H)$, and $\sigma_{o}^{2}(n, H)$, in order to reflect this fact.

I. 3 Description of Data

During the period from 1949 to 1954 the Central Radio Propagation Laboratory of the National Bureau of Standards had contracts with the following agencies to measure the hourly medians of field strength of a large number of commercial television stations and FM radio stations over the United States:

University of Washington

University of Illinois

University of Texas

Pennsylvania State College

United Broadcasting Company

Collins Radio Corporation

Federal Communications Commission

In addition, CRPL operated transmitters on Cheyenne Mountain and Pikes Peak and at Fort Carson near Colorado Springs in Colorado. Radio transmission loss over paths from these transmitters was measured at sites near Kendrick, Karval, Haswell, and Sheridan Lake, Colorado, and near Garden City and Anthony, Kansas, and Fayetteville, Arkansas.

Data collected from these various sources were put on IBM punch cards and listed in descending order of field strength within each of the eight time blocks of Table I-1. A recent NBS Technical Note [Williamson, Fuller, et al , 1960], tabulates some of these data within summer and winter (all day) time blocks. The total possible number of hours of data in a full time block ranges from 1288 for a seven-hour period to 910 for a five-hour period. No time block was completely filled with data since there were times when either the transmitter was off the air for some time or the receiver was out of service. The largest number of hours actually recorded for a time block was 1199 while the lowest was eight. The average number of hourly medians per time block was 365. From these two thousand 6-month, 6-hour groups of data, 73 were selected, representing 29 different propagation paths and a wide range of frequency, distance, angular distance, and antenna height. Of the 73 sets of data, 51 time blocks were nearly full, including more than 700 of the total possible number of T observed hourly medians. The major propagation path characteristics for these data are listed by Williamson et al [1960]. Their selection was based on the following criteria:

1. In general, recordings were selected representing as nearly full time blocks as possible.

2. The paths selected cover a wide geographical area of the United States to get sampling of a variety of terrain and climatic conditions.

3. A wide range of frequency is represented in the study.

4. Time blocks were selected which had a minimum number of "greater than" and "less than" values. Sometimes field strength goes above the highest value that can be measured with the equipment in use or drops into the noise level. These values were listed as "greater than" the highest value which could be measured or "less than" the lowest value above the noise level. They will be referred to later as cut-off values.

To obtain the weights derived in this report, each of the 73 selected time blocks was divided into smaller and smaller consecutive non-overlapping groups from the first to the last day in each time block.

In determining the median of each of the K samples of size n days, "cut-off values" in a sample were counted as valid pieces of data if all the "greater thans" were above and the "less thans" were below the median value. If "cut-off" values affected the median, as for instance when one or more "less than" was above the median or when the median itself was a "cut-off" value, these data were eliminated from the analysis.

I.4 Analysis of the Effect of Sample Length on the Variability of Long-Term Medians

Given K consecutive non-overlapping samples of length n days recorded over a given path within a given time block, the mean, $L_k(n)$, of each of the K samples was approximated by its median; then the variance of these medians about their mean L_y was calculated for each group of K medians:

$$s_o^2(n) = \frac{1}{K} \sum_{k=1}^{K} [L_k(n) - L_y]^2 \qquad \text{(I-34)}$$

where L_y and $L_k(n)$ are defined by (I-24) and (I-25).

Corresponding to the 73 values of $s_o^2(n)$ and to ten pre-selected values n = 1/H, 0.5, 1, 2, 5, 10, 15, 30, 60, and 90 days, there were 730 values of sample variance as defined by (I-23). For n = 1/H, τ = 1; for n = 0.5, τ = 3 in the four time blocks where H = 6, and τ is alternately 2 and 3 for H = 5 and alternately 3 and 4 for H = 7. Studying these values of s_o^2, it was apparent that they depend upon the angular distance, θ, corresponding to each of the 29 propagation paths represented. The angular distance is the angle between horizon rays from transmitter and receiver. Methods for its determination and its importance to various aspects of radio wave propagation by diffraction and tropospheric forward scatter are discussed in a number of recent reports, [Rice et al, 1959; Norton, Rice and Vogler, 1955]. The symbol $s_o^2(n, \theta)$ will be used now to denote variances defined by (I-34).

Figure I-1 shows $s_o^2(n, \theta)$ for the four fixed values n = 1/H, 1, 10, and 30 days plotted versus the angular distance, θ. Also shown on Figure I-1 is the function

$$f_1(\theta) = [(\theta - 0.3) \exp(-0.003\ \theta^2) + 2] \qquad \text{(I-35)}$$

which was selected to fit these data as well as any other simple arbitrary function of θ having a single maximum between finite values $f_1(0)$ and $f_1(\infty)$. The selection of a function of θ which would fit the data well enough to be usable was simplified by the following process: overlapping intervals were chosen along the abscissa scale of the data plot, and for each interval the median ordinate was plotted against the median abscissa. The curve represented by (I-35) was chosen as the simplest one that could be made to go through or very near to these median values and which would at the same time extrapolate to reasonable values for $\theta = 0$ and $\theta \to \infty$. The decision as to what is a reasonable value for $\theta \to \infty$ was made by studying <u>all</u> the data compiled by Williamson et al [1960], rather than only the data used in this study. The set of points for 47 milliradians corresponds

THE VARIANCE OF n - DAY MEDIANS VS SAMPLE LENGTH AND ANGULAR DISTANCE, θ

THE CURVES SHOW $f_1(\theta)\, g_1(n)$ FOR EACH VALUE OF $f_1(\theta) = [(\theta - 0.3) \exp(-0.003\,\theta^2) + 2]$

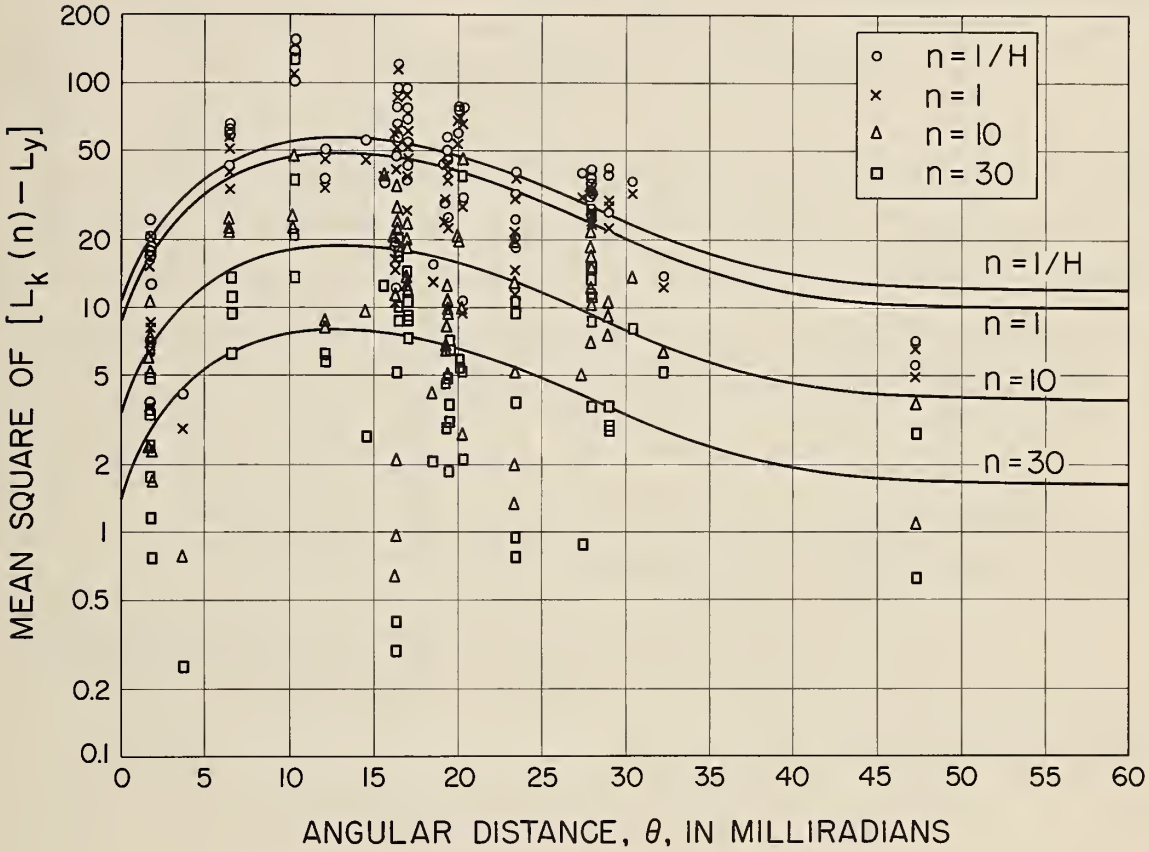

Figure I–1

to time blocks with fewer than 700 hours of recording available. Figure I-1 shows $f_1(\theta)$ normalized to fit the data, as explained in Step 1, below.

Note that Figure I-1 shows $s_o^2(n, \theta)$ plotted on a logarithmic scale; it is assumed that

$$\ell n [s_o^2(n, \theta)] = E \{\ell n [s_o^2(n, \theta)]\} + \epsilon , \qquad \text{(I-36)}$$

where ϵ is a random variable with a variance independent of θ, but dependent on n; the scatter of $\ell n[s_o^2(n, \theta)]$ shown on Figure I-1 seems consistent with this assumption. It is proposed to determine $f(\theta)$ by least squares curve fits of the data $\ell n[s_o^2(n, \theta)]$ to functions of the form $\ell n\, f(\theta) + \ell n g(n)$. The steps in this process are:

1. As a first estimate of g(n), define $g_1(n)$ for each of the ten preselected values of n as the median of the 73 values of $s_o^2(n, \theta)/f_1(\theta)$ available for a given n.

2. As a second estimate of $f(\theta)$, use the 730 values of $\ell n(s_o^2/g_1)$ to determine, by unweighted least squares, coefficients A and B for the assumed relation

$$\ell n\, f_2(\theta) = A + \ell n [(\theta - B) \exp (-0.003\, \theta^2) + 2] . \qquad \text{(I-37)}$$

The results are A = 0.0560, B = 1.167, exp A = 1.0576, so

$$f_2(\theta) = 1.0576 [(\theta - 1.167) \exp (-0.003\, \theta^2) + 2] \qquad \text{(I-38)}$$

is obtained as a second estimate of $f(\theta)$.

3. Estimate the variance of $\ell n(s_o^2)$ for each n:

$$\text{variance of } \ell n(s_o^2) = \frac{1}{72} \sum_{i=1}^{73} \{\ell n [s_i^2/f_2(\theta_i)] - \frac{1}{73} \sum_{j=1}^{73} \ell n [s_j^2/f_2(\theta_j)]\}^2 \qquad \text{(I-39)}$$

4. Denote by the symbol w(n) a weight defined as the reciprocal of each variance defined by (I-39):

Table I-2

u	n_u	$w(n_u)$	$g_1(n_u)$	u	n_u	$w(n_u)$	$g_1(n_u)$
1	1/H	2.92	5.98	6	10	1.19	1.95
2	0.5	2.91	5.84	7	15	1.06	1.40
3	1	2.75	5.07	8	30	0.92	0.83
4	2	2.43	3.54	9	60	0.53	0.45
5	5	1.82	2.41	10	90	0.27	0.14

5. Determine a weighted average value y_i of $\ell n(s_o^2/g_1)$ for $i = 1, 2, 3, \ldots, 73$ and find by weighted least squares coefficients A, B, C for the assumed relation

$$\ell n[f_3(\theta)] = A + \ell n[(\theta - B)\exp(-0.003\,\theta^2) + C], \qquad \text{(I-40)}$$

where the data fitted by least squares to (I-40) are

$$y_i = y(\theta_i) = \{\sum_{u=1}^{10} w(n_u)\,\ell n[s_{iu}^2(n_u, \theta_u)/g_1(n_u)]\}/\sum_{u=1}^{10} w(n_u) \qquad \text{(I-41)}$$

(See Table I-2). As explained at the beginning of this section, it may be assumed that $\ell n(s_o^2) = \ell n(fg) + \epsilon$, where ϵ is a zero-mean random variable whose variance $1/w(n)$ is independent of θ. The least squares determinations of the coefficients in (I-40) which define the third estimate $f_3(\theta)$ of $f(\theta)$ are A = 0.1155, B = 1.9, C = 2.6.

Next, the year-to-year variance σ_γ^2 defined by (I-27) is estimated. There are available 65 pairs of "full" time blocks for successive years, and 25 triplets, each comprising three successive years of observations in the same time block over the same path. For

this purpose, wherever more than 700 hours of observations are available, a time block is considered full. Make the following assumption:

$$E(\sigma_\gamma^2) \equiv \sigma_o^2(180) = C\, f_3(\theta) \equiv f(\theta) \qquad \text{(I-42)}$$

Define C using the pooled variance of year-to-year variances determined from the 65 pairs and 25 triplets described above, where Δ_i is the deviation of a time block median from the average of a pair or triplet of "full" time blocks:

$$C = \frac{\sum_{i=1}^{205} [\Delta_i^2 / f_3(\theta)]}{205-65-25} = 0.76155 \qquad \text{(I-43)}$$

From (I-39), (I-42), and (I-43),

$$E(\sigma_\gamma^2) = f(\theta) = 0.7\,[(\theta - 1.9)\exp(-0.003\,\theta^2) + 2.6] \qquad \text{(I-44)}$$

The year-to-year variance $f(\theta)$ is plotted as Figure 14 of the main body of this paper.

Now the assumption that $s_o^2(n, \theta) = f(\theta)\, g(n)$ is modified as

$$\sigma_o^2(n, \theta)/f(\theta) \equiv g(n, H) = \{f(\theta) + E[s_o^2(n, H, \theta)]\}/f(\theta) \qquad \text{(I-45)}$$

Here, $s_o^2(n, H, \theta)$ is the same as $s_o^2(n, \theta)$, but the H is fixed at 5, 6, or 7, and the requirement is added that only time blocks containing more than 700 hours of observations are to be used in estimating $g(n, H)$. Among the 73 time blocks used to define $f(\theta)$, 21 correspond to H = 5, 29 to H = 6, and only one to H = 7, of those representing more than 700 hourly median values of transmission loss. Table I-3 lists median values of $[f(\theta) + s_o^2(n, H, \theta)]/f(\theta)$ for H = 5 and H = 6 hours and for n = 1/H,

0.5, 1, 2, 5, 10, 15, 30, 60, 90 days as estimates $\hat{g}$ of g. Corresponding values of τ are also listed, as well as the final values of g, whose calculation will shortly be described.

Table I-3

Median Values of $[f(\theta) + s_o^2(n, H, \theta)]/f(\theta) = \hat{g}(n, H)$.

$$\sigma_o^2(n) = f(\theta)\, g(n, H)$$

H = 5:

n	τ	$\hat{g}$	g
1/5	1	6.47	6.96
1/2	2.5	6.42	6.06
1	5	5.50	5.40
2	10	4.62	4.60
5	25	3.06	3.57
10	50	2.79	2.87
15	75	2.54	2.50
30	150	1.96	1.96
60	300	1.51	1.51
90	450	1.19	1.30
180	900	-	1.00

H = 6:

n	τ	$\hat{g}$	g
1/6	1	11.79	12.90
1/2	3	10.52	10.26
1	6	9.22	8.44
2	12	6.25	6.80
5	30	4.55	4.85
10	60	3.73	3.67
15	90	2.54	3.09
30	180	1.95	2.28
60	360	1.62	1.67
90	540	1.11	1.38
180	1080	-	1.00

Since g(n, H) is the ratio of the variance of an n-day mean to the variance of a yearly mean, g(180, H) = 1 for any H; this explains the last line of Table I-3.

Someuseful relations are summarized and combined as follows:

$$z_h(\tau) = \frac{1}{\tau} + \frac{2}{\tau^2} \sum_{q=1}^{\tau-1} (\tau - q)\, \rho_h(q) \qquad \text{(I-19)}$$

$$E[\sigma_o^2(n)] = \sigma_\xi^2 z_h(\tau), \quad \tau = nH \tag{I-46a}$$

$$E(\sigma_\gamma^2) = \sigma_\xi^2 z_h(T) = \sigma_o^2(180) = f(\theta) \tag{I-46b}$$

$$g(n, H) \equiv \sigma_o^2(n)/f(\theta) = z_h(\tau, H)/z_h(T, H) \tag{I-47a}$$

$$g(1/H, H) = z_h(1, H)/z_h(T, H) = 1/z_h(T, H), \tag{I-47b}$$

$$z_h(\tau, H) = g(\nu, H)/g(1/H, H). \tag{I-48}$$

Define

$$x(\tau) \equiv \frac{\tau^2}{2}\left[z(\tau) - \frac{1}{\tau}\right] = \sum_{q=1}^{\tau-1} (\tau - q)\, \rho_h(q), \quad h(\tau) \equiv g(n, H) - 1 . \tag{I-49}$$

Then,

$$x(\tau) - x(\tau - 1) = \sum_{q=1}^{\tau-1} \rho_h(q) \tag{I-50}$$

$$\rho_h(\tau) = x(\tau + 1) + x(\tau - 1) - 2x(\tau)$$

$$= \frac{2 + (\tau + 1)^2 h(\tau + 1) + (\tau - 1)^2 h(\tau - 1) - 2\tau^2 h(\tau)}{2g(1/H, H)} \tag{I-51}$$

The hour-to-hour serial correlation $\rho_h(\tau)$ for H = 5 and for H = 6 was somewhat arbitrarily assumed to be of the form

$$\rho_h(\tau) = \frac{(1 + a\tau)^k}{1 + ka\tau} , \tag{I-52}$$

and values a = 3, k = 0.6 for H = 5 and a = 4.2, k = 0.5 for H = 6 were found to give good agreement between the statistical model and the data listed in Table I-3. The method of procedure was to select arbitrary values of g(1/H, H), a, and k, and to compare calculated values of $g(n) = g(1/H, H)z_h(\tau)$ with the data, plotting both g and τ on logarithmic scales: The parameter k determines the slope of g(n, H) at large τ, the parameter "a" moves the curve parallel to the log τ axis, and the parameter g(1/H, H) moves the curve up or down, parallel to the log g axis. Values of g(1/H, H) listed in Table I-3 were determined last, to satisfy the condition $g(180, H) \equiv 1$. Figure I-2 is a picture of the curves and data of Table I-3. Figure I-3 shows $\rho_h(\tau)$ plotted versus τ for H = 5 and H = 6. The functional form given by (I-52) is proportional to τ^k/τ for large τ and therefore has a Fourier cosine transform for $0 < k < 1$, satisfying the Khintchine theorem [Takács, 1960], which specifies a necessary and sufficient condition for a correlation function. For small τ, (I-52) approaches $1 - k^2 a^2 \tau^2$, which has a slope of zero at $\tau = 0$.

Next, (I-29) was used to calculate the serial correlation $\rho(n)$ of daily mean values separated by n days for H = 5 and H = 6. Figure I-4 shows these two autocorrelation functions.

The major difference between g(n) and $\rho_h(\tau)$, or $\rho(n)$ for Time Blocks 2 and 5 and the other time blocks arises not from the fact that H is less, but from the fact that there is little diurnal trend of the data in the afternoon time blocks. It is assumed that for Time Blocks 7 and 8 the functions g(n) and $\rho(n)$ are the same as those labeled H = 6, and that if one hour a day were recorded in any of these time blocks, $\rho(n, H)$ should be set equal to $\rho_h(\tau H, H)$. The dashed curves of Figure I-4 represent these functions.

With one more assumption, the final estimates of $\sigma_o^2(n, H)$ for Time Blocks 2 and 5 (H = 5), Time Blocks 1, 3, 4, 6, 7, 8 (H = 6),

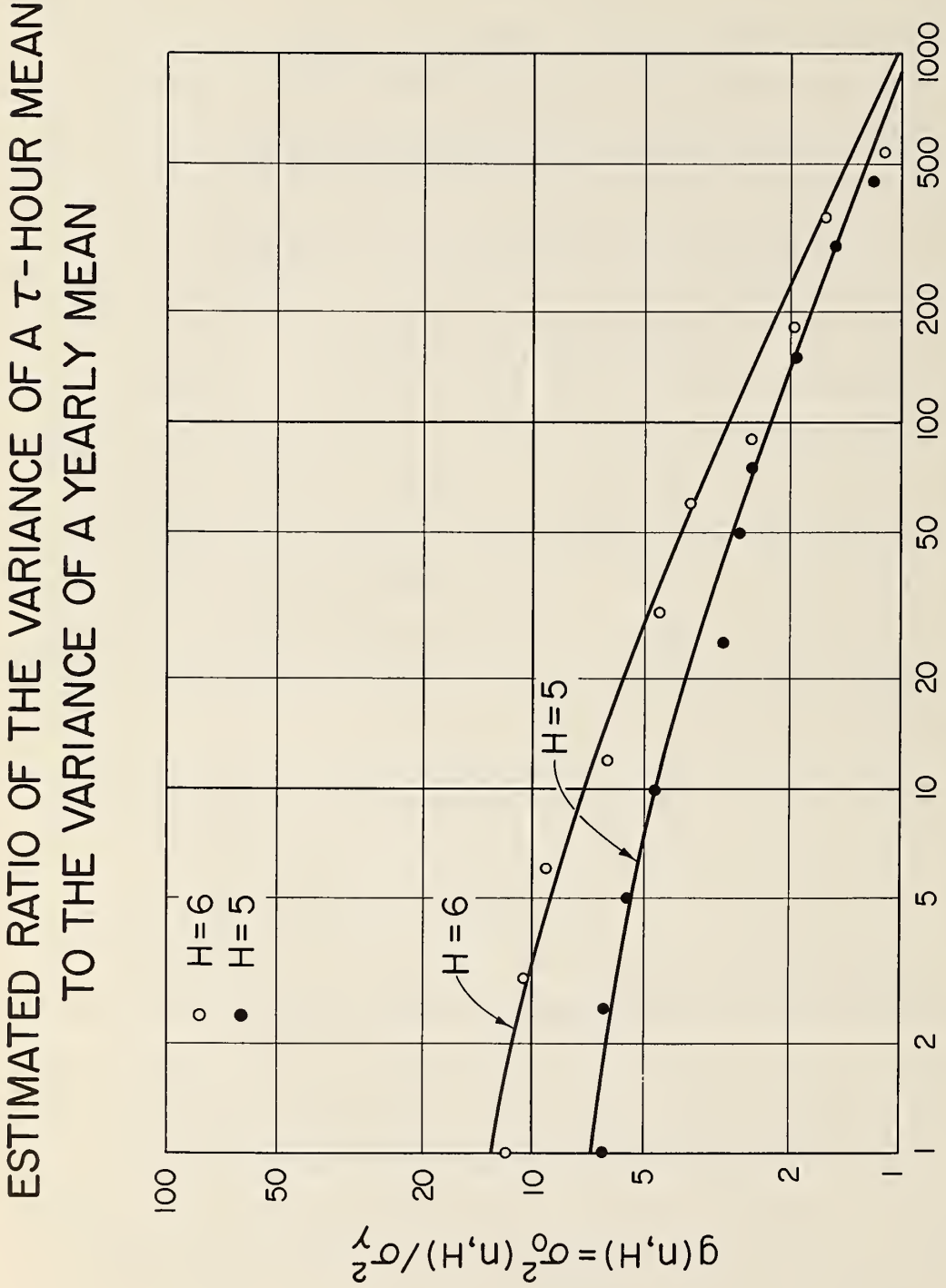
ESTIMATED RATIO OF THE VARIANCE OF A τ-HOUR MEAN
TO THE VARIANCE OF A YEARLY MEAN
g(n,H) = σ₀²(n,H)/σ_y²
100
50
20
10
5
2
1
H=6
H=5
H=6
H=5
1
2
5
10
20
50
100
200
500
1000
τ = NUMBER OF HOURS IN A RECORDING PERIOD

Fig. I-2

SERIAL CORRELATION OF HOURLY MEDIAN TRANSMISSION LOSS

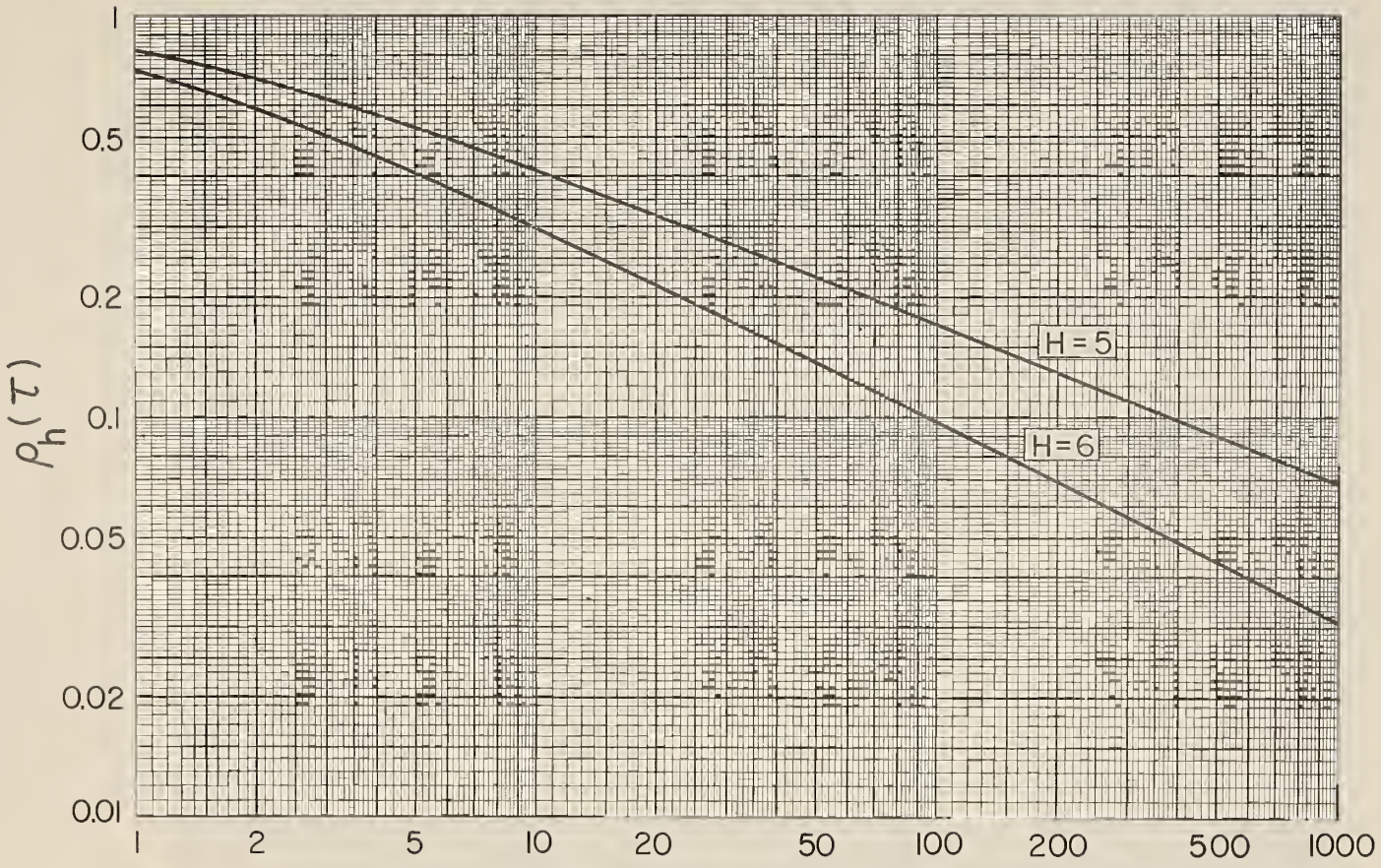

Figure I-3

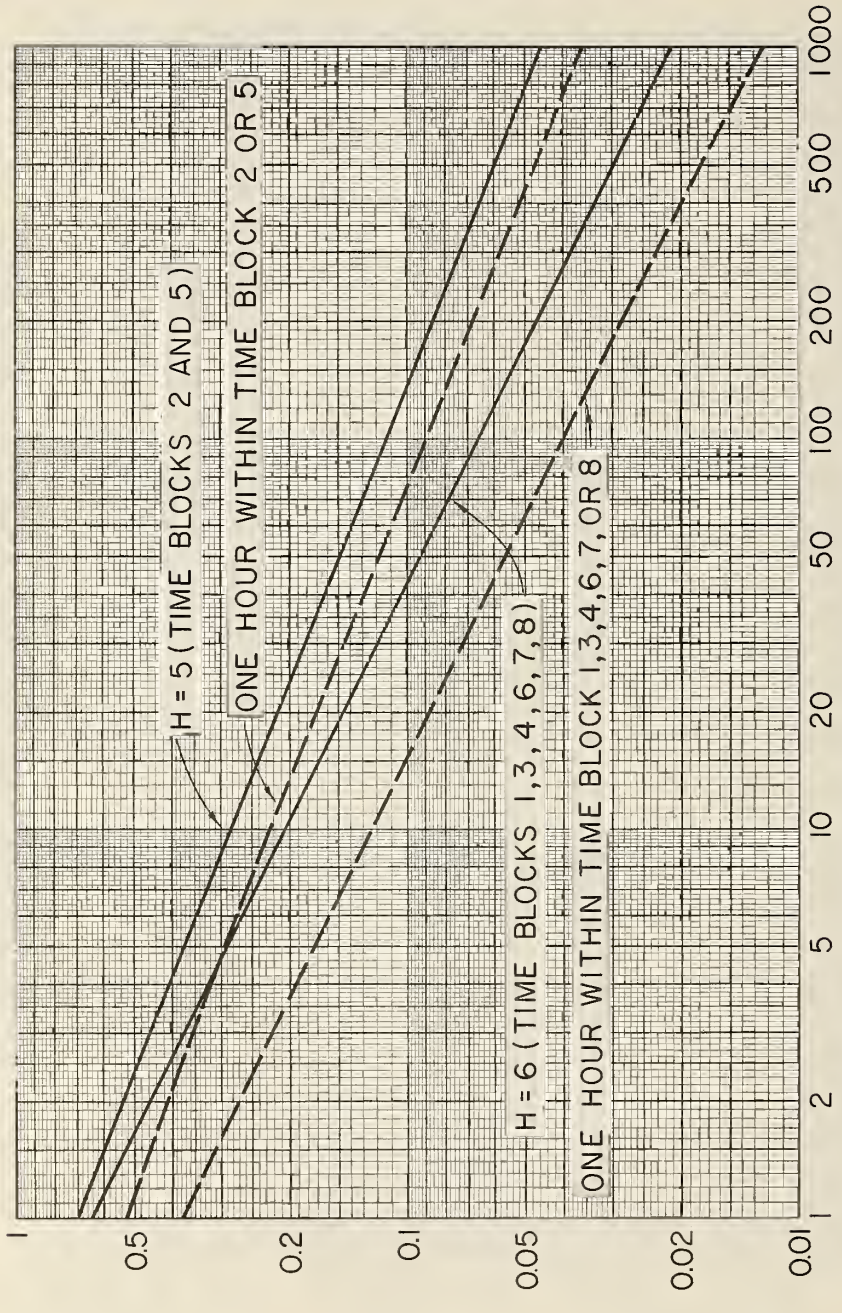
SERIAL CORRELATION OF DAILY MEAN TRANSMISSION LOSS
ρ (n)
1
0.5
0.2
0.1
0.05
0.02
0.01
H = 5 (TIME BLOCKS 2 AND 5)
ONE HOUR WITHIN TIME BLOCK 2 OR 5
H = 6 (TIME BLOCKS 1,3,4,6,7,8)
ONE HOUR WITHIN TIME BLOCK 1,3,4,6,7, OR 8
1
2
5
10
20
50
100
200
500
1000
n DAYS = SEPARATION OF DAILY MEAN VALUES IN A SINGLE TIME BLOCK

Fig. I-4

and all hours (all day and all year) may be plotted. Assuming that data obtained in any one time block are statistically independent of data obtained in any other, the variance $\sigma_o^2(n, H)$ for all hours is a weighted average: $\sigma_o^2(n, 24) = [2\sigma_o^2(n, 5) + 6\sigma_o^2(n, 6)]/8$. The heavy solid curve of Fig. 15 of the main body of this paper shows this estimate. As indicated, two of the curves in Fig. 15 show $\sigma_o^2(n, 5)$ and $\sigma_o^2(n, 6)$ from Fig. I-2, and two represent $\sigma_o^2(n, 1)$ for Time Blocks 2, 5, and 1, 3, 4, 6, 7, 8, respectively. This latter estimate is obtained from (I-32), replacing σ_λ^2 by $\sigma_\xi^2(H)$ and $\rho(s, H)$ in (I-30) by $\rho_h(sH, H)$.

The curves of Fig. 15 may be used to assign weights to mean or median values of transmission loss observed for n consecutive days in any of the time blocks of Table I-1. For other larger time blocks or where hours or days are not recorded consecutively, the statistical model of Section I.3 may still be used to calculate estimates of $\sigma_o^2(n, H)$, with assumptions similar to those of the preceding paragraph. A weight is defined as the reciprocal of the total variance of the quantity being considered. The variance $\sigma_o^2(n, H)$ includes time-varying equipment and reading errors and some of the prediction errors arising from not taking sufficient account of time trends and appropriate propagation mechanisms in the prediction methods. As (I-33) shows, a path-to-path equipment and reading error variance is added to $\sigma_o^2(n, H)$ to obtain the variance $\sigma_{oe}^2(n, H)$ of an n-day median value $L_k(n)$ about the "true" path median $L_c + \delta_c$.

I.5 The Prediction Uncertainty $\sigma_c^2(p)$ for Arbitrary Values of Time Availability, p

Let $L_o(p, n)$ denote the observed transmission loss exceeded by (100-p) per cent of the hourly medians recorded during an n-day period, and let $L_o(p, \infty)$ represent an infinite-time value, with $L_c(p)$

the corresponding calculated transmission loss. Replace (I-2) with

$$L_o(p,n) = L_c(p) + \delta_c(p,n) + \delta_e, \tag{I-53}$$

$$\lim L_o(p,n) = L_o(p,\infty) = L_c(p) + \delta_c(p) + \delta_e \tag{I-54}$$

Both $L_o(p,n)$ and $L_o(p,\infty)$ include a measurement error δ_e in addition to a path-to-path prediction error $\delta_c(p)$. Assuming that

$$L_c(50) = L_c, \quad \delta_c(50) = \delta_e \tag{I-55}$$

and that the mean and median of hourly medians L_t are the same for an infinite-time sample,

$$L_o(50,\infty) = L_c + \delta_c + \delta_e. \tag{I-56}$$

The prediction uncertainty $\sigma_c^2(p)$ is the path-to-path variance of the difference between the calculated percentile $L_c(p)$ and a "true" value, $L_o(p,\infty) - \delta_e$:

$$\sigma_c^2(p) = E\{[L_c(p) - L_o(p,\infty) + \delta_e]^2\} = E[\delta_c^2(p)] \tag{I-57}$$

Data used to estimate $\sigma_c^2(p)$ involve $L_o(p,n)$ rather than $L_o(p,\infty)$, but for this analysis the effect of finite samples is considered negligible compared to the large path-to-path variance of $L_o(p,n)$. Both in the main body of the paper and in what follows, $L_o(p)$ is used as an abbreviated form of $L_o(p,n)$.

Predicted and observed values of basic transmission loss, $L_{bc}(p)$ and $L_{bo}(p)$ were used to estimate $\sigma_c^2(p)$ as follows:

(A) For time blocks 2 and 4 and for 70 propagation paths, the mean square and variance of $L_{bc}(p) - L_{bo}(p)$ were determined for p = 1%, 10%, 50%, 90%, and 99%.

(B) For all hours and a total of 80 paths for two frequencies and two distance ranges (80 and 120 miles), the mean square and variance of $L_{bc}(p) - L_{bo}(p)$ were determined for the same values of p as in (A). (This was also done for time blocks 2 and 4, expected to represent fairly extreme conditions, and results were almost the same.)

Ideally, estimates of $\sigma_c^2(p)$ should be based on a comparison of observed and calculated values $L_{bo}(p)$ and $L_{bc}(p)$ at each percentage level p for a wide diversity of propagation paths for which all-day, all-year cumulative distributions are available. Data set (A) represent a wide diversity of paths, but not all hours, and (B) represents all hours over a large number of paths which are located in a single region in Ohio.

Long-term recordings over a large number of paths would be needed to establish accurately $\sigma_c^2(p)$ for each possible combination of the prediction parameters. The mean error of prediction will average to zero over the entire range of propagation path parameters represented by the available data, but this bias is not expected to be zero in a given region for given values of distance, angular distance, antenna height, frequency, and surface refractivity. Here, the mean square deviation of observed from predicted values of transmission loss, $\sigma_c^2(p) + \sigma_e^2$, is the sum of (1) a variance about the mean prediction error, (2) the square of this bias, and (3) the equipment and reading error σ_e^2.

The variance of prediction error about its mean value was assumed independent of all prediction parameters except p and was estimated from data set (B), observed and predicted values for p = 1%, 10%, 50%, 90% and 99% of all hours corresponding to two Ohio FM stations, each recorded for one year at 80 and 120 miles over a total of 80 propagation paths. The first row of Table I-4 lists the

average values for these variances as a function of the percentage of time availability p.

The mean square error of prediction for Time Blocks 2 and 4 is listed in Row 2 of Table I-4, averaging values for 70 paths at each percentage level [data set (A)]. Tentative estimates of $\sigma_c^2(p) + \sigma_e^2$ appear in Row 3 of Table I-4, as the sum of variance and mean square bias from Rows 1 and 2. Rows 4 and 5 show the final variance σ_c^2 adjusted to 12.73 db^2 at p = 50%, and the corresponding standard deviations are given in Row 6. The variances $\sigma_c^2(p)$ are plotted versus the time availability p in Fig. I-5. The standard deviation, $\sigma_c(p)$ is shown as a function of the time availability p by the broken line on Fig. 9 in the main body of the paper.

Table I-4

Steps Used in Estimating Standard Deviations $\sigma_c(p)$

	db^2 for per cent p of all hours				
	1%	10%	50%	90%	99%
(1) Average variance $E\{[\Delta(p) - \overline{\Delta}]^2\}$ from Ohio data.	69.44	39.07	19.81	19.03	29.31
(2) Mean square bias from TB 2 and TB 4 data, normalized to zero at p = 50%.	1.08	0.22	0.00	0.75	2.38
(3) Sum of (1) and (2).	70.52	39.29	19.81	19.78	31.69
(4) (3) minus the average of the year-to-year variances 4.75 db^2	65.77	34.54	15.06	15.03	26.94
(5) (4) adjusted to 12.73 db^2 at p = 50%	63.44	32.21	12.73	12.70	24.61
(6) Standard deviation $\sigma_c(p)$ in db.	7.97	5.68	3.57	3.56	4.96

PATH-TO-PATH VARIANCE

THE VARIANCE OF BASIC TRANSMISSION LOSS $L_{bo}(p)$ EXCEEDED FOR p PERCENT OF ALL HOURS, RELATIVE TO THE CALCULATED VALUE $L_{bc}(p)$

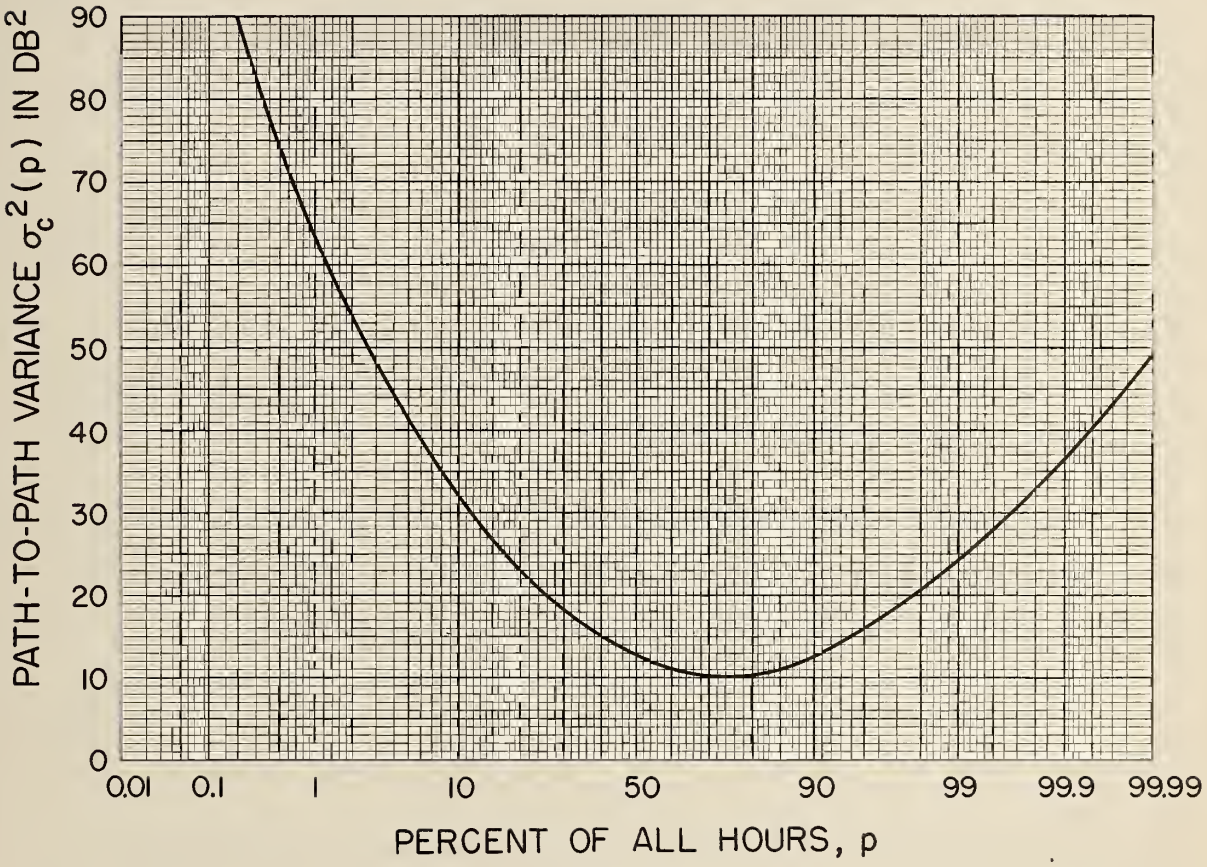

Fig. I-5

I.6 Estimation of $\sigma_o^2(p, n)$

The variance of $L_o(p, n)$ relative to the infinite-time percentile value $L_o(p, \infty)$ given by (I-54) is written as

$$\sigma_o^2(p, n) = E\{[L_o(p, n) - L_o(p, \infty)]\} \qquad \text{(I-58)}$$

For p = 50 per cent, $\sigma_o^2(p, n) = \sigma_o^2(50, n) = \sigma_o^2(n)$ which was estimated in Section I.4:

$$\sigma_o^2(50, n) = f(\theta)\, g(n, H) , \qquad \text{(I-59)}$$

and for any particular combinations of values of n, H, and θ, the appropriate curves of Figs. 14 and 15 are used. See the discussion in connection with (I-45) and (I-47a).

In order to obtain the variance $\sigma_o^2(p, n)$ for values of p other than 50%, the assumption is made that a similar relation exists here as for the variance $\sigma_c^2(p)$ assigned to the calculated values; i.e.,

$$\sigma_o^2(p, n) = \sigma_o^2(50, n)\, h(p) , \qquad \text{(I-60)}$$

where h(p) is given by $\sigma_c^2(p)/\sigma_c^2(50)$, and values may be determined from the $\sigma_c(p)$ curve of Fig. 9. Noting that $\sigma_c^2(50) = 12.73$, (I-59) may be rewritten using (I-60), resulting in

$$\sigma_o^2(p, n) = 0.0786\, g(n, H)\, f(\theta)\, \sigma_c^2(p) \qquad \text{(I-61)}$$

This equation is designated as (30) in the main body of the paper. It has already been mentioned that the procedures used to derive $\sigma_{oe}(p, n)$, especially the relation between $\sigma_o(50, n)$ and $\sigma_o(p, n)$ as well as $\sigma_c(50)$ and $\sigma_c(p)$ constitute the best available estimates to date. The

entire problem is being restudied, and it is expected that these relations will be formulated later on a statistically more refined basis. The final results, however, are not expected to differ materially from the ones obtained using the methods outlined here, so that the procedures given in this paper will result in reasonably good estimates.

APPENDIX II

ESTIMATING PREDICTION UNCERTAINTY FOR ONE PATH USING MEASUREMENTS MADE OVER ANOTHER PATH

This problem has been discussed briefly in Section 6 of the main body of the paper. Here a detailed derivation of (35) in Section 6 is given, which is a formula for calculating the standard deviation σ_{tb}. This standard deviation is assigned to the transmission loss estimate L_{tb} for a Path "b" Both L_{tb} and σ_{tb} depend on calculated values for Paths a and b, measurements for Path a, and an assumed correlation coefficient ρ_{ab} between the prediction errors δ_{ca} and δ_{cb}. All concepts have been explained in Section 6 and Appendix I. Equation (35), which is to be derived, is repeated here:

$$\sigma_{tb}^2 = \sigma_{cb}^2 + \sigma_{ca}^2 - \sigma_{ta}^2 - 2\sigma_{ca}\sigma_{cb}\rho_{ab}(1 - \sigma_{ta}^2/\sigma_{ca}^2) \qquad \text{(II-1)}$$

For convenience, the notation in this appendix will be simplified compared to the notation in Appendix I. The relationships to be developed will apply to any value of time availability. The observed transmission loss exceeded for p per cent of the hours in a T-hour recording over Path a, for instance, is L_{oa}:

$$\text{For Path a, } L_o(p, n) = L_{oa} \qquad \text{(II-2)}$$

The "true" infinite-time mean value $L_o(p, \infty) - \delta_e$ for Path a is L_a:

$$\text{For Path a, } L_o(p, \infty) - \delta_e = L_a \qquad \text{(II-3)}$$

Calculated values $L_c(p)$ for Paths a and b are L_{ca} and L_{cb}:

$$L_{ca} = L_{ca}(p) = L_a - \delta_{ca}(p)\ , \qquad \text{(II-4)}$$

$$L_{cb} = L_{cb}(p) = L_b - \delta_{cb}(p) , \qquad \text{(II-5)}$$

Variances of the random prediction errors $\delta_{ca}(p)$ and $\delta_{cb}(p)$ are defined by (I-57) and are written as σ^2_{ca} and σ^2_{cb}, respectively. Instead of regarding L_{ca} and L_{cb} as fixed and L_a and L_b as random, it is convenient here to regard the "true" values L_a and L_b as fixed, and the calculated values L_{ca} and L_{cb} as depending on random determinations of the prediction parameters for Paths a and b.

Similarly, the variance of the observed percentile L_{oa} relative to the true value L_a is given by (I-58) or (I-60) plus σ^2_e:

$$\sigma^2_e + \sigma^2_{oa}(p, n) = E[(L_{oa} - L_a)^2]. \qquad \text{(II-6)}$$

Reciprocals of these variances are weights:

$$w_{ca} = 1/\sigma^2_{ca}, \quad w_{cb} = 1/\sigma^2_{cb} \qquad \text{(II-7)}$$

$$w_{oa} = 1/[\sigma^2_{oa}(p, n) + \sigma^2_e] \qquad \text{(II-8)}$$

It was assumed that measurements are available only for Path a.

The improved prediction, L_{ta}, for Path a is analogous to (27) of Section 6 of the main body of the paper, and is written here as:

$$L_{ta} = \frac{w_{oa} L_{oa} + w_{ca} L_{ca}}{w_{oa} + w_{ca}} \qquad \text{(II-9)}$$

where the variance σ^2_{ta} assigned to L_{ta} is the reciprocal of the sum of the weights w_{oa} and w_{ca}:

$$\sigma^2_{ta} = \frac{1}{w_{ta}} = \frac{1}{w_{oa} + w_{ca}} \qquad \text{(II-10)}$$

From standard statistical texts, the correlation coefficient ρ_{xy} between the quantities x and y is given by

$$\rho_{xy} = \frac{E(xy) - E(x)\,E(y)}{\sigma_x \cdot \sigma_y} \qquad \text{(II-11)}$$

where E denotes expected values, as before, and σ_x^2 and σ_y^2 are the variances of x and y, respectively. Also, the variance of a sum of three terms

$$u = x + y + z \qquad \text{(II-12)}$$

is given by

$$\sigma_u^2 = \sigma_x^2 + \sigma_y^2 + \sigma_z^2 + 2\sigma_x \sigma_y \rho_{xy} + 2\sigma_x \sigma_z \rho_{xz} + 2\sigma_y \sigma_z \rho_{yz} \qquad \text{(II-13)}$$

This may now be applied to (34) of Section 6 which gives the estimated relation between calculated and improved prediction values of Paths "a" and "b" and is repeated here:

$$L_{tb} = L_{ta} + (L_{cb} - L_{ca}). \qquad \text{(II-14)}$$

Using (II-13),

$$\sigma_{tb}^2 = \sigma_{ta}^2 + \sigma_{ca}^2 + \sigma_{cb}^2 - 2\sigma_{ta} \sigma_{ca} \rho_{12} + 2\sigma_{ta} \sigma_{cb} \rho_{13} - 2\sigma_{ca} \sigma_{cb} \rho_{23} \qquad \text{(II-14)}$$

where

$$\rho_{12} \equiv \rho_{L_{ta} L_{ca}}, \quad \rho_{13} \equiv \rho_{L_{ta} L_{cb}}, \text{ and } \rho_{23} = \rho_{ab} \equiv \rho_{L_{ca} L_{cb}}.$$

The first two correlation coefficients are now expressed in terms of the last one, as for instance,

$$\rho_{12} = \frac{E[L_{ta} L_{ca}] - E(L_{ta})E(L_{ca})}{\sigma_{ta} \sigma_{ca}} = \frac{E[(L_{ta} - L_a)(L_{ca} - L_a)] - E[(L_{ta} - L_a)]E[(L_{ca} - L_a)]}{\sigma_{ta} \sigma_{ca}} \qquad \text{(II-15)}$$

Any constant value (L_a), subtracted from each of two variables, does not affect their correlation.

From (II-9),

$$L_{ta} - L_a = \frac{w_{oa}(L_{oa} - L_a) + w_{ca}(L_{ca} - L_a)}{w_{oa} + w_{ca}} \qquad \text{(II-16)}$$

$$E[(L_{ta} - L_a)] = \frac{1}{w_{ta}}\{w_{oa} E[(L_{oa} - L_a)] + w_{ca} E[(L_{ca} - L_a)]\} = 0 \qquad \text{(II-17)}$$

$$E(L_{ca} - L_a)] = E[\delta_{ca}] = 0 \qquad \text{(II-18)}$$

$$E[(L_{ta} - L_a)(L_{ca} - L_a)] = \frac{1}{w_{ta}}\{w_{oa} E[(L_{oa} - L_a)(L_{ca} - L_a)] + w_{ca} E[(L_{ca} - L_a)^2]\} \qquad \text{(II-19)}$$

$$E[(L_{oa} - L_a)(L_{ca} - L_a)] = 0 \qquad \text{(II-20)}$$

as errors of prediction and observation are assumed to be independent. As $E[(L_{ca} - L_a)^2] = \sigma^2_{ca}$, (II-15) is reduced to

$$\rho_{12} = \frac{\sigma^2_{ta} w_{ca} \sigma^2_{ca}}{\sigma_{ta} \sigma_{ca}} = \frac{\sigma_{ta}}{\sigma_{ca}} \qquad \text{(II-21)}$$

Similarly,

$$\rho_{13} = \frac{E[L_{ta} L_{cb}] - E[L_{ta}]E[L_{cb}]}{\sigma_{ta} \sigma_{cb}} = \frac{E[(L_{ta} - L_a)(L_{cb} - L_a)] - E[(L_{ta} - L_a)]E[L_{cb} - L_a)]}{\sigma_{ta} \sigma_{cb}} \qquad \text{(II-22)}$$

where $L_{cb} - L_a = L_b - L_a - \delta_{cb}$, and $L_b - L_a$ is a constant.

$$E[(L_{ta} - L_a)(L_{cb} - L_a)] = \frac{1}{w_{ta}} \{w_{oa} E[(L_{oa} - L_a)(L_b - L_a - \delta_{cb})] + w_{ca} E[(\delta_{ca} \cdot \delta_{cb})]\}$$

(II-23)

According to (II-11), $E[(\delta_{ca} \cdot \delta_{cb})] = \rho_{ab} \sigma_{ca} \sigma_{cb}$. The first term on the right hand side of (II-23) and both factors of the product $E[(L_{ta} - L_a)]$ times $E[(L_{ca} - L_a)]$ in (II-22) are zero, so that

$$\rho_{13} = \sigma_{ta}^2 \frac{\sigma_{ca}}{\sigma_{ca}^2} \frac{\sigma_{cb} \rho_{ab}}{\sigma_{ta} \sigma_{cb}} = \frac{\sigma_{ta}}{\sigma_{ca}} \rho_{ab} \qquad \text{(II-24)}$$

Finally, substituting the results for ρ_{12} and ρ_{13} into (II-14) and remembering that ρ_{23} has been denoted ρ_{ab}, the expression given as (II-1) is obtained:

$$\sigma_{tb}^2 = \sigma_{ta}^2 + \sigma_{ca}^2 + \sigma_{cb}^2 - 2\sigma_{ta} \sigma_{ca} \frac{\sigma_{ta}}{\sigma_{ca}} + 2\sigma_{ta} \sigma_{cb} \frac{\sigma_{ta}}{\sigma_{ca}} \rho_{ab} - 2\sigma_{ca} \sigma_{cb} \rho_{ab}$$

$$= \sigma_{ta}^2 + \sigma_{ca}^2 + \sigma_{cb}^2 - 2\sigma_{ta}^2 + 2\sigma_{ta}^2 \frac{\sigma_{cb}}{\sigma_{ca}} \rho_{ab} - 2\sigma_{ca} \sigma_{cb} \rho_{ab}$$

$$= \sigma_{cb}^2 + \sigma_{ca}^2 - \sigma_{ta}^2 - 2\sigma_{ca} \sigma_{cb} \rho_{ab} \left(1 - \frac{\sigma_{ta}^2}{\sigma_{ca}^2}\right) \qquad \text{(II-1)}$$

This result is identical to (35) given in Section 6:

The special case where $\sigma_{ca} = \sigma_{cb}$, $\rho_{ab} = 1$, and the paths are identical has already been mentioned in Section 6. In this case, (II-1) reduces to $\sigma_{tb}^2 = \sigma_{ta}^2$, as it should.

If the two paths, Path a and Path b, are so different that the correlation coefficient ρ_{ab} between the errors δ_{ca} and δ_{cb} assigned to the calculated values may be set equal to zero, (II-1) is reduced to

$$\sigma_{tb}^2 = \sigma_{ca}^2 + \sigma_{cb}^2 - \sigma_{ta}^2 \qquad \text{(II-25)}$$

In this case no improvement for Path b is obtained on the basis of measurements for Path a, as σ^2_{tb} will always be larger than σ^2_{cb}. The latter is the prediction uncertainty of the calculated value for Path b without any measurements, and in this case it will be more advantageous to use L_{cb} than L_{tb}. The improved prediction uncertainty σ^2_{ta} for Path a will, of course, be always smaller than σ^2_{ca}, based only on calculated values, and the right-hand side of (II-25) will always be larger than σ^2_{cb}.

The case of most interest in practical applications is the one where the paths are nearly equal (i.e., in the same general area of similar meteorological or terrain characteristics, with perhaps one of the terminals identical). In this case the prediction uncertainties σ^2_{ca} and σ^2_{cb} may be set equal to each other, but the correlation coefficient ρ_{ab} is not necessarily unity:

$$\sigma^2_{ca} = \sigma^2_{cb} = \sigma^2_c \tag{II-26}$$

and (II-1) is transformed to

$$\sigma^2_{tb} = \sigma^2_{ta}(2\rho_{ab} - 1) + 2\sigma^2_c(1 - \rho_{ab}). \tag{II-27}$$

Dividing by σ^2_c, and denoting as r^2 the prediction improvement ratio σ^2_{tb}/σ^2_c for Path "b", r^2 may be obtained as a function of the prediction improvement ratio for Path "a" (for which the measurements are available), $\sigma_{ta}/\sigma^2_c = k^2$, and the correlation coefficient ρ_{ab}:

$$r^2 = k^2(2\rho_{ab} - 1) + 2(1 - \rho_{ab}) \tag{II-28}$$

Curves for r^2 have been calculated and are shown on Fig. II-1. Only values of $r^2 < 1$ represent an improvement in the prediction for

Path "b" ($\sigma_{tb}^2 < \sigma_c^2$). Fig. (II-1) shows that ρ_{ab} has to be at least 0.5, and the improvement for Path "b", of course, depends on the degree of improvement $k^2 = \sigma_{ta}^2/\sigma_c^2$ obtained by measurements for Path "a". For $k^2 = 1$, ρ_{ab} drops out of (II-28) and $r^2 = 1$ for any value of ρ_{ab}.

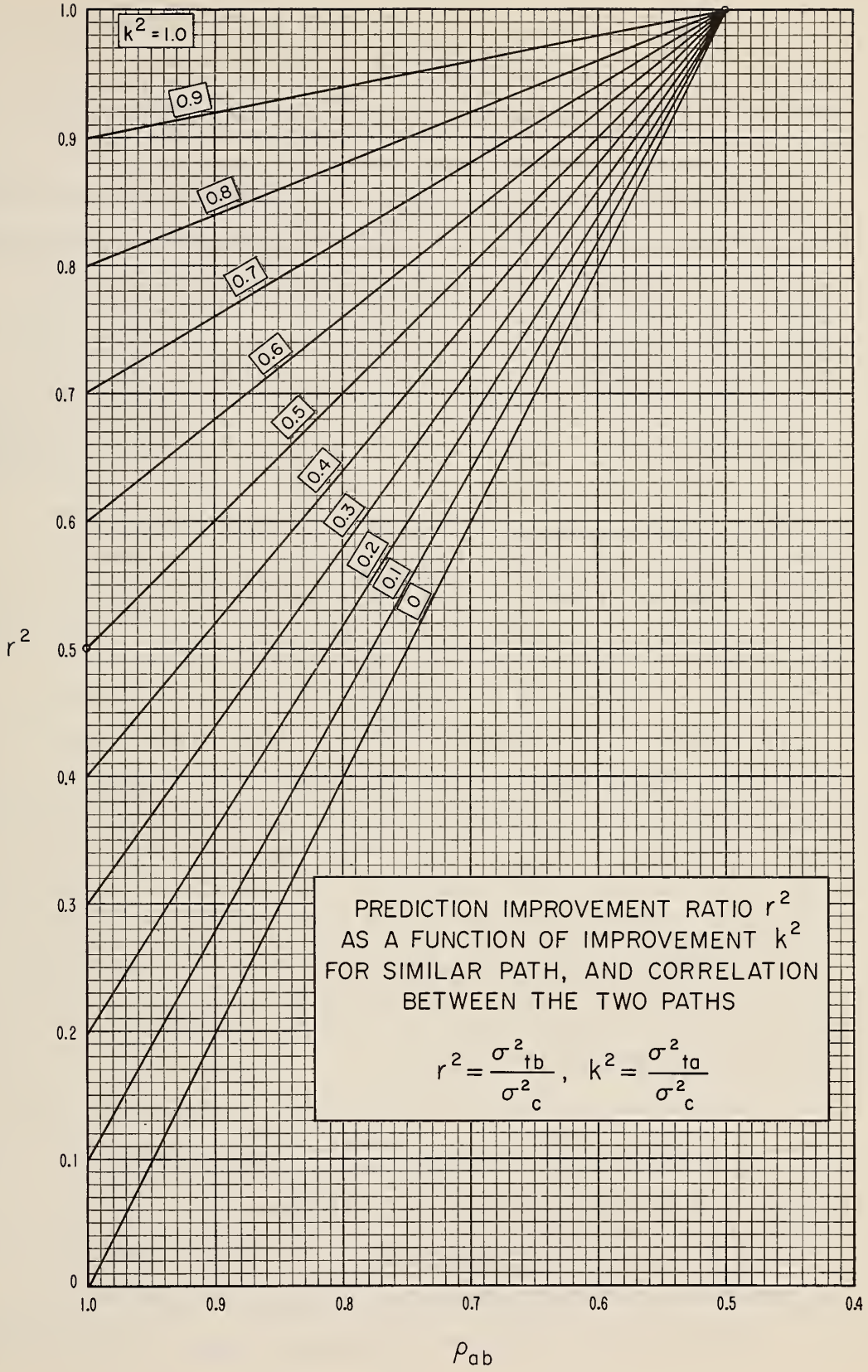
$k^2 = 1.0$
0.9
0.8
0.7
0.6
0.5
0.4
0.3
0.2
0.1
0
r^2
1.0
0.9
0.8
0.7
0.6
0.5
0.4
ρ_{ab}
PREDICTION IMPROVEMENT RATIO r^2
AS A FUNCTION OF IMPROVEMENT k^2
FOR SIMILAR PATH, AND CORRELATION
BETWEEN THE TWO PATHS
$r^2 = \frac{\sigma^2_{tb}}{\sigma^2_c}$, $k^2 = \frac{\sigma^2_{ta}}{\sigma^2_c}$

Figure II-1

APPENDIX III

THE EFFECTIVE NOISE FIGURE OF A RECEIVING SYSTEM

For several years now the concepts of an effective noise figure of a radio receiving system and of an effective input noise temperature have been found to be quite useful at the Central Radio Propagation Laboratory of the National Bureau of Standards. An operating noise factor was originally defined in a paper by North [1942], and characterizes the performance of the entire receiving system as contrasted to the receiver noise figure which characterizes only the performance of the receiver itself. Later, Norton [1953] gave a slightly more general expression for this factor and designated it as an effective noise figure. Thus the effective noise figure makes appropriate allowance for the external noise picked up by the receiving antenna as well as the noise introduced by the receiver itself, together with the effects of any losses in the antenna circuit and in the transmission line. The purposes of this appendix are to derive equation (1) in Section 2, to provide a more general formulation for the effective noise figure of a receiving system, to describe its general properties, and to relate it to the effective input noise temperature of the receiving system. In contrast to the approach to unity of the noise figure of an essentially noise-free network, the effective noise figure of an essentially noise-free receiving system approaches zero.

Essentially all of the basic concepts used in this discussion originated in the early papers by Burgess [1941], North [1942] and Friis [1944] and in the discussion by North [1945] of the paper by Friis. A precise definition of the noise figure of a four-terminal network was given by Friis [1944], and his definition forms the basis for the following formulation of the effective noise figure of a receiving system.

All signal and noise powers will be expressed in watts. It will be convenient in this appendix to make use of the concept of available power, i.e., the power which would be available in the output of a generator if the output circuit were matched to the generator impedance. It is evidently desirable to calibrate a signal generator in terms of its open circuit voltage v, and then its available power is given simply by $s_g = v^2/(4 R_g)$ for a generator with impedance $Z_g = R_g + jX_g$. Note that the available power from the generator has the desirable property of being independent of the load impedance, and this desirable property makes this concept especially useful for the definition and measurement of noise figures.

Let the impedance of the load be $Z_\ell = R_\ell + jX_\ell$; now it may be shown that the ratio of the available signal power s_g to the signal power s_ℓ delivered to the load is given by:

$$\frac{s_g}{s_\ell} = \frac{|Z_g + Z_\ell|^2}{4 R_g R_\ell} \equiv \ell_m \geq 1 \qquad \text{(III-1)}$$

The mismatch loss factor ℓ_m will be equal to 1, and the delivered power s_ℓ will be equal to the available power s_g when the load and generator impedances are matched, i.e., when $R_\ell = R_g$ and $X_\ell = -X_g$. Since it is confusing to use the decibel scale when noise powers are added, the convention of using lower case letters to denote powers in watts, or power ratios, will be adopted, and capital letters will be used to denote their decibel equivalents. For example, p_o will denote the available signal power at the terminals of the receiving antenna expressed in watts, and $P_o = 10 \log_{10} p_o$ dbw.

The gain, $g_{n\nu}$, of a four-terminal network for a c.w. frequency ν is defined as the ratio of the available signal power, s_o, at the output terminals of the network to the available signal power, s_g, at the output terminals of the signal generator.

$$g_{n\nu} = s_o / s_g \qquad (s_o / s_g \geq 1) \qquad \text{(III-2)}$$

Alternatively, the loss factor, $\ell_{n\nu}$, of a four-terminal network is given by:

$$\ell_{n\nu} = s_g / s_o \qquad (s_g / s_o \geq 1) \qquad \text{(III-3)}$$

Note that $g_{n\nu}$ and $\ell_{n\nu}$ inherently contain a mismatch factor ℓ_m determined from the signal generator and network input impedances, and thus depend upon the generator impedance as well as upon the characteristics of the network itself. The four-terminal network will have some kind of band-pass characteristic, and the gain, g_n, is often defined as the maximum gain in this pass band. More precisely, g_n should be considered to be the gain for the c.w. frequency ν at which the noise figure is to be specified or for the modulated band of frequencies typical of signals expected to be transmitted through the network. Let $s_{g\nu}$ denote the available signal power density per cycle per second in the modulated band of frequencies intended to be transmitted through the network. Now the network gain for a modulated band of signal frequencies may be expressed in the following form:

$$g_n = \frac{\int_0^\infty s_{g\nu}\, g_{n\nu}\, d\nu}{\int_0^\infty s_{g\nu}\, d\nu} = \frac{s_o}{s_g} \qquad \text{(III-4)}$$

Similarly the network loss for a modulated band of frequencies may be expressed in the following form:

$$\ell_n = \frac{\int_0^\infty s_{g\nu}\, d\nu}{\int_0^\infty (s_{g\nu}/\ell_{n\nu})\, d\nu} = \frac{s_g}{s_o} \qquad \text{(III-5)}$$

Since the gain will vary over the pass band of the network, we will follow North [1945] and define its effective noise bandwidth in cycles per second as:

$$b = \frac{1}{g_n} \int_{\nu_1}^{\nu_2} g_{n\nu}\, d\nu = \frac{1}{h\, g_n} \int_0^\infty g_{n\nu}\, d\nu \qquad \text{(III-6)}$$

In the above, ν_1 and ν_2 are chosen so as to include only the principal response of the network, i.e., a band of frequencies in which the desired signal power density is a maximum, and which is sufficiently wide so that $g_{n\nu 1}$ and $g_{n\nu 2}$ are negligibly small relative to the maximum value of $g_{n\nu}$ within this band. The factor h in (III-6) is a measure of any spurious responses which may be present in the receiver. The discussion in this appendix refers particularly to superheterodyne receivers and might have to be modified for other types of receivers. Note that $h \geq 1$ and may sometimes be greater than 2 for superheterodyne receivers with little or no selectivity at the frequency converter input. In such receivers, spurious responses will be generated by cross modulation of signals or noise on various frequencies appearing on the frequency converter grid of the receiver. The frequency converter mixes the signal $s_{g\nu d}$ on a desired frequency ν_d within the principal response band ν_1 to ν_2 with the oscillator frequency ν_o of the receiver to produce a signal with intermediate frequency $\nu_i = \pm(\nu_d - \nu_o)$. Additional undesired voltages may

arise in the intermediate frequency output by virtue of beats between the m^{th} harmonic of the oscillator frequency and the n^{th} harmonic of a spurious signal or noise with radio frequency ν_u not in the band ν_1 to ν_2 to produce the w^{th} subharmonic of the intermediate frequency. The spurious frequencies ν_u which may produce such additional responses in the intermediate frequency output may be determined from the following relation:

$$\pm (n \nu_u - m \nu_o) = \nu_i / w \qquad \text{(III-7)}$$

The above may be solved for ν_u by setting n, m, and w equal to various integers and ν_i equal to some value within the range $|\nu_1 - \nu_o|$ to $|\nu_2 - \nu_o|$;the most important spurious response usually corresponds to n = m = w = 1, and the spurious frequencies ν_u for this response differ by $2\nu_i$ from the frequencies ν_d within the principal response band. We will assume that the noise voltages in the principal and in the spurious responses are not correlated so that the resulting noise power in the receiver intermediate frequency output is simply the sum of the output noise powers arising from the several responses; this assumption may not be valid in the case of atmospheric or man-made noise, and in such cases the factor h would require a different evaluation.

Note that it would have been possible to define the noise bandwidth by integrating over the entire band, thus obtaining the larger bandwidth hb. However, the intermediate frequency band in which the noise finally appears has the bandwidth b, and this is the motivation for the definition (III-6). Receivers having spurious responses will have noise figures based on the definition of b given by (III-6) which are larger by the factor h than the noise figures of corresponding receivers not having such responses.

Note that g_n and thus b will depend upon the frequency, or band of frequencies, for which g_n is determined. When we later consider several networks in tandem, b is to be determined using g_n and $g_{n\nu}$ as determined from the values of s_g and s_o available at the input and output, respectively, of this chain of networks. It will later be convenient to use the db ratio of b to one cycle per second, $B = 10 \log_{10} b$.

The noise figure, f_n, of a four-terminal network was defined by Friis [1944] as the ratio of the available signal-to-noise ratio at the signal generator terminals to the available signal-to-noise ratio, r_o, at its output terminals, with the available noise at the signal generator terminals set equal to the reference available Johnson noise power, kt_ob, from a resistance at the absolute reference temperature t_o.

$$f_n = \frac{s_g/(kt_ob)}{r_o} \qquad \text{(Friis' Original Definition)} \qquad \text{(III-8)}$$

In the above, k is Boltzman's constant. If n_o denotes the available noise power at the output, the output available signal-to-noise ratio $r_o = s_o/n_o$, and when this, together with (III-2) or (III-3) are substituted in (III-8), the following alternative definitions are obtained for the noise figure of a network in terms of the available output noise power, n_o, and loss factor ℓ_n or gain g_n:

$$f_n = n_o \ell_n/(kt_ob) = n_o/(g_n kt_ob) \qquad \text{(Equivalent Definitions)} \qquad \text{(III-9)}$$

The above definitions will now be used to derive an expression for the noise figure of the simple network of Fig. III-1 with loss ℓ_n caused by its resistance, R_n, at an absolute temperature t_n. Let the resistance, R_g, of the signal generator be at the reference temperature t_o. The available signal power from the signal generator at the network input terminals is given in terms of its open circuit voltage, v, by:

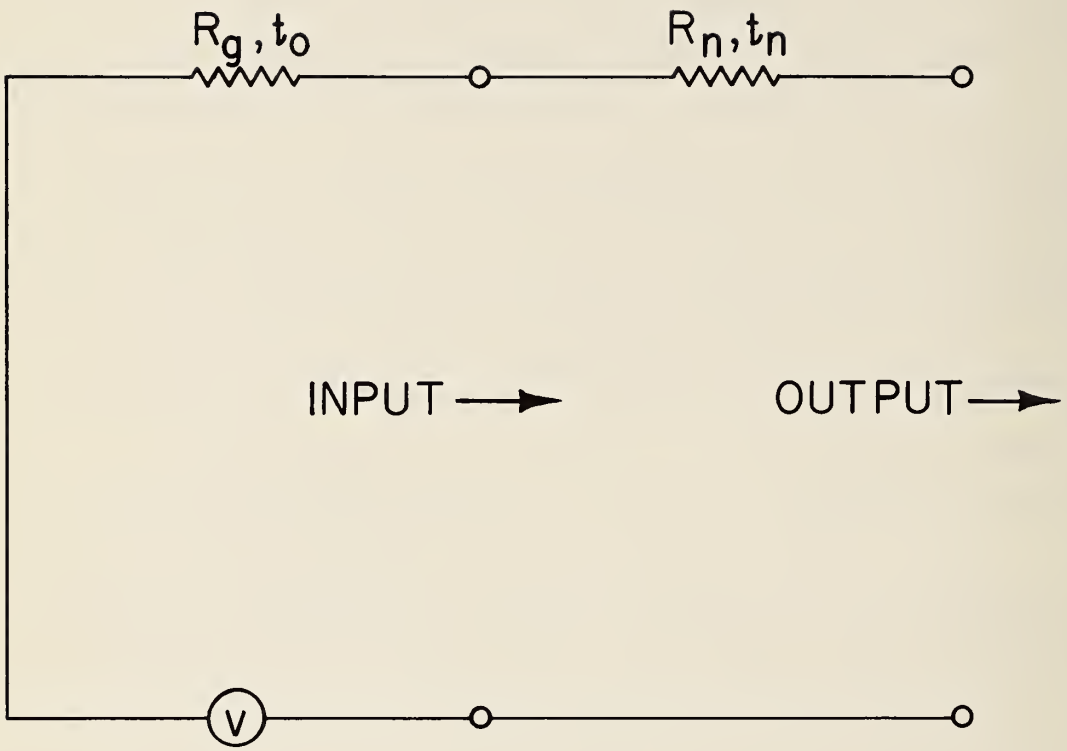

$$f_n = 1 + (\ell_n - 1)(t_n / t_o)$$

$$\ell_n = (R_n + R_g) / R_g$$

Figure III-1

$$s_g = v^2/(4R_g) \tag{III-10}$$

and the available signal power at the network output terminals is given by:

$$s_o = v^2/[4(R_g + R_n)] \tag{III-11}$$

Thus, from (III-3):

$$\ell_n = s_g/s_o = (R_g + R_n)/R_g \tag{III-12}$$

is obtained.

The available noise power at the output of the network of Fig. III-1 is given by the weighted average of the Johnson noises from the resistances R_g and R_n at temperatures t_o and t_n:

$$n_o = kb\left\{\frac{R_g t_o + R_n t_n}{R_g + R_n}\right\} = \frac{kb}{\ell_n}\{t_o + t_n(\ell_n - 1)\} \tag{III-13}$$

When this is substituted in (III-9), the result is:

$$f_n = 1 + (\ell_n - 1)(t_n/t_o) \tag{III-14}$$

Note that the noise figure f_n depends upon the generator impedance as well as upon the characteristics of the network itself. Note also that the noise figure of a passive network at the reference temperature t_o is simply equal to its loss factor, i.e., when $t_n = t_o$, it follows from (III-14) that $f_n = \ell_n$.

Next, (III-14) will be derived in another way, and it will be shown that it is applicable in general to any lossy passive network with loss ℓ_n and temperature t_n, i.e., having arbitrary input and output impedances. Note that the noise output, n_o, of the lossy network can be expressed as the sum of the two terms:

$$n_o = kb\, t_n + \frac{kb(t_o - t_n)}{\ell_n} \tag{III-15}$$

The first term would represent the available Johnson noise power from the network if its source resistance were also at the temperature t_n, while the second term represents a correction arising from the fact that the temperature t_o of the source resistance is different from that of the network, either higher or lower. When n_o, as given by (III-15), is substituted in the noise figure definition (III-9), (III-14) is obtained as before.

Using the above definitions and conventions, the effective noise figure of the receiving system illustrated on Fig. III-2 may now be discussed. Let p_a be the available signal power from the loss-free receiving antenna, let p_o be the available signal power from the actual receiving antenna, i.e., the available signal power at the antenna circuit output terminals, and let ℓ_c be the loss factor of the receiving antenna circuit; thus $p_a = \ell_c p_o$. Let t_c denote the effective absolute temperature of the antenna circuit, and (III-14) may be used to determine the noise figure of the antenna circuit network:

$$f_c = 1 + (\ell_c - 1)(t_c/t_o) \qquad \text{(III-16)}$$

Similarly the noise figure of the transmission line network with absolute temperature t_t and the line loss factor ℓ_t is given by:

$$f_t = 1 + (\ell_t - 1)(t_t/t_o) \qquad \text{(III-17)}$$

The noise figure of the receiver itself will be designated f_r.

Friis [1944] gives an expression for the noise figure of three networks in tandem. This will be used to determine the noise figure of the three-network system (c), (t), and (r) of Fig. III-2:

$$f_{ctr} = f_c + \ell_c(f_t - 1) + \ell_c \ell_t(f_r - 1) \qquad \text{(III-18)}$$

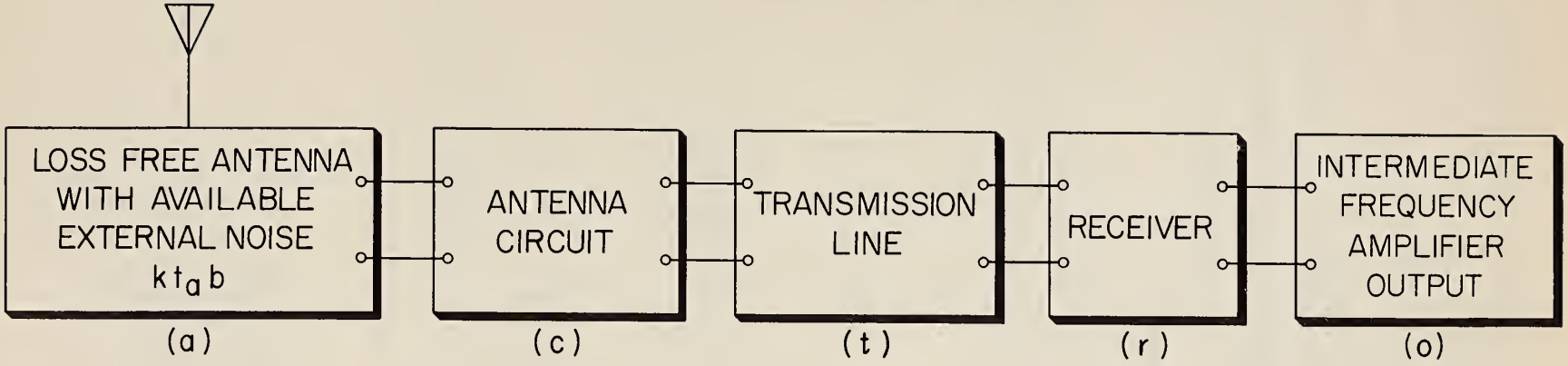

$$f = 1 + h\,(f_a - 1) + (\ell_c - 1)(t_c / t_o) + \ell_c\,(\ell_t - 1)(t_t / t_o) + \ell_c\,\ell_t (f_r - 1)$$

$$t_e = f\,t_o$$

Figure III-2

It will be convenient to represent the external noise power in the band $d\nu$ which is available at the terminals of the loss-free receiving antenna by $k t_{a\nu} d\nu$ where $t_{a\nu}$ is the receiving antenna noise temperature at the frequency ν. Representative values of $t_{a\nu}$ are given by Crichlow [1955] and by the C.C.I.R. [1956 and 1959] for frequencies $\nu < 10^8$ and are given by Blake [1961] for frequencies within the range $10^8 < \nu < 10^{10}$. Several useful additional sources of information relative to $t_{a\nu}$ are available in the January 1958 Radio Astronomy Issue of the Proceedings of the I.R.E. Now the available noise power n at the output of the complete receiving system may be represented, with the antenna replacing the signal generator having a reference temperature t_o, as the sum of two terms:

$$n = f_{ctr}\, k b t_o g_{ctr} + k \int_o^\infty (t_{a\nu} - t_o)\, g_{ctr\nu}\, d\nu \qquad \text{(III-19)}$$

In practice, $g_{ctr\nu}$ may sometimes best be determined from its components using the relation $g_{ctr\nu} = g_{r\nu}/(\ell_{c\nu}\ell_{t\nu})$. The first term in (III-19) would represent the available noise power at the output of the receiving system if $t_{a\nu} = t_o$ for all values of ν, while the second term represents a correction arising from the difference between $t_{a\nu}$ and t_o. Since the integral in (III-19) has the limits 0 to ∞, it allows properly for all of the spurious responses as well as for the principal response.

It is useful now to define an effective antenna noise temperature t_a:

$$t_a = \frac{\int_o^\infty t_{a\nu} g_{ctr\nu}\, d\nu}{\int_o^\infty g_{ctr\nu}\, d\nu} = \frac{\int_o^\infty t_{a\nu} g_{ctr\nu}\, d\nu}{h b g_{ctr}} \qquad \text{(III-20)}$$

Using this value of t_a, (III-19) may be expressed:

$$n = f_{ctr}\, k b t_o\, g_{ctr} + k h b (t_a - t_o)\, g_{ctr} \qquad \text{(III-21)}$$

If this value of n is substituted in (III-9) for n_o, and g_{ctr} for g_n, the following expression is obtained for the effective noise figure of the receiving system:

$$f = h(t_a/t_o) + (f_{ctr} - h) \qquad \text{(III-22)}$$

Finally, if we replace (t_a/t_o) by f_a, substitute (III-18) for f_{ctr}, (III-17) for f_t and (III-16) for f_c, the following general expression for the effective noise figure of the receiving system described by the network of Fig. (III-2) is obtained:

$$f = 1 + h(f_a - 1) + (\ell_c - 1)(t_c/t_o) + \ell_c(\ell_t - 1)(t_t/t_o) + \ell_c \ell_t (f_r - 1) \qquad \text{(III-23)}$$

For the special case of a receiver with no spurious responses so that h = 1 and in which the antenna circuits and transmission line are at the reference temperature t_o, it follows that $f_c = \ell_c$, $f_t = \ell_t$, and (III-23) becomes:

$$f = f_a - 1 + f_c f_t f_r = f_a - 1 + \ell_c \ell_t f_r \qquad (t_c = t_t = t_o \text{ and } h = 1) \qquad \text{(III-24)}$$

The above is the expression for the effective noise figure previously given by Norton [1953].

This effective noise figure concept has been adopted by the Consultative Committee on International Radio [1956 and 1959]. Examples of its application are given in several recent reports of the Central Radio Propagation Laboratory [Crichlow et al, 1955; Norton, 1956; Rice et al, 1959; Florman and Tary, 1961; and Air Force Technical Order, 1961].

The effective noise figure is useful for determining the relation between the signal power, p_a, available from the loss-free receiving antenna and the corresponding signal-to-noise ratio r at the receiver output. It is usually more convenient and is essential in the case of FM receivers to consider r to be the predetection signal-to-noise ratio available at the output of the intermediate frequency amplifier. Now, if f is substituted in (III-8) for f_n, p_a for s_g, and r for r_o, the result is:

$$p_a = f\, r\, k\, t_o\, b \qquad \text{(III-25)}$$

Just as Friis defined the noise figure of a four-terminal network as the ratio of the input available signal-to-reference-noise ratio to the output available signal-to-noise ratio: $f_n = [s_g/(k t_o b)]/r_o$. here the effective noise figure of a receiving system has been defined to be the ratio of the available signal-to-reference-noise ratio from the loss-less receiving antenna to the receiver output available signal-to-noise ratio: $f = [p_a/(k t_o b)]/r$. As pointed out by Friis, definitions in terms of available signal and noise powers rather than for necessarily matched conditions are advantageous since the use of mismatch conditions in amplifier input circuits often lead to a reduction in the noise figure of networks containing such amplifiers, [Llewellyn, 1931; Haus and Adler, 1958; Haus et al, 1960].

Expressed in decibels, (III-25) may be written

$$P_a = F + R + B - 204 \text{ dbw} \qquad \text{(III-26)}$$

where $F = 10 \log_{10} f$, $R = 10 \log_{10} r$, and $10 \log_{10} k t_o = -204.00$ when $t_o = 288.39^o$ and $k = 1.38044 \times 10^{-23}$ [Cohen et al, 1957]; since t_o must be somewhat arbitrarily chosen in any case, the above value was assigned so that the constant in (III-26) is equal to 204.

If P_r denotes the power radiated from the transmitting antenna, then the radio path transmission loss [Norton, 1959]

$L \equiv P_r - P_a = P_t - L_t - P_a = L_b - G_p$, where $P_r = P_t - L_t$ and the remaining terms in this equation are defined on pages 3 and 4. Now the following simple equation is obtained for determining the transmitter power P_t required to provide a given predetection signal-to-noise ratio R:

$$P_t = L_b - G_p + L_t + F + R + B - 204 \text{ dbw} \qquad \text{(III-27)}$$

Note that the effective noise figure f for a noise-free receiving system, i.e., with $t_a = f_a = 0$, $f_c = f_t = 1$ and $f_r = h$ is equal to zero. We may establish that $f_r = h$ for a noise-free receiver with spurious responses as follows. The noise n available at the output of such a receiver may be expressed:

$$n = k t_o \int_o^\infty g_{r\nu} \, d\nu \qquad \text{(III-28)}$$

If we substitute this value in (III-9), we obtain:

$$f_r = \frac{1}{g_r b} \int_o^\infty g_{r\nu} \, d\nu = h \qquad \text{(III-29)}$$

In fact, practical receiving systems have been developed with effective noise figures f substantially less than unity, so that F is actually negative; for example, DeGrasse et al [1960] have reported a value of F = -12 db.

Some experimenters prefer to specify the performance of low noise receiving systems in terms of an effective input noise temperature t_e, and this is related to f and t_o or to h, t_a and f_{ctr} by $t_e = f t_o = h t_a + (f_{ctr} - h) t_o$. However, it appears from the above discussion that the effective input noise temperature t_e depends upon the antenna impedance, the spurious responses of the receiving system

and the modulation characteristics of the signals intended to be received. Consequently, it would appear to be better to use f, t_o and b to provide a measure of the expected performance of a receiving system rather than adding one more to the already large number of different temperature concepts [Ko, 1961] currently in use in the electronic engineering literature. In this connection, reference may also be made to recent discussions by Rhodes [1961] and Talpey [1961]. The reference temperature $t_o = 288.39^o$ is preferred for the reason given above, but corresponding noise figures would be less than 0.024 db larger than those specified relative to a reference temperature $t_o = 290^o$; however, the use of a reference temperature $t_o = 1^o K$ would lead to noise figures which would be 24.6 db larger.

A temperature in degrees Kelvin may be related to temperatures in degrees centigrade or in degrees Fahrenheit by the relations:

$$t_{Kelvin} = 273.16 + t_{Centigrade} = 255.38 + (5/9)\, t_{Fahrenheit} \qquad \text{(III-30)}$$

If the signal generator used for receiver noise figure measurements has its impedance at a temperature t_g rather than t_o, then a term $[1-(t_g/t_o)]\,h$ should be added to the value so measured to determine f_r. It follows that an error in f_r of less than $\pm 0.1h$ will be made if t_g lies within the range $260^o K$ to $317^o K$, i.e., within the range $-13^o C$ to $44^o C$ or within the range $8^o F$ to $111^o F$.

The effective noise figure of the receiving system could be referred to the receiver input terminals rather than to the terminals of the loss-free receiving antenna. It would then be smaller by the factor $\ell_c \ell_t$ and would thus not represent a proper measure of the noise performance of the entire receiving system. The loss-free receiving antenna terminals clearly represent the only proper reference point for the effective noise figure of most communications receiving systems,

although an argument can be made [Dyke, 1961] by the radio astronomers for referring the effective noise figure and the corresponding effective input noise temperature to outer space--the location of their target--by including tropospheric and ionospheric losses with appropriate temperatures in determining f.

In radiometry, the desired signal is the noise available from the loss-free receiving antenna, and such a signal will be present in the spurious responses as well. In this case g_{ctr} and b, as defined by (III-4) and (III-6) are indeterminate; however, the factor $h\,b\,g_{ctr}$, which is required in (III-10) for the evaluation of t_a, may be evaluated [See (III-6)] by:

$$h\,b\,g_{ctr} = \int_0^\infty g_{ctr\nu}\,d\nu \qquad \text{(III-31)}$$

The radiometer measures only an <u>average</u> antenna temperature t_a, and it is evident by (III-20) that the presence of spurious responses over a wide band will not yield a good estimate of $t_{a\nu}$ if this has different values for the different receiver responses. Furthermore, the output noise voltages from various parts of the response band must be uncorrelated to the same extent as those from the calibrating white noise source for a valid determination of t_a.

Normally the effective noise figure of a receiving system would not be measured directly; instead each of its components would be measured, and then (III-23) used to combine these components. The following systematic procedure may be followed for determining each of these components under the actual conditions of matching or mismatching of the various elements in the receiving system. Let R_a denote the theoretical radiation resistance of the receiving antenna referred to its input terminals, and let R_m be its measured input resistance; in this case $\ell_c = R_m/R_a$. This method of determining ℓ_c may sometimes be used at low radio frequencies where R_m and R_a often differ substantially; a more general discussion including the

effects of insulator losses is given by Crichlow [1955]. At the higher frequencies, ℓ_c will usually be negligibly different from unity; however, in the case of reception with a unidirectional rhombic terminated in its characteristic impedance, ℓ_c may be greater than 2 [Harper, 1941], since nearly half of the received power is dissipated in the terminating impedance and some is dissipated in the ground. Next the transmission line loss factor ℓ_t is measured as the ratio s_g/s_o where s_g denotes the available power from a signal generator at the input to the line with its impedance adjusted so as to be equal to the measured impedance of the receiving antenna, and s_o denotes the resulting available power at the output of the line, i.e., the power which would be delivered to an output impedance which matches the output impedance of the line with the antenna connected to the input to the line. Finally, the noise figure f_r of the receiver is to be determined by using a c.w. signal generator at its input having the same impedance as the above-defined output impedance of the transmission line. Let s_d denote the available signal power at the frequency ν from the generator with its impedance at temperature t_g which is required to double the receiver output power (signal plus noise) relative to the output noise power with the signal generator turned off; then $f_r = [s_d g_{r\nu}/(g_r k t_o b)] + [1-(t_g/t_o)] h$. The above procedures will yield the appropriate values of ℓ_c, ℓ_t and f_r to be used in (III-17) for the actual conditions of matching of the transmission line either to the receiving antenna or to the receiver. It will always be desirable to match the line to the receiving antenna, since this will result in the smallest value for ℓ_t and will eliminate echoes which could be quite objectionable on long lines. However, it will sometimes be advantageous to mismatch the transmission line to the receiver and thus minimize f_r; this latter point is discussed in the paper by Llewellyn [1931] and in the I. R. E. Standards [Haus et al, 1960]. Next, $g_{ctr\nu}$ is determined over a frequency range which includes all of the receiver responses, and g_{ctr}, b, h and t_a are then determined by means of their defining equations (III-4), (III-6), and (III-20).

The use of a dispersed signal source [noise generator] has been recommended [Haus et al, 1960] as a simpler method of measurement of the receiver noise figure since the bandwidth need not be separately measured in determining f_r. However, if this method is used in the case of a multiple response receiver, it is essential that the noise density from the generator be constant over a band which includes all of the receiver responses, and the apparent noise figure obtained in this way must be increased by the factor h in order to determine f_r; thus it would still be necessary in this case to measure both b and h in order to determine the noise figure of a multiple response receiver. Furthermore, the ultimate use of f_r is for the determination of p_a, and it is evident by (III-25) that its determination requires an equally accurate determination of both b and f. Consequently, the specification of the noise performance of a receiving system (or of a receiver) requires the determination of b and h as well as f (or f_r). Note that b should be made somewhat larger than the band ideally required for the reception of the desired signal, in order to accommodate relative drifts of the transmitter and receiver oscillators.

The over-all merit of a receiving system is best measured by $p_m = f r_m k t_o b \equiv r_m k t_e b$ where r_m denotes the minimum value of r required in the system considered for a specified grade of service. Although p_m provides a direct and unambiguous measure of the merit of a receiving system, it should not be overlooked that a reduction in p_m can sometimes be achieved by the use of very wide band modulation schemes, and the use of such wide bands is not necessarily desirable for the efficient use of the spectrum; in many cases the use of higher power transmitters and narrower modulation bands might well be advantageous.

In measuring an available loss or gain of a four-terminal network, it may be inconvenient in some cases to make the signal generator output impedance the same as the output impedance of the preceding networks and the load impedance equal to the network output impedance with its

input connected to the preceding networks. There are two cases in which this can be avoided. In case the load impedance is matched to the network output impedance, we may determine ℓ_n or g_n by (III-2) or (III-3) by replacing s_g by $s_g \ell_{mnp}/\ell_{mng}$ where ℓ_{mnp} denotes the mismatch factor (III-1) between the network input impedance and the output impedance of the preceding networks while ℓ_{mng} denotes the mismatch factor between the network input impedance and the signal generator impedance; when the signal generator impedance is made equal to the impedance of the preceding networks, $\ell_{mnp} = \ell_{mng}$ and no correction is involved. In case the signal generator impedance is made equal to the output impedance of the preceding networks, we may determine ℓ_n or g_n by (III-2) or (III-3) by replacing s_o by $s_\ell \ell_{mo\ell}$ where s_ℓ denotes the power delivered to the load and $\ell_{mo\ell}$ denotes the mismatch factor between the network output impedance and the load impedance.

Many radio relay systems contain a duplexer between the transmission line and the receiver so as to permit simultaneous transmission and reception from a single antenna. In case this duplexer has the same absolute temperature t_t as that of the transmission line, we may modify (III-23) as follows to determine the effective noise figure of a receiving system containing such a duplexer: ℓ_t is now measured as the ratio s_g/s_o where, as before, s_g denotes the available power from a signal generator at the input to the line with its impedance equal to that of the receiving antenna, but s_o is now the resulting power available at the output of the duplexer. In addition, the following term is added to (III-23): $\frac{\ell_c \ell_t}{g_r k t_o b} \int_o^\infty p_{d\nu}\, g_{r\nu}\, d\nu$ where $p_{d\nu}$ is the undesired local transmitter power density available at the output of the duplexer; it is assumed that the receiver output voltages arising from this source from the various responses are uncorrelated.

It is important to emphasize that the noise figure of a receiver, or of any four-terminal network, depends upon a mismatch factor ℓ_m between the source and the network, and thus depends upon the source impedance as well as the characteristics of the network itself. In particular, the effective noise figure of a receiving system depends upon the impedance of the receiving antenna.

In those cases, particularly at the lower frequencies, where the transmitting and receiving antenna circuit losses are large, it might appear to be advantageous to use the concept of system loss $L_s \equiv P_t' - P_o$ where P_t' is the power input to the transmitting antenna and P_o is the available power from the actual lossy receiving antenna. In this case and assuming a single response receiver with h = 1, (III-27) may be written:

$$P_t' = L_s + F_s + R + B - 204 \text{ dbw} \qquad \text{(III-32)}$$

$$F_s \equiv 10 \log_{10}\{(t_{as}/t_o) + (\ell_t - 1)(t_t/t_o) + \ell_t(f_r - 1)\} \quad (h=1) \qquad \text{(III-33)}$$

Here F_s is the effective noise figure of the receiving system referred now to the terminals of the actual lossy receiving antenna, and $kt_{as}b$ represents the external noise available at the terminals of the lossy receiving antenna. Note, however, that $(t_{as}/t_o) = \{f_a + (\ell_c - 1)(t_c/t_o)\}/\ell_c$, and thus ℓ_c and t_c must still be known for a proper determination of the performance of the system. For this reason it appears that (III-32) is no simpler to use than (III-27) and, of course, these two equations must yield identical results when each of their terms is properly evaluated.

In many applications, particularly where atmospheric noise is involved, t_a and f_a will be quite variable with time, and in such cases it is useful to consider f to be a random variable and to describe it in terms of appropriate statistical characteristics. In still other applications, such as space-satellite communications, f will be found to vary with the receiving antenna orientation since t_a will vary as the antenna is pointed in different directions.

At very high frequencies or at very low temperatures, the available noise power from a source at absolute temperature t will be less than ktb by the factor $(h\nu/kt)/\{\exp(h\nu/kt) - 1\}$ as was shown by Nyquist [1928]; here h denotes Planck's constant. Since $(h\nu/kt) = 0.0479932\ \nu(Gc/s)/t$ [Cohen et al, 1957], this correction represents less than 0.1 decibel reduction in the available noise power when $\nu(Gc/s)/t$ is less than 0.955895, i.e., when $\nu < 276$ Gc/s at the reference temperature t_o or when $\nu < 9.5$ Gc/s for a temperature $t = 10^{o}K$. Balazs [1957] has shown that the Johnson noise power available from a conductor also depends on the shape of the conductor at very high frequencies.

There has been some discussion in the literature [Haus and Adler, 1957 and Siegman 1961] of difficulties with "negative" resistances and their associated "negative" temperatures in some types of amplifiers; such considerations are important, however, only in the design and description of the various internal components of the receiver. In those cases where the receiver output impedance has a negative resistance, r may be re-interpreted to be the signal-to-noise ratio in the load impedance rather than the available signal-to-noise ratio at the intermediate frequency output. With the use of this convention in such cases, the noise figure f_r of any practical stable receiver can still be defined since such a receiver must have positive source and load resistances with positive temperatures at its input and output.

It is sometimes possible to reduce the effective noise figure f of a receiving system and thus to improve its performance by rearranging the order of its component parts. To see how this may be accomplished, we may use the formula of Friis for two networks in tandem. For two networks p and q, with noise figures f_p and f_q, the two networks in tandem with p preceding q will have a noise figure given by:

$$f_{pq} = f_p + (f_q - 1)/g_p \qquad \text{(III-34)}$$

Alternatively, if q precedes p, we have:

$$f_{qp} = f_q + (f_p - 1)/g_q \qquad \text{(III-35)}$$

From the above we obtain the condition which must be satisfied for $f_{pq} < f_{qp}$:

$$f_p + (f_q - 1)/g_p < f_q + (f_p - 1)/g_q \qquad (\text{For } f_{pq} < f_{qp}) \qquad \text{(III-36)}$$

We will first consider the conditions under which it is advantageous to use a preamplifier p at the antenna terminals preceding the transmission line represented by network q. In this case $g_q = 1/\ell_t$ and $f_q = 1 + (\ell_t - 1)(t_t/t_o)$ so that we may write for the reduction in f with the preamplifier preceding the transmission line:

$$\Delta f \equiv f_{qp} - f_{pq} = (\ell_t - 1)\{(f_p - 1) + (t_t/t_o)(1 - \frac{1}{g_p})\} \qquad \text{(III-37)}$$

Since Δf is inherently positive, it follows that f will <u>always</u> be decreased by having a preamplifier precede the transmission line, and this reduction represents an improvement, expressed in decibels, given by $\Delta F = -10 \log_{10}\{(f_{pq} + \Delta f)/f_{pq}\}$.

Consider next the question of which of two amplifiers in a chain should precede the other. In this case we may subtract 1 from each side of (III-36) and, provided $g_p > 1$ and $g_q > 1$, we may re-write this inequality in the form:

$$\frac{f_p - 1}{1 - \frac{1}{g_p}} < \frac{f_q - 1}{1 - \frac{1}{g_q}} \qquad \begin{array}{l}(\text{For } f_{pq} < f_{qp} \text{ provided} \\ g_p > 1 \text{ and } g_q > 1)\end{array} \qquad \text{(III-38)}$$

If the above inequality is satisfied, it will be advantageous to have the amplifier p precede the amplifier q.

Acknowledgements: This appendix was written after discussions with E. F. Florman and W. Q. Crichlow, both of whom independently derived the expression (III-14) by arguments differing from those given herein. Discussions with L. V. Blake of the Naval Research Laboratory also proved to be helpful.

REFERENCES

Air Force Technical Order, Ground Telecommunications Performance Standards, Part 5 of 6, Tropospheric Systems, prepared by the Central Radio Propagation Laboratory of the National Bureau of Standards under sponsorship of the Ground Electronics Engineering and Installation Agency (Directorate of Engineering, ROZM), United States Air Force, T.O. 31-Z-10-1, published under authority of the Secretary of the Air Force (June 15, 1961).

Balazs, Nandor L., Thermal fluctuations in conductors, Phys. Rev. vol. 105, no. 3, pp. 896-899, (Feb. 1957).

Barghausen, A. F., and C. F. Peterson, Path loss measurements versus predictions for long distance tropospheric scatter circuits, submitted for publication in the IRE Transactions on Communication Systems (1961).

Bennett, C. A., and N. L. Franklin, Statistical analysis in chemistry and the chemical industry, p. 86 and Table 1 of Appendix, 689-693, (John Wiley and Sons, Inc., New York, N.Y., 1954).

Blake, L. V., Recent advancements in basic radar range calculation technique, IRE Transactions on Military Electronics, vol. MIL-5, no. 2, pp. 154-164 (April, 1961).

Burgess, R. E., Noise in receiving aerial systems, Proc. Phys. Soc., vol. 53, pp. 293-304 (May 1941).

C.C.I.R., Report No. 65, Report on revision of atmospheric radio noise data (Warsaw, 1956, available as a separate document from the International Telecommunications Union, Geneva, or in Vol. I of the Documents of the VIIIth Plenary Assembly of the C.C.I.R., Warsaw, 1956).

C.C.I.R., Documents of the IXth Plenary Assembly, III, 223-256, Los Angeles, (1959).

Cohen, E. R., K. M. Crowe, and J. W. M. Dumond, The fundamental constants of physics, (Interscience Publishers, New York, N.Y., 1957).

Crichlow, W. Q., D. F. Smith, R. N. Morton, and W. R. Corliss, Worldwide radio noise levels expected in the frequency band 10 kc to 100 Mcs, NBS Circular 557 (August 1955); the derivation in this report for f is correct only in the case where t_c and t_t are equal to t_o.

DeGrasse, R. W., D. C. Hogg, E. A. Ohm, and H. E. D. Scovil, Ultra-low noise receiving system for satellite or space communication, Proc. Nat. Elect. Conf. 15, 370-379 (1959); also published as Bell Telephone System Monograph 3624 (August, 1960).

Dyke, E., Corrections and coordination of some papers on noise temperature, Proc. IRE, 49, No. 4, pp. 814-815, (April 1961).

Feller, W., An introduction to probability theory and its applications (John Wiley and Sons, Inc., New York, N. Y., 1950).

Florman, E. F., and J. J. Tary, Required signal-to-noise ratios, carrier power and bandwidth to achieve a given performance of multichannel radio communication systems, to be submitted for publication as an NBS Technical Note (1961).

Friis, H. T., Noise figures of radio receivers, Proc. IRE 32, No. 7, pp. 419-422 (July 1944).

Harper, A. E., Rhombic antenna design, D. Van Nostrand Co., 1941.

Hartman, W. J., and R. E. Wilkerson, Path antenna gain in an exponential atmosphere, J. Research NBS 63D (Radio Prop.), No. 3, 273-286 (Nov.-Dec. 1959).

Haus, H. A., W. R. Atkinson, G. M. Branch, W. B. Davenport, Jr., W. H. Fonger, W. A. Harris, S. W. Harrison, W. W. McLeod, E. K. Stodola and T. E. Talpey, Representation of noise in linear twoports, Proc. IRE 48, No. 1, 60-74 (January, 1960).

Haus, H. A., and R. B. Adler, An extension of the noise figure definition, Proc. IRE 45, No. 5, 690-691 (May 1957).

Haus, H. A., and R. B. Adler, Optimum noise performance of linear amplifiers, Proc. IRE 46, No. 8, 1517-1533 (August 1958).

Kirby, R. S., Measurement of service area for television broadcasting, IRE Transactions on Broadcast Transmission Systems, PGBTS-7, 22-30 (February 1957).

Kirby, R. S., and F. M. Capps, Correlation in VHF propagation over irregular terrain, IRE Transactions on Antennas and Propagation AP-4, No. 1, 77-85 (January 1956).

Kirby, R. S., H. T. Dougherty, and P. L. McQuate, VHF propagation measurements in the Rocky Mountain region, IRE Transactions on Vehicular Communication PGVC-6, 13-19 (July 1956). See Fig. 6.

Ko, H. C., Temperature concepts in modern radio, Microwave Journal 4, No. 6, 60-65 (June 1961).

Llewellyn, F. B., A rapid method of estimating the signal-to-noise ratio of a high gain receiver, Proc. IRE 19, No. 3, 416-421 (March 1931).

North, D. O., The absolute sensitivity of radio receivers, RCA Review 6, 332-343 (Jan. 1942).

North, D. O., Discussion on noise figures of radio receivers, by H. T. Friis, Proc. IRE 33, No. 2, 125-127 (Feb. 1945).

Norton, K. A., Transmission loss in radio propagation, Proc. IRE 41, No. 1, 146-152 (Jan. 1953).

Norton, K. A., Point-to-point radio relaying via the scatter mode of tropospheric propagation, IRE Transactions on Communication Systems CS-4, No. 1, 39-49 (March 1956).

Norton, K. A., System loss in radio-wave propagation, Proc. IRE 47, No. 9, 1661 (Sept. 1959).

Norton, K. A., P. L. Rice, and L. E. Vogler, The use of angular distance in estimating transmission loss and fading range for propagation through a turbulent atmosphere over irregular terrain, Proc. IRE 43, No. 10, 1488-1526 (Oct. 1955).

Nyquist, H., Thermal agitation of electric charge in conductors, Phys. Rev. 32, No. 1, 110-113 (July 1928).

Rand Corporation, A million random digits with 100,000 normal deviates, (The Free Press Publishers, Glencoe, Illinois, 1955).

Rice, P. L., A. G. Longley, and K. A. Norton, Prediction of the cumulative distribution of ground wave and tropospheric wave transmission loss (Part I), NBS Technical Note 15, PB 151374, (July 1959). Order by PB number from the Office of Technical Services, U.S. Department of Commerce, Washington 25, D.C. Foreign remittances must be in U.S. exchange and must include one-fourth of the publication price to cover mailing costs. $1.50.

Rhodes, D. R., On the definition of noise performance, Proc. IRE 49, No. 1, p. 376 (Jan. 1961).

Siegman, A. E., Thermal noise in microwave systems, The Microwave Journal 4, No. 3, 81-90 (Mar. 1961); 4, No. 4, 66-73 (Apr. 1961); and 4, No. 5, 93-104 (May 1961).

Takács, L., Stochastic processes (John Wiley and Sons, Inc., New York, N.Y., 1960).

Talpey, T. E., Comment on "On the Definition of Noise Performance" by D. R. Rhodes, Proc. IRE 49, No. 1, 376-377 (Jan. 1961).

Williamson, D. A., V. L. Fuller, A. G. Longley, and P. L. Rice, A summary of VHF and UHF tropospheric transmission loss data and their long-term variability, NBS Technical Note 43, PB 151402 (Mar. 1960). Order by PB number from the Office of Technical Services, U. S. Department of Commerce, Washington 25, D.C. Foreign remittances must be in U.S. exchange and must include one-fourth of the publication price to cover mailing costs. $2.25.

U. S. DEPARTMENT OF COMMERCE
Luther H. Hodges, *Secretary*

NATIONAL BUREAU OF STANDARDS
A. V. Astin, *Director*

THE NATIONAL BUREAU OF STANDARDS

The scope of activities of the National Bureau of Standards at its major laboratories in Washington, D.C., and Boulder, Colorado, is suggested in the following listing of the divisions and sections engaged in technical work. In general, each section carries out specialized research, development, and engineering in the field indicated by its title. A brief description of the activities, and of the resultant publications, appears on the inside of the front cover.

WASHINGTON, D.C.

Electricity. Resistance and Reactance. Electrochemistry. Electrical Instruments. Magnetic Measurements. Dielectrics.

Metrology. Photometry and Colorimetry. Refractometry. Photographic Research. Length. Engineering Metrology. Mass and Scale. Volumetry and Densimetry.

Heat. Temperature Physics. Heat Measurements. Cryogenic Physics. Equation of State. Statistical Physics.

Radiation Physics. X-ray. Radioactivity. Radiation Theory. High Energy Radiation. Radiological Equipment. Nucleonic Instrumentation. Neutron Physics.

Analytical and Inorganic Chemistry. Pure Substances. Spectrochemistry. Solution Chemistry. Standard Reference Materials. Applied Analytical Research.

Mechanics. Sound. Pressure and Vacuum. Fluid Mechanics. Engineering Mechanics. Rheology. Combustion Controls.

Organic and Fibrous Materials. Rubber. Textiles. Paper. Leather. Testing and Specifications. Polymer Structure. Plastics. Dental Research.

Metallurgy. Thermal Metallurgy. Chemical Metallurgy. Mechanical Metallurgy. Corrosion. Metal Physics. Electrolysis and Metal Deposition.

Mineral Products. Engineering Ceramics. Glass. Refractories. Enameled Metals. Crystal Growth. Physical Properties. Constitution and Microstructure.

Building Research. Structural Engineering. Fire Research. Mechanical Systems. Organic Building Materials. Codes and Safety Standards. Heat Transfer. Inorganic Building Materials.

Applied Mathematics. Numerical Analysis. Computation. Statistical Engineering. Mathematical Physics. Operations Research.

Data Processing Systems. Components and Techniques. Digital Circuitry. Digital Systems. Analog Systems. Applications Engineering.

Atomic Physics. Spectroscopy. Infrared Spectroscopy. Solid State Physics. Electron Physics. Atomic Physics.

Instrumentation. Engineering Electronics. Electron Devices. Electronic Instrumentation. Mechanical Instruments. Basic Instrumentation.

Physical Chemistry. Thermochemistry. Surface Chemistry. Organic Chemistry. Molecular Spectroscopy. Molecular Kinetics. Mass Spectrometry.

Office of Weights and Measures.

BOULDER, COLO.

Cryogenic Engineering. Cryogenic Equipment. Cryogenic Processes. Properties of Materials. Cryogenic Technical Services.

Ionosphere Research and Propagation. Low Frequency and Very Low Frequency Research. Ionosphere Research. Prediction Services. Sun-Earth Relationships. Field Engineering. Radio Warning Services.

Radio Propagation Engineering. Data Reduction Instrumentation. Radio Noise. Tropospheric Measurements. Tropospheric Analysis. Propagation-Terrain Effects. Radio-Meteorology. Lower Atmosphere Physics.

Radio Standards. High Frequency Electrical Standards. Radio Broadcast Service. Radio and Microwave Materials. Atomic Frequency and Time Interval Standards. Electronic Calibration Center. Millimeter-Wave Research. Microwave Circuit Standards.

Radio Systems. High Frequency and Very High Frequency Research. Modulation Research. Antenna Research. Navigation Systems.

Upper Atmosphere and Space Physics. Upper Atmosphere and Plasma Physics. Ionosphere and Exosphere Scatter. Airglow and Aurora. Ionospheric Radio Astronomy.


NBS